

CEA-N-1561

KFK 1581

- Note CEA-N-1561 -

- KFK 1581 -

Centre d'Etudes Nucléaires de Cadarache  
Division d'Etudes et de Développement des Réacteurs  
Département de Physique des Réacteurs et de Mathématiques Appliquées  
Service des Expériences Critiques et de Physique des Réacteurs

---

Institut für Angewandte Systemtechnik und Reaktorphysik  
Projekt Schneller Brüter  
Gesellschaft für Kernforschung M.B.H. Karlsruhe

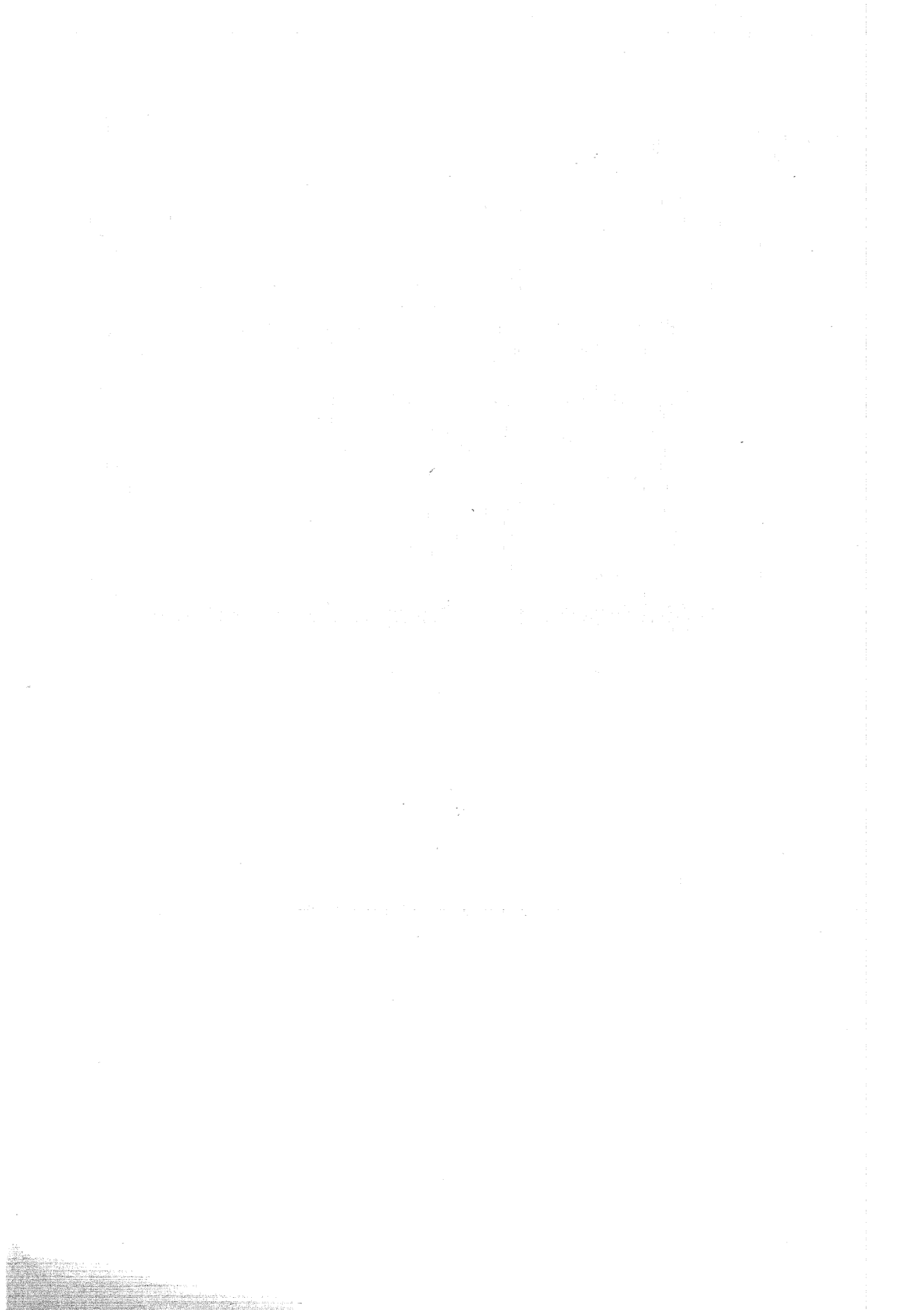
## PHYSICS INVESTIGATIONS OF SODIUM COOLED FAST REACTORS

### CORE Z1 MASURCA IN SNEAK-ASSEMBLY 6D

*Compiled by*

*Philippe HAMMER and Fritz PLUM*

- SEPTEMBER 1972 -



CEA-N-1561 - Philippe HAMMER - Fritz PLUM

PHYSIQUE DES REACTEURS RAPIDES REFROIDIS AU SODIUM : ETUDE DU RESEAU Z1 MASURCA DANS L'ASSEMBLAGE SNEAK 6 D.

Sommaire. - Le but de cette note est de présenter les résultats des mesures faites sur le milieu Z1 de MASURCA à combustible Plutonium chargé dans l'expérience critique SNEAK 6D à Karlsruhe au cours de l'année 1970 : la composition de ce milieu est voisine de celle de la zone centrale d'un réacteur rapide de 250 MWe.

Les expériences ont été réalisées en étroite coopération par les physiciens des laboratoires de Cadarache et de Karlsruhe selon un programme établi en commun par les deux équipes et orienté vers l'étude de deux types de paramètres :

- les paramètres cellule (spectre- Laplacien matière- indices de spectres) qui caractérisent la cellule Z1 MASURCA et permettent de tester l'adaptation des jeux de sections efficaces aux calculs de ce type de milieu.
- les paramètres projet (masse critique- distribution de puissance- vide sodium- échauffement  $\gamma$ - barres de contrôle) dont la mesure est destinée à connaître et éventuellement améliorer la qualité des méthodes de calculs utilisées pour prévoir ces grandeurs dans les projets en cours (PHENIX - SNR).

Ce rapport présente simultanément les résultats expérimentaux et les évaluations qui en ont été données tant à Karlsruhe qu'à Cadarache. Lorsque les méthodes de calcul diffèrent dans les deux laboratoires, elles sont toutes deux présentées et leurs résultats confrontés à ceux de l'expérience.

1972

94 p.

Commissariat à l'Energie Atomique - France

CEA-N-1561 - Philippe HAMMER - Fritz PLUM

PHYSICS INVESTIGATIONS OF SODIUM COOLED FAST REACTORS CORE Z1 MASURCA IN SNEAK-ASSEMBLY 6 D.

Summary. - This report aims to present the results of the measurements performed on the Plutonium core Z1 MASURCA built in the SNEAK 6D facility at Karlsruhe during 1970. This core is close to the central zone of a 250 MWe power fast reactor.

These experiments were carried out in close cooperation between Karlsruhe and Cadarache physicists according to a common program settled by the two laboratories and devoted to the study of two kinds of parameters :

- cell parameters (spectrum- material bubbling- spectral indices), characterizing the Z1 MASURCA cell, which allow to check the validity of the cross-section sets for predicting the neutron balance in such a medium.
- design parameters (critical mass- sodium void- power distribution  $\gamma$  heating- control rods) which are studied in order to check and eventually to improve the calculation methods used to predict those quantities for the present designs (PHENIX - SNR).

This report presents simultaneously the experimental results and the analysis of the measurements performed either at Karlsruhe or at Cadarache. When the calculation methods used in both laboratories are different, both of them are presented and compared to the experimental results.

1972

94 p.

Commissariat à l'Energie Atomique - France



Centre d'Etudes Nucléaires de Cadarache  
Division d'Etudes et de Développement des Réacteurs  
Département de Physique des Réacteurs et de Mathématiques Appliquées  
Service des Expériences Critiques et de Physique des Réacteurs

---

Institut für Angewandte Systemtechnik und Reaktorphysik  
Projekt Schneller Brüter  
Gesellschaft für Kernforschung M.B.H. Karlsruhe

## PHYSICS INVESTIGATIONS OF SODIUM COOLED FAST REACTORS

### CORE Z1 MASURCA IN SNEAK-ASSEMBLY 6D

*Compiled by*

*Philippe HAMMER\* and Fritz PLUM\*\**

- \* Centre d'Etudes Nucléaires de Cadarache - DEDR/DPRMA/SECPR
- \*\* Institut für Angewandte Systemtechnik und Reaktorphysik - Projekt Schneller Brüter - Gesellschaft für Kernforschung M.B.H. - Karlsruhe



THE SNEAK 6D EXPERIMENTS WERE PERFORMED AND ANALYZED BY :

G.F.K. : MM. BICKEL - BÖHME - DÖRFEL - HELM -  
JOURDAN - PLUM - WERLE - WITTEK -  
PILATE (BELGONUCLEAIRE)

CADARACHE : MM. BARRE - BRUNET - CAMPAN - CAUMETTE -  
CHAUDAT - DESPRETS - GOLINELLI - HAMMER -  
JEANDIDIER - LERIDON

1. The first part of the document discusses the importance of maintaining accurate records of all transactions and activities. It emphasizes that this is crucial for ensuring transparency and accountability in the organization's operations.

2. The second part of the document outlines the various methods and tools used to collect and analyze data. It highlights the need for consistent and reliable data collection processes to support informed decision-making.

3. The third part of the document focuses on the role of technology in modern data management. It discusses how advanced software solutions can streamline data collection, storage, and analysis, leading to more efficient and accurate results.

4. The fourth part of the document addresses the challenges associated with data security and privacy. It stresses the importance of implementing robust security measures to protect sensitive information from unauthorized access and breaches.

5. The fifth part of the document concludes by summarizing the key findings and recommendations. It reiterates the importance of a data-driven approach and provides actionable steps for improving data management practices within the organization.

## CONTENTS

### INTRODUCTION

#### I - DESCRIPTION OF THE ASSEMBLY SNEAK 6D

I.1. Core media

I.2. Realization of the core

#### II - CRITICALITY

#### III - PROTON RECOIL SPECTRA MEASUREMENTS

III.1. Experimental configurations

III.2. Counter characteristics

III.3. Measured and evaluated spectra

III.3.1. G.F.K. results

III.3.2. CADARACHE results

III.4. Comparison between G.F.K. and CADARACHE measured spectra

#### IV - REACTION RATE TRAVERSES

IV.1. Measurements performed

IV.2. G.F.K. calculations of the traverses

IV.3. Experimental buckling evaluation

IV.4. Reflector savings

IV.5. Axial power distribution

#### V - SPECTRAL INDICES AT THE CORE CENTER

V.1. Experimental results

V.1.1. Measurements performed

V.1.2. Experimental corrections to the measured data

V.1.3. Calculated corrections to the measured data

V.2. Comparison between calculated and measured results

#### VI - SODIUM VOID

VI.1. Experiments performed

VI.2. G.F.K. calculations

VI.3. CADARACHE calculations

VI.4. Conclusions

#### VII - AXIAL $\gamma$ -HEATING TRAVERSE

VIII - CONTROL RODS

- VIII.1, Shut down reactivity of the various rods
  - VIII.1.1. Measurements performed
  - VIII.1.2. G.F.K. evaluation
  - VIII.1.3. CADARACHE calculations
    - VIII.1.3.1. Experimental radii
    - VIII.1.3.2. Calculated radii
    - VIII.1.3.3. Comparison between experimental and calculated results
  - VIII.1.4. Comparison between the G.F.K. and CADARACHE analysis
- VIII.2. Reaction rates in presence of rods
  - VIII.2.1. G.F.K. analysis
  - VIII.2.2. CADARACHE analysis

CONCLUSION

## INTRODUCTION

The core SNEAK 6D to which this report is devoted belongs to the SNEAK-6 assemblies which have been built at the Karlsruhe research center between February 1970 and September 1970. The aim of this arrangement was to study a central core zone of 17 % enrichment in plutonium fissile isotopes, a value which is close to the central zone enrichment of the SNR and the PHENIX projects.

In the SNEAK 6D core the central zone which was to be studied was built with the MASURCA rodlets. This assembly completed the French program devoted to the study of PHENIX zones : this program includes the R1 and R2 uranium cores built in MASURCA, and the plutonium cores Z2 built in MASURCA and Z1 built in SNEAK.

The MASURCA fuel which is made of an alloy U-Pu-Fe is quite different from the  $\text{PuO}_2$ - $\text{UO}_2$  platelets previously used for the central zone in the SNEAK 6A and 6B cores. This should permit a comparison between two media with almost the same enrichment in fissile isotopes, but with different cell-geometry (see ref. [1]).

The experimental program for this core was prepared and realized by physicists of both German and French teams and the analysis of the results was performed simultaneously at Cadarache and at Karlsruhe.

## I. - DESCRIPTION OF THE ASSEMBLY SNEAK 6D

### 1.1. Core media

The SNEAK 6D core (see fig. 1/2) contains three cylindrical zones :

— the central zone (Z1M) loaded with the Z1-MASURCA cells. The Z1-MASURCA cell whose description is given in fig. 3 contains three rodlets of the U-Pu-Fe alloy and one rodlet of depleted uranium with twelve rodlets of diluent (ferrit and sodium). The U-Pu-Fe and the depleted uranium rodlets are cylindrical with a diameter of 12,7 mm. The diluent rodlets have a square section (12.7 x 12.7 mm). The fuel enrichment in fissile isotopes is 17 %. The MASURCA plutonium contains 8.4 % of Pu-240;

— a buffer zone (Z1A), containing Z1A SNEAK cells whose homogeneous composition is quite close to the Z1M-composition. The SNEAK-cell, described in more detail in ref. [1], is built with SNEAK platelets according to fig. 3.

The fuel enrichment in fissile isotopes is 15.5 %. The SNEAK-plutonium contains 7.7 % of Pu-240;

— a driver zone, loaded with R1-cells (see ref. [1]) which contains uranium whose mean enrichment is 22 % (see fig. 3).

### 1.2. Realization of the core

The Z1-MASURCA zone was built free of control rods. The fuel rodlets used were 60 and 30 cm long except in one of the four central tubes where they were 45 cm long for the foil measurements (see section V.1). The cladding of the rodlets is 0.2 mm thick except at the top and the bottom where the thickness of the cap is 2 mm for the short rodlets and 4 mm for the long rodlets.

— In the SNEAK zones neither the Z1- nor the R1-SNEAK elements contained an integer number of cells. To fit the core height exactly one had put at the upper and lower ends of each element rest-cells whose composition was close to the composition of the normal cells and whose thickness was chosen to fit the core height. Those rest-cells are described in more detail in ref. [1].

— The cells located in the midplane of the core along the N.S. diameter of the reactor were modified to permit the installation of the radial channel for the measurements.

— In the R1 - and Z1-SNEAK zones some element positions were occupied by control

rods which were filled with uranium platelets in the core region. In the criticality calculations the presence of control rods is taken into account by calculating for each zone including such rods mean concentrations (see tab. 1 / 2 :  $k_{eff}$  concentrations) which correspond to the homogenisation of each zone including the control rods.

The MASURCA-zone consisted of 96 elements. The buffer zone Z1-SNEAK surrounding the central zone contained 160 elements. The R1 zone contained 113 elements.

The axial breeder blanket covering the MASURCA-zone was loaded with Na and  $UO_2$ -MASURCA rodlets. In the Z1-SNEAK zone the axial blanket consisted of Na and  $UO_2$  platelets, and in the R1-zone of Al and  $UO_2$  (because of lack of Na platelets). The radial blanket was loaded with depleted uranium. The atom densities of the blankets are given in Table 2.

The geometrical characteristics of the clean critical core are the following ones :

Zone	Z1-MAS.	Z1-SNEAK	R1-SNEAK	Radial blanket	Axial blanket
R cm	30.07	49.1	58.95	92.12	-
H cm	91.45	89.4	89.4	150.00	thickness: 40.65

The fuel inventory in the core was approximately :

Pu-MASURCA (Z1 M) 126 kg

Pu-SNEAK (Z1 A) 217 kg

$U^{235}$  (Total core) 259 kg

$U^{238}$  (Total core) 2 632 kg.

II. - CRITICALITY

The criticality of the clean critical core has been evaluated with the cross-section sets MOXTOT and NAP (26 groups) at Karlsruhe and with the CADARACHE set (25 groups) on the French side. The principle of the evaluation is to calculate the  $k_{eff}$  of the assembly in two-dimensional cylindrical geometry with the multigroup diffusion approximation and then to take into account the corrections corresponding to heterogeneity, transport and cylinderisation.

For the German sets the elastic scattering cross-sections have been improved by weighting them with the actual spectrum of the core under consideration (REMO-correction : see ref. [2]).

In the French set the improvement of the elastic scattering cross-sections is performed systematically, with the use of a 600 group weighting spectrum calculated for every core determination of the 25 group cross-sections. The geometry of the core is given in Fig. 1. The corrections were calculated in one dimensional geometry (except the cylinderisation correction) with energy - and composition dependent bucklings at Karlsruhe, with non energy dependent buckling at Cadarache. The results of the criticality calculations are the following :

	MOXTOT	NAP	CADARACHE
$k_{eff}$ (Homog. 2D)	0.9866	0.9696	0.99172
REMO	0.0037	0.0085	-
Heterogeneity	0.0091	0.0098	0.00561
Transport (S8)	0.0046	0.0046*	0.00592
Cylinderisation	-0.0025	-0.0025*	-0.00165
Final value	1.0015	0.9900	1.00160
Estimated error of the $k_{eff}$ calculation	0.00064	0.00064	0.00064
Experimental value	1.00014 ± 0.00004		

\* These values have been taken over from the MOXTOT-set.

The uncertainty of the final value of  $k_{eff}$  calculated with the French set was estimated according to the usual method used in Cadarache and it was assumed that this uncertainty would be of the same magnitude for the MOXTOT and NAP sets. It is mainly due to the approximations made to perform the various corrections.

Taking into account this uncertainty for each final calculated value one can see that the MOXTOT as well as the CADARACHE sets overestimate slightly the  $k_{eff}$  value while the NAP set underestimates it strongly.

The final values obtained with the MOXTOT and the CADARACHE sets are in a good agreement, but this agreement is partly due to compensating discrepancies :

- The heterogeneity estimate done at Karlsruhe is much higher than the effect calculated at Cadarache. This may be due to the fact that while the cross-sections corresponding to the heterogeneous media were evaluated by the same process at both places, the homogeneous media were not defined in the same way. At Karlsruhe the homogeneous cross-sections used in the heterogeneity correction (so called "quasi-homogeneous" cross-sections) were evaluated by a cell calculation in which all the dimensions were decreased by a factor of  $10^3$ , while the homogeneous cross-sections used in the two-dimensional  $k_{eff}$  calculation were calculated straightforward from the averaged atom densities. At Cadarache in every case the homogeneous cross-sections were evaluated directly from the averaged atomic densities.

Anyway, the strong heterogeneity is due to the structure of the MASURCA-cell built with metal rodlets. Let us say for comparison that the heterogeneity effect of SNEAK 6B (see ref. [1]) built with oxide platelets is negative and close to 0.001 in  $K_{eff}$ .

- The cylinderisation-effect evaluated at Karlsruhe for this core is also higher than the one obtained at Cadarache, and higher than the previous effects evaluated on the 6A, 6B cores (see ref. [1]). This discrepancy is under investigation.
- The transport effect which was calculated with the same procedure (S8) by both groups differs by 25 % between Cadarache and Karlsruhe. It should be mentioned that this discrepancy is of the same order of magnitude for the three cores 6A, 6B, 6D and is probably the consequence of the different assumptions made on each side.

### III. - PROTON RECOIL SPECTRA MEASUREMENTS

#### III.1. Experimental configurations

The measurements were performed in the center of the core in position 17 / 20 (see Fig. 2). The experimental configurations of the core used either by the Karlsruhe team or by the Cadarache team are the following :

1. The clean critical core with all shim rods out ( $B_4C$  in the core) and all safety rods dropped ( $B_4C$  in). The corresponding  $k_{eff}$  is close to 0.95. In this configuration measurements were made by both laboratories.
2. The clean critical core with all safety and shim rods located in the Z1-SNEAK zone occupying their normal position (fuel inserted) and all shim rods of the R1-zone out. In this case the steady state of the reactor is at  $k_{eff} \approx 0.98$ . The measurements in this configuration were only performed by Cadarache. The highest possible flux was reached which provided a counting rate of about 10 000 cp/s above 10 KeV.

In the following configurations the measurements were only performed by the G.F.K. team :

3. The "small core" corresponding to the clean critical configuration diminished by 105 edge elements with all the shim rods at their normal position (fuel inserted) and none of the safety rods dropped.
4. The small core preceedingly defined with 9 shim rods out of the core ( $B_4C$  in) and no safety rod dropped.

#### III.2. Counter characteristics

The following tables give the characteristics of the counters which were used by the G.F.K. and by the Cadarache team :

G.F.K. counters

Nr.	Geometry	Active volume diameter length (cm)	Filling	Energy range
1	cylindrical	3.5    9.4	3 atm $CH_4$	400-1 400 KeV
2	spherical	3.94	4 atm $H_2$	150- 600 KeV
3	spherical	3.94	2 atm $H_2$	10- 400 KeV with $\gamma$ -n- discrimination
4	spherical	3.94	1 atm $H_2$	50-250 KeV

Cadarache counters

Nr.	Diameter mm	Length mm	Filling	Energy range	Best resolution
1	22	75	1 atm. H <sub>2</sub> -CH <sub>4</sub> (80%-20%)	10 - 200 KeV	4 %
2	22	75	4 atm. H <sub>2</sub> -CH <sub>4</sub> (80%-20%)	150 - 500 KeV	6 %
3	22	75	4 atm. CH <sub>4</sub>	300 -1500 KeV	10 %

Fig. 4 shows the arrangement of each type of counter-German and French - in the SNEAK tube. The detailed descriptions of the electronic apparatus are given in ref. [3] and [4]. In every case a  $\gamma$ -n discrimination is used.

III.3. Measured and calculated spectra

For each configuration the evaluation of the measured proton spectrum was performed by unfolding the spectrum with calculated response matrices. The contribution of high energy neutrons (above 1.4 MeV) was deduced from a calculated spectrum. Before unfolding, the proton spectrum is smoothed at the expense of some per cent in the energy resolution. A more detailed description of the treatment of the rough experimental results is available in ref. [3] and [4].

III.3.1. G.F.K. results

Fig. 5 and Fig. 6 show the results of the spectrum measurements in the smaller cores (configurations 3 and 4) together with the corresponding 208-group calculated spectra. The precision of measured points is better than  $\pm 10$  %.

For this comparison pairs of neighbouring groups in the calculated spectra were combined to one to get an energy resolution comparable with that of the measurements. Calculation and experiment both show a slight hardening of the spectrum when the shim rods are inserted into the small core. In Table 3 the results of different calculations and measurements have been summarized after integration over the ABN-groups. For each of the configuration 1, 3 and 4 the calculations were normalized to the experimental integral value between 100 KeV and 1.4 MeV, since one assumes the error on the measured spectra to increase from 10 % to approximately 15 % below 100 KeV. The 208-group calculations agree well with the measurements while the 26-group calculations performed with the MOXTOT set (see Table 3) show a strong discrepancy with the measurement in the region of the oxygen resonance at 430 KeV in spite of the fact that a REMO-correction was applied to the calculations.

### III.3.2. CADARACHE results

#### a/ Measurements done in configuration 2.

The measurements performed in that configuration are particularly interesting, since they were performed at  $k_{eff} \simeq 0.98$ , i.e. not very far from the critical state, and since the influence of the boron rods inside the R1-zone of the reactor is of small importance for the spectrum in the center. The results are shown in Fig. 7 after wall effect corrections are been applied. These corrections are made assuming that the spectrum is known above 1.4 MeV (see ref. [4]).

Two kinds of comparison can be made, one concerning the fine structure, the other the macrogroup spectrum.

The fine structure comparison, which above a few KeV is particularly influenced by slowing down effects, is done with a 208 group calculation (G.F.K. calculation). As stated above, group resolution and counter resolution are similar in this case. The agreement here is fairly good.

For a survey over the total neutron population a macrogroup comparison is more convenient. For this macrogroup comparison a 25 group calculation is used which is the result of the condensation of a 600 group spectrum as usual with the CADARACHE set. The 25 group calculation is performed with the diffusion approximation on the homogeneous medium, since one assumes the homogeneous spectrum represents rather well the measured one. Measurement and calculation are normalized over the range 15 to 1 350 KeV.

The discrepancies (Experiment-Calculation)/Calculation for that range are shown on Fig. 8. They could be partly explained by the way in which the slowing down was calculated at Cadarache at the time the measurements were performed.

#### b/ Measurements done in configuration 1.

Some difficulties with the  $\gamma$ -n discrimination system in this measurements led to experimental results which were meaningful only above 60 KeV. A comparison between the measurements in this configuration and at  $k_{eff} \simeq 0.98$  gives the following results (both measurements were normalized to the signal of a D.C. chamber located outside the core) :

Energy (KeV)	1 350 - 820	820 - 498	498 - 302	302 - 183	183 - 111	111 - 67.4
$\frac{\phi \text{ config. 2}}{\phi \text{ config. 1}}$	1.21	1.12	1.12	1.07	1.14	1.12

The experimental error is about  $\pm 3$  % per group. Considering this, the shapes of the two spectra both normalized between 67.4 and 1 350 KeV agree fairly well except for the high energy group.

#### III.4. Comparison between G.F.K. and CADARACHE measured spectra

In order to get a comparison over the broadest possible energy range we compared the spectrum of configuration 3 (G.F.K.-measurements) with the spectrum of configuration 2 (CADARACHE-measurements). In doing so we have to apply small corrections taking into account the slight modification of the spectrum with varying core size. In comparing the fine structure spectra this correction was not made.

The fine spectra do not show systematic discrepancies but a difference in resolution which may arise from the counters or from the smoothing of the proton spectra before differentiation. This is particularly true in the 28 KeV iron resonance region (see Fig. 9). An important result is that the general slope between 1.35 MeV and 15 KeV agrees within 6 %.

For the macrogroup comparison the lethargy-width  $\Delta u$  was chosen as 0.5. In this case the spectrometer resolution is of small importance. The G.F.K. measurements done in configuration 3 were corrected for the smaller core size. Table 4 summarizes the results. As the assumed error bars are about 3 % per group, except in the lowest energy group where they are close to 10 %, the results agree except for the groups 11 and 12. But if we compare the sum of these two groups the difference is only 4 %. This is due to the fact that the iron resonance is near the boundary of these groups and that therefore the resolution affects in this case the neutron distribution between them.

#### IV. - REACTION RATE TRAVERSES

The axial and radial fission rate distributions were measured in SNEAK in order to get information on the quality of the traverse calculations in the core and the axial blanket and by  $B_m^2$  determination on the quality of the cell calculations and the cross-section sets used. Furthermore they should give some information on the blanket characteristics (reflector savings).

##### IV.1. Measurements performed

For measuring the axial and radial fission rate distributions fission chambers with a diameter of 8 mm and an active length of 20 mm were used. Their deposits were respectively made of U 235, U 238, Np 237 and Pu 239.

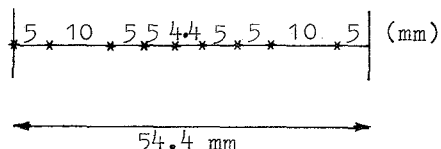
The measurements were performed axially in the element 17/20 (see fig. 2) where a channel was constructed by replacing the  $Fe_2O_3$  rodlets between the four Na rodlets by a guiding tube. Radially the measurements were done along the N-S diameter of the reactor in the core midplane in a channel shifted by half an element to the West.

In each position of the chamber 60 000 impulses were counted twice in order to get a statistical error less than 3 %. By means of a pilot-rod which was located at the core-radial blanket boundary the power was kept constant manually.

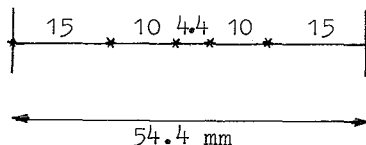
Fluctuations which still appeared were eliminated by using two monitors which were working as D.C. chambers.

Axially the fission rates were measured each centimeter.

Radially in each tube of the Z1-MASURCA zone the fission rates were measured at the following nine positions :



In the tubes of the Z1-SNEAK zone the fission rates were measured in five positions :



The positions of the chambers were accurate to 0.1 mm. In each case the fission rates were registered on line.

The measured fission rates are plotted on the fig. 10 to 17 where one can see also the polynomials which were adjusted on the experimental distributions. Axially one can see (Fig. 11 and 13) that there is a local perturbation in the distributions of the U 238 and Np 237 fission rates. This perturbation is due to the caps of the rodlets (total thickness : 6 mm). Radially one can see the fine structure of the Z1-MASURCA cell which is emphasized by the fission chambers with threshold characteristics (see Fig. 15 and 17).

#### IV.2. G.F.K. calculations

In the axial as well as in the radial measurements the immediate vicinity of the chambers contained practically only structural material. So the heterogeneity model shown in Fig. 18 loses its validity and the assumption was made that the measurements should be best represented by simple two dimensional homogeneous diffusion calculations. Fig. 19, 20 and 21 show the measured and calculated results for the normalized axial fission rate traverses per atom of U 235, U 238 and Pu 239. It turns out that the results of these calculations performed with 26 groups in (r, z) geometry using the MOXTOT set agree well with the measured rates in spite of the fact that  $k_{eff}$  was not strictly equal to 1 in the rate calculations. The same is true for the radial fission rate traverse of U 238 shown in Fig. 22 though the simple diffusion calculation is of course not able to represent the fine structure due to the cells.

#### IV.3. Experimental buckling evaluation

The experimental value of the material buckling of the Z1 MASURCA zone has been deduced from the fission rate traverses according to the method used at CADARACHE (see ref. [5]).

One must mention two particular points :

- Axially the polynomial adjustment was made with a polynomial of the following form :

$$A_0 + A_1 X^2 + A_2 X^4 + A_3 X^6$$

The expansion was limited to the degree 6 because of the loss of points in the U 238 and Np 237 traverses due to the local perturbation of the caps.

- Radially the fine structure which appears in the Np 237 and U 238 fission rate traverses has been smoothed observing that this fine structure had exactly the periodicity of the MASURCA-cell and that the radial distribution could be assumed to be of the form :

$$T(r) = f(r) [1 + g(r)]$$

where  $f(r)$  is the macroscopic distribution to which the polynomial expansion is

adjusted and  $g(r)$  is a periodic function, representing the fine structure, evaluated numerically.

The calculated traverses used for the regression (see ref. [5] for more details) were evaluated with the following approximations :

- diffusion, two dimensional (r,z) calculations with cross-sections taking into account the heterogeneity of the core cells (see Fig. 18 for the model used to describe the Z1-MASURCA cell);
- the detector material is assumed to be infinitely dilute.

The experimental results are then :

$$\begin{aligned} \text{Axial component of } B_m^2 : \quad & \alpha = 2.444 \quad \text{m}^{-1} \\ & \frac{\delta\alpha}{\alpha} = 0.13 \cdot 10^{-2} \\ & \alpha^2 = 5.974 \quad \text{m}^{-2} \end{aligned}$$

$$\begin{aligned} \text{Radial component of } B_m^2 : \quad & \beta = 3.003 \quad \text{m}^{-1} \\ & \frac{\delta\beta}{\beta} = 0.56 \cdot 10^{-2} \\ & \beta^2 = 9,018 \quad \text{m}^{-2} \end{aligned}$$

$$\begin{aligned} \text{Material Buckling : } B_m^2 &= \alpha^2 + \beta^2 \\ B_m^2 &= 14.99 \pm 0,12 \quad \text{m}^{-2} \end{aligned}$$

In the following table the experimental value is compared to the values found by cell calculation using the MOXTOT-set and the CADARACHE-set. The cell calculation was performed with ZERA code at Karlsruhe (see ref. [6]) and the HETAÏRE code at Cadarache (see ref. [7]).

$B_m^2 \quad (\text{m}^{-2})$	HOMOG.	HETEROG.	$\frac{E - C_{\text{HET}}}{C_{\text{HET}}}$
G.F.K.calculat.	14.429*	15.137	-0.9 %
CADARACHE calculat.	15.07	15.47	-3.1 %
EXPERIMENT	14.99 ± 0,12		

\* This value corresponds to the quasi-homogeneous section defined in chapter II.

One can notice that the G.F.K. heterogeneous calculation agrees quite well with the experimental value for this core. The discrepancy between the CADARACHE heterogeneous value and the experimental result is of the same order of magnitude as in the other cores of the same range (R1 - R2 - Z2).

The heterogeneous bucklings calculated at Cadarache and Karlsruhe differ by 2.1 % and this discrepancy is the sum of two effects :

a/ an effect due to the different sets used in Karlsruhe and Cadarache;

b/ a slight difference between the geometrical models used in cell-calculations performed in both places as it can be seen from Fig. 18.

In fact the second effect is negligible : calculations performed in Cadarache show that the difference between the two cell-models affects the calculated  $Bm^2$  only by 0.4 %.

The main discrepancy, coming from the sets themselves may be attributed for one part to the different evaluation of the difference production-absorption term :

$$\Sigma^+ = \nu\Sigma_f - \Sigma_a$$

and for another part to the different evaluation of the diffusion coefficient D. This is summarized in the following table, where  $\Sigma^+$ ,  $\nu\Sigma_f$ ,  $\Sigma_a$ , D are flux weighted energy averaged values.

One can see from that table that the main discrepancy is due to the  $\nu\Sigma_f - \Sigma_a$  term (3 %).

		$Bm^2 = \frac{\Sigma^+}{D}$ cm <sup>-2</sup>	D cm	$\Sigma^+ = \nu\Sigma_f - \Sigma_a$ cm <sup>-1</sup>
G.F.K. CALCULATIONS	HETERO (1)	15.137.10 <sup>-4</sup>	1.7504	26.50. 10 <sup>-4</sup>
	HOMO (2)	14.429.10 <sup>-4</sup>	1.7162	24.763.10 <sup>-4</sup>
	$\frac{(1) - (2)}{(2)}$	5 %	2 %	7 %
CADARACHE CALCULATION	HETERO (3)	15.47.10 <sup>-4</sup>	1.7654	27.313.10 <sup>-4</sup>
	HOMO (4)	15.07.10 <sup>-4</sup>	1.7414	26.183.10 <sup>-4</sup>
	$\frac{(3) - (4)}{(4)}$	2.8 %	1.4 %	4.2 %
<u>CAD. - G F K</u> CAD	$\frac{(3) - (1)}{(3)}$	+2.2 %	+0.8 %	3 %

#### IV.4. Reflector savings

From the axial component  $\alpha^2$  of the material buckling, one can deduce the reflect savings of the blanket by the well know relation :

$$\alpha = \frac{\pi}{h + 2 S_2}$$

where h is the core height and  $S_2$  the reflector savings.

This has been done systematically at Cadarache on the R1, R2, Z2 cores built in MASURCA.

The experimental and the calculated values for the reflector savings  $S_z$  of the  $UO_2$ -Na axial blanket covering the Z1-MASURCA zone are :

	EXPER.	CADARACHE CALCUL.	$\frac{E - C}{C}$
$\alpha \text{ cm}^{-1}$	0.02444 $\pm 0.00003$	0.02466	- 0.9 %
$S_z \text{ cm}$	18.5 $\pm 0.1$	18.49	0.4 %

The discrepancy  $\frac{E - C}{C}$  obtains here is of the same order of magnitude than the previous ones observed on the other R-Z cores.

#### IV.5. Axial power distribution

Fig. 23 shown the axial power distribution as evaluated from the experimental traverses or from the calculated ones (at Karlsruhe and Cadarache). Each power traverse was normalized to unity in the center of the core. For the evaluation of the experimental power traverse the rough experimental values of the spectral indices have been used (see section 5.1).

In the G.F.K. calculations, calculated values of homogeneous spectral indices were used while in the Cadarache calculations the rough experimental values were taken.

From Fig. 23 one can see that there is a good agreement between calculated and experimental results in the core region.

In the blanket one can notice that there is a good agreement between the G.F.K. and CADARACHE calculated power traverses and the experimental one. This is partly due to the good agreement between the calculation and the measurement of the U 238 traverse (see Fig. 20 for the G.F.K. U 238 traverse).

At the interface between core and blanket the power values are :

	EXPERIMENT	G.F.K. calculation	CADARACHE calculation	$\frac{E-C}{C}$ G.F.K.	$\frac{E-C}{C}$ CADARACHE
Core boundary	0.47	0.476	0.479	-1.3 %	-1.9 %
Blanket boundary	0.072	0.0716	0.0692	+0.6 %	+4 %

The discrepancies between experimental and Cadarache calculated values of the power at the interface are of the same order of magnitude as the ones observed in others cores of the same kind (built in SNEAK or in MASURCA). These discrepancies are due only to the model (diffusion-approximation) used for the traverse calculations since the same

spectral indices have been used in both experimental and calculated power traverses.

In the G.F.K. evaluation, the discrepancies between calculated and measured indices and the discrepancies due to the model applied to the traverse calculation may compensate each other.

V. - SPECTRAL INDICES AT THE CORE CENTER

The purpose of these measurements is to compare the experimental values of  $\sigma_{f8}/\sigma_{f5}$ ,  $\sigma_{cs}/\sigma_{f5}$ ,  $\sigma_{f3}/\sigma_{f5}$  corresponding to the fundamental mode to the values evaluated by a cell-calculation either with the German sets, MOXTOT and NAPPMB, or with the CADARACHE set.

V.1. Experimental results

V.1.1. Measurements performed

a/ Fission indices

Absolute values of the fission rates were deduced from reaction rate measurements made successively with the CADARACHE fission chambers and with the SNEAK flat fission chambers. Each chamber had been calibrated separately at HARMONIE according to a procedure developed at CADARACHE (see ref. [8]).

One had so the possibility to do an intercomparison between the two types of fission chamber and to check the consistence of the measurements.

These chambers were located in the axial channel built at the place of the ferrit rodlets in a position equivalent to the position 5 (see Fig. 24) of the element 17/20 (see Fig. 2). The values of the spectral indices deduced of the absolute measurements are not directly comparable to the calculated ones in the cell-models of Fig. 18 mainly because of the perturbation due to the channel.

To make them comparable complementary foil measurements were made in positions 1, 2, 3 and 4 (see Fig. 24) in element 18/19 (see Fig. 2) and in a reference position (7) in the channel of element 17/20. In the element 18/19 the 60 and 30 cm fuel rodlets were replaced by 45 cm rodlets so that the foil measurements could be performed in the core midplane.

The rates  $R_k(i)$  resulting from the foil measurements in position  $i$  ( $i = 1, 2, 3, 4$ ) were normalized to the reference measurement  $R_k(7)$  for each isotope  $k$ . In this way one can define the ratio  $\bar{R}_k$  which is given by

$$\bar{R}_k = \frac{\sum_i R_k(i) N_k(i)}{R_k(7) \sum_i N_k(i)}$$

where  $N_k(i)$  is the atom density number of isotope  $k$  per cm length of each fuel rodlet. The final spectral index  $I_{k/5}$  which is comparable to the calculated one will then be :

$$I_{k/5} = \left( \frac{\sigma_f^k}{\sigma_f^5} \right)_{\text{chamber}} \times \frac{\bar{R}_k}{\bar{R}_5}$$

b/ Capture index  $\sigma_{cs}/\sigma_{fs}$

The capture index  $\sigma_{cs}/\sigma_{fs}$  was measured with respect to the value of the same index in the thermal column of HARMONIE.

The final value was obtained in two steps :

— one measured the ratio : 
$$K_1 = \frac{\langle \sigma_{cs} \phi (Z_1) \rangle}{\langle \sigma_{cs} \phi_{th} \rangle}$$

where  $\phi (Z_1)$  is the flux at the position of the foil

and  $\phi_{th}$  the flux in the thermal column;

— then one measured the ratio : 
$$F_1 = \frac{\langle \sigma_{fs} \phi (Z_1) \rangle}{\langle \sigma_{fs} \phi_{th} \rangle}$$

If one admits that the fission cross section  $\sigma_{fs}$  and the capture cross section  $\sigma_{cs}$  are well known in the thermal column, then one can get the value of the index  $\sigma_{cs}/\sigma_{fs}$  in the  $Z_1$  MASURCA zone from the ratio  $K_1/F_1$ . Further details on this method are given in ref. [9].

Depleted U foils (0.43 % U 235) were used to measure  $\langle \sigma_{cs}, \phi(Z_1) \rangle$ ,  $\langle \sigma_{cs}, \phi_{th} \rangle$  and  $\langle \sigma_{fs}, \phi_{th} \rangle$ . Highly enriched foils (93 % U 235) were used to measure  $\langle \sigma_{fs}, \phi(Z_1) \rangle$ .

The foils were disposed in the SNEAK tube 17/20 as it was described hereabove for the fission index measurements.

V.1.2. Experimental corrections to the measured data

Two experimental corrections must be applied to the preliminary rough results to take into account the following effects :

- the size of the detectors which are different in the Pu-rodlets (diameter 12.1 mm) and in the depleted U-rodlets (diameter 12.7 mm). All the results were evaluated by taking 12.1 mm as the reference value;
- the steel thickness (0.1 mm) at the top and bottom of the 45 cm rodlets. (The measurements for evaluating that effect were performed in MASURCA R2, see ref. [10]).

The following table gives the rough experimental results after combination of the values measured in the positions 1, 2, 3, 4 and 7 and the results after correcting for the two effects mentioned above.

Indices	Rough values	Corrected values
$\sigma_c^8/\sigma_f^5$	0.125	0.1251
$\sigma_f^8/\sigma_f^5$	0.0287	0.02911
$\sigma_f^8/\sigma_f^5$	0.99	0.9845

V.1.3. Calculated corrections to the measured data

In order to derive the fundamental mode values from the experimental data the following corrections have been estimated by the usual methods used in Cadarache (see ref. [10]).

- A curvature correction to get the rates corresponding to the center of the core from the measured rates.
- A correction which accounts for the presence of harmonics.
- A correction for the dilution effects : to take into account the difference between the dilutions of chamber and foils on one hand, and between the fuel and the foils on the other hand.

It was found that the influence of the SNEAK tube on the measurements of the U238 fission rate is negligible. This is quite understandable as the distance between the tube and the fuel rodlets is much shorter than the high energy free paths.

In the following table one can compare the final experimental values after all corrections have been applied with the rough results :

Indices	Rough results	Final corrected values	Precision
$\sigma_{f8} / \sigma_{f5}$	0.125	0.125	$\pm 1.2 \%$
$\sigma_{f8} / \sigma_{f5}$	0.0287	0.0293	$\pm 1.7 \%$
$\sigma_{f8} / \sigma_{f5}$	0.99	0.983	$\pm 1.6 \%$

The precisions indicated above include the precision of measurements (and thermal calibration for  $\sigma_{f8}$  and  $\sigma_{c8}$ ) as well as the estimated uncertainties of the calculated corrections.

V.2. Comparison between calculated and measured results

The cell calculations were performed with the ZERA code (see ref. [6]) in Karlsruhe using the MOXTOT and NAPPMB sets according to the cell model shown in Fig. 18. At Cadarache the same type of calculation was performed with the HETAÏRE code (see ref. [7]) using the CADARACHE set and the cell model also shown in Fig. 18. A comparison between the final corrected experimental indices and the calculated ones is given in the following table :

Indices	Final corrected experimental values E	Calc. MOXTOT C	MOXTOT $\frac{E - C}{C}$	Calc. NAPPMB C	NAPPMB $\frac{E - C}{C}$	Calc. CADARACHE C	SETR $\frac{E - C}{C}$
$\sigma_{c8}/\sigma_{f5}$	0.125	0.1265	- 1.2 %	0.1454	-14.0 %	0.1251	-0.1 %
$\sigma_{f8}/\sigma_{f5}$	0.0293	0.02582	+13.5 %	0.02798	+ 4.7 %	0.0275	+6.5 %
$\sigma_{f9}/\sigma_{f5}$	0.983	0.9020	+ 9.0 %	0.9531	+ 3.1 %	0.975	+0.8 %

One can see that the MOXTOT set, evaluated more recently than the NAPPMB set at Karlsruhe, brings only an improvement for the ratio  $\sigma_{c8}/\sigma_{f5}$  with respect to the NAPPMB set. The ratios  $\sigma_{f8}/\sigma_{f5}$  and  $\sigma_{f9}/\sigma_{f5}$  are underestimated by the MOXTOT and NAPPMB set but the discrepancy is particularly large for the MOXTOT set. This tendency has already been observed at other cores like SNEAK-6A/6B (see ref. [1]). The CADARACHE set gives results in good agreement with the measurements for  $\sigma_{c8}/\sigma_{f5}$  and one observes an underestimation of about 6 % for the ratio  $\sigma_{f8}/\sigma_{f5}$ . This discrepancy is similar to the one observed in the previous cores MASURCA-R2,Z2 (see ref. [10]).

VI. - SODIUM VOID

VI.1. Experiments performed

The sodium void effect was measured in the central zone of SNEAK-6D for increasing heights, step by step, beginning at the center :

1. in the four central elements;
2. in the sixteen central elements.

The heights of the voided zones were successively : 10.2 , 50.8 , 71.1 , 91.45 (cm)

The corresponding measured reactivities are given in the tables of the following section VI.2.

VI.2. G.F.K. calculations

All sodium void calculations were performed using twodimensional, first order perturbation theory in (r,z) geometry and heterogeneity corrected MOXTOF cross-sections in the 26 group diffusion approximation. In the following tables one can compare the calculated G.F.K. values with the experimental ones :

a/ 4 central elements voided,  $\beta_{\text{eff}} = 0.00397$

Up to a height H (cm)	Experiment cents	Calculation cents	$\frac{\text{Calculation}}{\text{Experiment}}$
10.2	+0.94	+1.03	1.10
20.0	/	+1.90	/
50.8	+2.97	+2.95	0.99
71.1	+1.84	+1.63	0.89
91.45 (total height)	-1.18	-1.24	1.05

b/ 16 central elements voided,  $\beta_{\text{eff}} = 0.00397$

Up to a height H (cm)	Experiment $\rho$	Calculation $\rho$	$\frac{\text{Calculation}}{\text{Experiment}}$
10.2	+3.41	+3.79	1.11
20.0	/	+7.02	/
50.8	+12.03	+10.61	0.88
71.1	+7.05	+5.23	0.74
91.45 (total height)	/	-6.11	/

The experimental accuracy is here and for all the other reactivity measurements near critical (see chapter VIII) about  $\pm 5\%$  of the absolute reactivity value. This is mainly due to the uncertainty in the calibration of the shim rods, to temperature drifts and to the geometrical reproducibility.

In the case of the sodium voids corresponding to the four central elements it is interesting to notice that the calculated and measured values of the reactivity agree within about 10 %, even in the case of the total height where a change of sign occurs in the reactivity effect. Fig. 25 shows the measured reactivity changes in 6D caused by voiding the four central elements up to a height H. The figure shows also corresponding calculational results for the core 6D using quasihomogeneous (see chapter II) and heterogeneity corrected cross-sections. It is interesting to see that calculation and experiment agree only if heterogeneity corrected cross-sections are used. Because of the few points which were used to sketch the curves of Fig. 25, the curves are supposed to give only a qualitative impression of the sodium void reactivity behaviour.

For the voided zones corresponding to sixteen elements one can observe that the agreement between calculation and experiment becomes worse as the voided zone becomes larger, at least as long as the sodium void effect is positive. Since the fluxes near the center of the core are varying only slightly with respect to the radial direction the void effect with 16 elements should be about a factor of 4 larger than that with 4 elements. Actually one gets :

Height H (cm)	I	II	II/I
	4 x Void in 4 central Elements(cents)	Void in 16 central Elements(cents)	
10.2	+ 3.76	+ 3.41	0.90
50.8	+11.88	+12.03	1.01
71.1	+ 7.36	+ 7.05	0.95

### VI.3. Cadarache calculations

The sodium void-effect was calculated according to two methods :

- a/ The reference method which has been used up to now at Cadarache. A first perturbation calculation is performed by varying the atom density of sodium in the zone under study. The reference calculation has been done twodimensionally in the multigroup diffusion approximation (12 groups). The cross-sections used are only corrected for the influence of heterogeneity on the resonant selfshielding.
- b/ A new method, similar to the G.F.K. procedure, is tested at present. It uses also first order perturbation, however the cross-sections used take into account the complete heterogeneity of the undisturbed and disturbed (voided) media. Only the central void was obtained by this method, using a zerodimensional diffusion-approximation in 25 groups.

The results obtained for the larger central sodium void (16 elements, H = 10.2 cm) related to the experimental value are the following ones :

	With method a/	With method b/
$\frac{C}{E}$	1.67	1.5

Evaluating the sodium void for the four central elements the calculational and experimental traverses were separately normalized to one on the central value. All calculations were only performed using method a/. The results are shown in the following table :

H (cm)	10.2	50.8	71.1	91.4
$\frac{C}{E}$	1.00	1.17	1.78	-1.96

#### VI.4. Conclusions

The G.F.K. calculations are closer to the experimental results than those of Cadarache. It may be mentioned that the overestimation of the central value observed at Cadarache is higher than the one which is usually obtained on MASURCA cores (30 %).

The good prediction of the reactivity variation versus core height (in the case of four elements) by the G.F.K. calculations must be emphasized. One should however notice that the REMO correction, which is rather important in calculating a sodium void effect, has not yet been included in the G.F.K. calculations presented here.

For the Cadarache evaluation of the axial traverse the calculations performed up to now are not satisfactory. Method b/ - 2 dimensions, heterogeneity corrected cross-sections and 25 groups - is just tested. A better evaluation is expected.

## VII. - AXIAL $\gamma$ -HEATING TRAVERSE

$\gamma$ -radiation produces fluorescent centers in silver activated phosphorescent glasses. The density of the fluorescent centers is a quantity which is proportional to the  $\gamma$ -radiation which was absorbed by the glasses. By excitation with UV-light the fluorescent radiation of the centers is emitted and can be measured with a photomultiplier. The connection between the  $\gamma$ -energy absorbed and the intensity of the fluorescent radiation is established by means of  $\gamma$ -sources with known intensities. Using the well known ratio of the average  $\gamma$ -absorption coefficients of steel and glass the  $\gamma$ -heating in steel can be calculated by measuring the intensity of the fluorescent radiation.

Beside of that the  $\gamma$ -radiation there is also a small contribution of neutrons to the generation of fluorescent centers. For calculating the  $\gamma$ -heating the fluorescent intensity has to be corrected for this contribution. To perform the correction the neutron-sensitivity of the glasses and the neutron flux in the position of the detector must be known. The neutron-sensitivity was measured with fast neutrons, with an accuracy of about 40 %.

In SNEAK-6D the central, axial  $\gamma$ -heating traverse was measured. The glass-dosimeters with the dimensions 8 x 8 x 4.7 mm were placed inside the element in position (17/20) (see Fig. 2). They were irradiated over a period of 50 minutes at a reactor power of 350 watt.

The neutron fluxes at the different detector positions which were needed to correct for the contribution of the neutrons were found by extrapolating the U 235 fission rate, measured in the center of the element in position (13/14), by means of calculated radial and axial traverses. To get an estimation of the neutron flux from the fission rate a calculated neutron spectrum was used. The contribution of the neutrons to the total effect is for the core about 3 % and for the blanket about 12 %. Therefore the uncertainty in the neutron sensitivity of 40 % affects the calculated  $\gamma$ -heating only by about 1.2 % and 4.8 % respectively. Fig. 26 shows the corrected  $\gamma$ -heating traverse. The total experimental error is for the core region about 6 % and for the blanket about 12 %. The ratio of  $\gamma$ -heating over fission rate is approximately constant in the core as well as in the blanket (see Fig. 27).

## VIII. - CONTROL ROD EXPERIMENTS

The experimental program devoted to control rods was designed by the French team and had the particular purpose to provide important additional information to the systematic studies performed in the  $R_2$  and  $R_1$  cores built in MASURCA (see ref. [11]), with respect to two points :

### — shut down reactivity analysis -

The first goal was to measure the relative values of various absorbers or diluents for a given size of the rods under study, and of various sections of the rods for a given absorber or diluent. These control rod experiments included the study of rods whose section was close to the PHENIX rod cross-section ( $140 \text{ cm}^2$ ). Another goal was to get the absolute values of the shut down reactivities independently of the  $\beta_{\text{eff}}$  value.

### — power distribution -

One wanted to measure the power distribution perturbation due to the rods.

The G.F.K. team could derive from these experiments complementary information to that obtained from the SNEAK 2C and SNEAK 6A control rod experiments (see ref. [12] and [13]), which were aimed at proper predictions for the control rods of the S.N.R.

### VIII.1. Shut down reactivity of the various rods

#### VIII.1.1. Measurements performed

The studied rods contained either diluent materials : Na - Al - stainless steel, or absorbers :  $B_4C$  - Ta, and were of various sizes.

The French side was particularly interested in the consideration of fully inserted rods in the center of the core as a first step of comparison between measurements and calculations.

In order to preserve symmetry the upper and lower axial blankets were kept free of diluent. In case of absorbers, the part of the rods located in the upper blanket was filled with  $B_4C$  for safety reasons. The experimental characteristics of the rods are summarized in the following table :

Nature of diluent or of absorber	Number of SNEAK tubes loaded	Cross section of the rods built $\text{cm}^2$	Loading of the part of the rod located in lower blanket	Loading of the part of the rod located in upper blanket
Na	1	29.59	$\text{UO}_2\text{-Na}$	$\text{UO}_2\text{-Na}$
Na	4	118.37	$\text{UO}_2\text{-Na}$	$\text{UO}_2\text{-Na}$
Al	4	118.37	$\text{UO}_2\text{-Na}$	$\text{UO}_2\text{-Na}$
S. Steel	4	118.37	$\text{UO}_2\text{-Na}$	$\text{UO}_2\text{-Na}$
Ta	4	118.37	$\text{UO}_2\text{-Na}$	$\text{B}_4\text{C}$
$\text{B}_4\text{C}$	1	29.59	$\text{UO}_2\text{-Na}$	$\text{B}_4\text{C}$
$\text{B}_4\text{C}$	4	118.37	$\text{UO}_2\text{-Na}$	$\text{B}_4\text{C}$

The following types of loading were used :

- a/ The sodium rod inserted in the core was made of one or four SNEAK tubes filled with MASURCA sodium rodlets.
- b/ The aluminium rod was built with four SNEAK tubes in which there were aluminium matrices filled with aluminium rodlets.
- c/ The tantalum rod was built with four SNEAK tubes containing aluminium matrices filled with tantalum rodlets (see sketch in table 6).
- d/ The boron carbide rods (1 or 4 SNEAK tubes) were made with SNEAK  $\text{B}_4\text{C}$  boxes. The enrichment of  $\text{B}_4\text{C}$  was 20 % in atoms of  $\text{B}_{10}$ .
- e/ The stainless steel rod was loaded with steel blocks of 2.5 cm height.

The atom densities of all the rods are given in table 5.

The reactivities were measured according to the SNEAK procedure :

- for measuring small reactivities sufficient edge elements were loaded to be as close as possible to criticality and so that the remaining reactivity change could be measured with the aid of calibrated shim rods;
- large reactivities were measured by summing up small reactivity changes measured in the above way.

The shim rods were recalibrated each time an important number (20 or more) of edge elements was added.

The edge elements ( $R_1$ -type) were added so as to keep the core shape as cylindrical as possible. All measured reactivities have an accuracy of approximately  $\pm 5\%$  on their absolute values.

The rods were studied from lower to higher values of shut down reactivities, i.e. in the following order :

1 Na - 4 Na - 4 Al - 4 S. Steel - 1 B<sub>2</sub>C - 4 Ta - 4 B<sub>4</sub>C

This has been done in several steps which are given in table 6, where one finds the measured reactivity in cents corresponding to each step with respect to the previous one.

VIII.1.2. G.F.K. evaluation

The evaluation of the control rod experiments was performed with the diffusion approximation (26 groups) in (r,z) geometry using the MOXTOT set with homogeneous cross-sections. In the calculations the shim and safety rods of SNEAK were supposed to occupy their normal position (fuel inserted in the core) and smeared over their respective zones (see "k<sub>eff</sub> atom densities" in table 1).

The following table contains the steps considered in the calculations and their respective calculated k<sub>eff</sub> values. In addition to these k<sub>eff</sub>, the delayed neutron fraction, β<sub>eff</sub>, was also calculated for each step in order to be able to convert the calculated reactivity Δk to cents with as realistic β<sub>eff</sub> values as possible, and in order to get an information on the variation of this quantity with changing rod configurations and increasing core size.

Core configuration		k <sub>eff</sub>	β <sub>eff</sub>	$\frac{(\beta_{eff})}{397.34-5}$
Rod inserted at the center of the core	Number of edge elements added to the clean critical core			
Clean critical core	5	0.9914/0	399.03-5	1.004
1 Na	5	0.9891/1	400.15-5	1.007
1 Na	19	0.9956/0	404.67-5	1.018
4 Na	19	0.9893/5	407.96-5	1.026
4 Al	19	0.9890/3	407.54-5	1.025
4 Al	25	0.9918/0	409.50-5	1.030
4 S. Steel	25	0.9908/1	409.40-5	1.030
4 S. Steel	25	0.9921/7	410.35-5	1.032
4 S. Steel with B <sub>4</sub> C in upper blanket	28	0.9911/4	410.62-5	1.033
4 S. Steel with B <sub>4</sub> C in upper blanket	31	0.9924/8	411.59-5	1.035
1 B <sub>4</sub> C	31	0.9893/8	411.99-5	1.036
4 Ta	31	0.9777/0	416.83-5	1.049
4 Ta*	101	1.0065/9	438.78-5	1.104
4 B <sub>4</sub> C	101	0.9930/7	445.39-5	1.120

\* This step was not realized in the experiment. The worth of 4 B<sub>4</sub>C elements with respect to 4 Ta elements was measured with subcritical method.

From the tabulated  $\beta_{\text{eff}}$  values hereabove, one sees that  $\beta_{\text{eff}}$  does not only increase with the increasing number of radial core elements but also with the increasing shut down reactivity of the central control rod, even though the first effect dominates. The latter effect is attributed to the fact that the control rod "displaces" the flux from the center towards the outer uranium zone. With respect to the clean critical core the maximum increase of  $\beta_{\text{eff}}$  is about 12 % in the case of 101  $R_1$  elements added and 4  $B_4C$  elements at the core center.

The calculated reactivity difference between two steps, expressed in cents, results from the difference between two  $k_{\text{eff}}$  values divided by the  $\beta_{\text{eff}}$  corresponding to the final core type. Through combination of such reactivity differences one gets the control rod worths which are shown in the table below. This table gives also the corresponding experimental results and the discrepancies  $\frac{E-C}{C}$  between calculated and measured reactivities. The reference core is here the clean critical core with five additional edge elements.

Type of measurement	Experimental result	Calculated result	$\frac{E-C}{C}$
1 Na → Reference core	-52.3 ¢	-57.2 ¢	-8.6 %
4 Na → Reference core	-197.7 ¢	-210.4 ¢	-6 %
4 Al → Reference core	-210.9 ¢	-218.3 ¢	-3.4 %
4 SS → Reference core	-234.2 ¢	-242.5 ¢	-3.4 %
4 SS <sup>(+)</sup> → Reference core	-258.0 ¢	-267.6 ¢	-3.6 %
4 SS <sup>(+)</sup> → 4 SS	-23.8 ¢	-25.1 ¢	-5.2 %
1 $B_4C$ <sup>(+)</sup> → Reference core	-316.1 ¢	-342.8 ¢	-7.8 %
1 $B_4C$ <sup>(+)</sup> → 1 Na	-263.8 ¢	-285.6 ¢	-7.6 %
4 Ta'' <sup>(+)</sup> → Reference core	-552.7 ¢	} -623.0 ¢	-11.3 %
4 Ta <sup>(+)</sup> → Reference core	-546.3 ¢		-12.3 %
4 Ta'' <sup>(+)</sup> → 4 Al	-341.8 ¢	} -404.7 ¢	-15.5 %
4 Ta <sup>(+)</sup> → 4 Al	-335.4 ¢		-17.1 %
4 $B_4C$ <sup>(+)</sup> → Reference core	-898.4 ¢	-926.5 ¢	-3.0 %
4 $B_4C$ <sup>(+)</sup> → 4 Na	-700.7 ¢	-716.1 ¢	-2.2 %

(+) The part of the central rod located in the upper blanket is filled with  $B_4C$ .

In a somewhat detailed form the same results are repeated in table 7.

It should be noted that the reactivity with respect to reference core of the light materials such as Na, Al, S.Steel is fairly well calculated (to a few percent) in comparison with SNEAK 6A. Detailed examinations showed that this improvement in the analytical results is due little to the transition from 4 energy-groups (6A) to 26 groups

(6D) but rather to the presence of the axial breeder blanket over the diluent rods in SNEAK 6D which creates a lower leakage at the position of these rods.

In SNEAK 6A an important leakage is due to the fact that the rod was filled with diluent even in the upper axial blanket.

The numerical accuracy of the  $k_{\text{eff}}$  calculations is about  $5 \cdot 10^{-5}$  : using the smallest  $\beta_{\text{eff}}$  value of  $399 \cdot 10^{-5}$ , a maximum numerical error of  $\pm 2,5 \%$  for the calculated results is found for that source of uncertainty.

#### Complementary G.F.K. calculations

A number of complementary calculations were made in order to make the comparison possible between the SNEAK 6D results and previous results obtained on the control rod experiments performed in a very similar way in SNEAK 6A and SNEAK 2C (see ref. [12]).

These complementary evaluations are described in ref. [13] to which one should therefore refer for full details.

In the following only the topics of the complementary calculations on SNEAK 6D are briefly summarized :

- The cases studied hereabove with the 2D (r,z) model were recalculated with the 2D (X,Y) and with the 3D (XY/Z synthesis) models.
- The most typical cases of the 26 groups study were recalculated with 4 groups, with both cross section sets NAP and MOXTOT.

This allow a methodical study of :

- a/ the use of the (r,z), (X,Y) and (XY,Z) geometrical models;
- b/ the condensation effect (from 26 groups to 4 groups).

#### a/ Geometrical models

The (X,Y) results are as satisfactory as it could be expected from such an approximate model : in particular the reactivity changes with respect to the reference core due to insertion of absorbers are well predicted. In the case of diluent materials (Na, Al, S. Steel) for which the axial neutron leakage plays an important role, the (X,Y) model is not able to reproduce correctly the experimental result, even when energy- and space-dependent buckling values extracted of (r,z) calculations are used.

The comparison of (r,z) and (X,Y/Z) results indicates a general increase of the calculated reactivity change from (r,z) to (X,Y/Z) by 1 to 5 %. This discrepancy is however mostly explained by the use of only one trial function in the synthesis for saving computer time. Other such comparisons, made namely in SNEAK 6A, indicate a discrepancy smaller than 2 %.

#### b/ Condensation effect

Already investigated for SNEAK 2C (see ref. [12]). The condensation effects are again

small, when adequate precautions concerning the condensation spectra are taken.

For SNEAK 6D, whatever the geometrical model may be, the largest effect due to condensation from 26 to 4 groups on reactivity changes is smaller than 3 % for the diluent material, and smaller than 1 % for the absorbers.

### VIII.1.3. Cadarache calculations

The SNEAK 6D control rod experiments were calculated with the same method that the one used for the previous control rod experiments performed in the  $R_2$  and  $R_1$  MASURCA cores, though the experimental method used in SNEAK differs slightly of the procedure used in MASURCA.

In order to avoid as much as possible the inaccuracies in reactivity comparisons which are due to conversion of  $\Delta k$  in cents, one calculates for each studied rod the difference between the critical radius with the rod inserted and the critical radius of the clean core. This calculated difference is then compared with the one deduced of the experimental radii.

#### VIII.1.3.1. Experimental radii

In the SNEAK 6D measurements a slight correction must be applied to the experimental radii obtained by cylinderisation since in each case the final adjustment to  $k_{eff} = 1$  was obtained by moving the shim rods.

To determine this correction one first deduces for each rod from the measured value  $\delta\rho$  of an edge element in cents the ratio  $\frac{\delta R}{\delta\rho}$ . It is possible then to transform the reactivity of the shim rods in an equivalent radius correction.

The following table gives the radii  $R_0$  corresponding to the cylinderisation, the correction  $r$  which has been applied to each value to take into account the insertion of the shim rods and the final values of the critical radii. The reference core is here the clean critical core.

Case	$R_0$ cm (cylinderised)	$r$ cm	$R_{ex}$ (Final value) cm	$\Delta R_{exp} = \begin{cases} R_{ex} \text{ (rod)} \\ R_{ex} \text{ (ref.)} \end{cases}$ cm
Reference	58.957	-0.083	58.874	0
1 Na	59.355	-0.072	59.283	0.409
1 $B_4C$	61.460	-0.030	61.430	2.556
4 Na	60.456	-0.038	60.418	1.544
4 Al	60.456	+0.090	60.546	1.672
4 SS	60.767	-0.073	60.694	1.82
4 Ta	63.496	-0.073	63.423	4.549
4 $B_4C$	66.538	-0.069	66.469	7.595

VIII.1.3.2. Calculated radii

The calculated critical radii are evaluated with the diffusion approximation (25 groups) by two dimensional calculations in (r,z) geometry with the CADARACHE cross-section set.

For each multiplying core medium the heterogeneous cross-sections were used. The rods and the blankets were supposed to be homogeneous media, and their cross-sections were weighted using a standard spectrum (see ref. [11]).

As it will be explained in more detail hereafter the transport effect is the only correction which was brought to these calculated critical radii. It was assumed here that the cylinderisation did not affect significantly the calculated results.

The following table gives the values of the critical radii  $R_D$  obtained for each of the rods inserted in the core center, and the corresponding variation  $\Delta R_D$  with respect to the reference value of the clean critical core. One will find also the associated experimental values  $R_{ex}$  and  $\Delta R_{exp}$ .

Case	EXPERIMENT		CALCULATION (Diffusion, (R,Z))	
	$R_{ex}$ cm	$\Delta R_{ex}$ cm	$R_D$ cm	$\Delta R_D$ cm
Ref. (no rod ins.)	58.874	0	59.2055	0
1 Na	59.283	0.409	59.8075	0.602
1 B <sub>4</sub> C	61.430	2.556	62.2211	3.016
4 Na	60.418	1.544	61.1554	1.950
4 Al	60.546	1.672	61.2587	2.053
4 SS	60.694	1.820	61.3655	2.160
4 Ta	63.423	4.549	64.8079	5.602
4 B <sub>4</sub> C	66.469	7.595	67.8	8.594

Transport correction

To take directly into account the transport effect one would have to calculate the various critical radii with a two dimensional transport code, thus getting the radius variation :

$$\Delta R_T = R_T (\text{rod}) - R_T (\text{ref})$$

where  $R_T (\text{rod})$  and  $R_T (\text{ref})$  are respectively the critical radii calculated with each rod and without the rod under consideration.

In fact one has calculated, in multigroup diffusion approximation :

$$\Delta R_D = R_D(\text{rod}) - R_D(\text{ref})$$

$\Delta R_T$  may be deduced from  $\Delta R_D$  if one is able to evaluate :

$$\Delta R_T = \Delta R_D + [R_T(\text{rod}) - R_D(\text{rod})] - [R_T(\text{ref}) - R_D(\text{ref})]$$

$$\Delta R_T = \Delta R_D + [\delta R_T(\text{rod}) - \delta R_T(\text{ref})]$$

In this last form, the transport correction which must be applied to  $\Delta R_D$  appears as the difference between the transport effect in the presence of the rod :  $\delta R_T(\text{rod})$  and the transport effect of the reference core :  $\delta R_T(\text{ref})$ .

It appears reasonable that this difference is mainly due to the radial component and therefore can be calculated in one dimension. Since it is calculated as  $\Delta k$  variation, for saving computer time, it is transformed into a radius variation by use of the following parameter :

$$\xi = \frac{\delta K/K}{2 \delta R/R} \quad (\text{see ref. [11]})$$

which has been evaluated for each calculated critical configuration.

The following table gives the transport effects  $\delta K$  evaluated in each case ( $S_4$ ), the corrections  $C_T$  to apply to the radius variations calculated with the diffusion approximation, the corrected radius variations  $\Delta R_C$ , and the percentage to which the transport corrections amount :

Case	Transport correction $\Delta K(\text{rod}) - \Delta K(\text{ref})$ pcm ( $10^{-5} \Delta K/K$ )	$C_T = \frac{\delta R_T(\text{rod})}{\delta R_T(\text{ref})}$ cm	$\Delta R_C$ cm	$\frac{C_T}{\Delta R_D}$
Reference clean critical	-	-	-	-
1 Na	-4	0.008	0.610	1.3 %
1 B <sub>4</sub> C	+9	-0.018	2.9986	0.6 %
4 Na	-2	0.004	1.954	0.3 %
4 Al	-1	0.002	2.055	0.1 %
4 SS	+9	-0.018	2.142	0.8 %
4 Ta	+21	-0.045	5.557	0.8 %
4 B <sub>4</sub> C	+82	-0.18	8.414	2.1 %

One should notice that this is less than 1 % in most cases, excepted for the 1 Na rod where it is 1.3 % and for the 4 B<sub>4</sub>C rod where it is 2 %.

VIII.1.3.3. Comparison between experimental and calculated results

A - Comparison of relatives values

The aim of this comparison is to see how the calculation estimates :

a/ the effect of increasing the rod size for a given diluent (Na) or absorber ( $B_4C$ );

b/ the effect, for a given size (4 SNEAK tubes), of changing the nature of the diluent or absorber.

— Influence of the rod size —

The following table gives the measured and calculated ratios of the radius variations obtained for the  $B_4C$  and the Na rods.

	EXP.	CALC.	$\frac{E - C}{C}$
$\frac{4 B_4C}{1 B_4C}$	2.971	2.806	6 %
$\frac{4 Na}{1 Na}$	3.775	3.203	18 %

One notices that the discrepancy between calculation and experiment is particularly high in the case of the diluent Na.

This seems to indicate that the procedure of calculation is not well suited to evaluate the diluent effect.

— Influence of nature of the absorber (or diluent)

For a given size of the rod, here 4 SNEAK tubes, calculated and measured relative variations of the radius are shown in the table below. The reference chosen here is the 4  $B_4C$ -rod.

	EXPERIMENT	CALCULATION	$\frac{E - C}{C}$
4 Na/4 $B_4C$	0.203	0.232	-12.5 %
4 Al/4 $B_4C$	0.220	0.244	-9.8 %
4 SS/4 $B_4C$	0.240	0.254	-5.5 %
4 Ta/4 $B_4C$	0.599	0.660	-9.2 %

One should mention that the discrepancy between calculation and experiment for the Na case is of the same order of magnitude as those which have been observed in similar cores before ( $R_1 - R_2$  built in MASURCA). The stainless steel, whose worth

relative to boron seems to be rather well predicted here, showed larger discrepancies in the MASURCA cores  $R_1$  and  $R_2$

B - Comparison of absolute values

In the following table the calculated variations of critical radii are given for each rod and are compared with the measured ones :

Rod	EXPERIMENT $\Delta R_{exp}$ cm	CALCULATION $\Delta R_C$ cm	$\frac{E - C}{C}$
1 Na	0.409	0.610	-33 %
1 $B_4C$	2.556	2.998	-15 %
4 Na	1.544	1.954	-24 %
4 Al	1.672	2.055	-19 %
4 S.S.	1.820	2.142	-15 %
4 Ta	4.549	5.557	-18 %
4 $B_4C$	7.595	8.414	-9.7 %

The discrepancies observed between measured and calculate  $\Delta R$  for the diluent rods (Na - Al - S. Steel) are of the same order of magnitude as the ones observed on other cores of the same family. This confirms that the procedure choosen to calculate these rods is not adequate.

In the case of tantalum it appears that the discrepancy observed, which is close to the one observed on the  $R_1$  MASURCA core, could be due to the tantalum cross-sections.

In case of 1  $B_4C$  the calculated value differs by 15 % from the measured one : this is quite an unusual discrepancy which was never observed before in uranium cores. This particular disagreement between calculation and experiment is now under investigation.

VIII.1.4. Comparison between the G.F.K. and CADARACHE analysis

Though the analysis methods used by G.F.K. and CADARACHE are somewhat different, some conclusions may be drawn from comparing the results given above for each analysis.

However, before looking at the discrepancies  $\frac{E - C}{C}$  obtained at KARLSRUHE and at CADARACHE, it is necessary to evaluate the uncertainty which must be applied to each  $\frac{E - C}{C}$  value to be able to draw a significant conclusion from the disagreement.

In the Cadarache evaluation one directly compares measured and calculated critical radii. Uncertainties arise only from the following corrections which must be applied:

- The experimental critical radius has to be corrected for the partial insertion of the shim rods. This correction has an uncertainty of about 15 %. This is due to the error of  $\pm 5\%$  in reactivities measured by calibrated rods and to the uncertainty in the worth of an edge element.
- The error in the calculated critical radius results mainly from the transport correction which was an uncertainty of about 25 % due to the S4 approximation used and to the conversion of reactivity to radius variation using the parameter

$$\xi = \frac{\Delta K/K}{2 \Delta R/R} \quad (\text{see ref. [11]})$$

The following table gives the uncertainties affecting the experimental and calculated values and the uncertainties which must be applied to the  $\frac{E-C}{C}$  values.

Rod	EXPERIMENT $\Delta R_{\text{exp}}$ cm	CALCULATION $\Delta R_{\text{T}}$ cm	$\frac{E-C}{C}$ %
1 Na	$0.409 \pm 0.023$	$0.610 \pm 0.002$	$-33 \pm 5.7$
1 B <sub>4</sub> C	$2.556 \pm 0.017$	$2.998 \pm 0.005$	$-15 \pm 0.7$
4 Na	$1.544 \pm 0.018$	$1.954 \pm 0.001$	$-24 \pm 1.2$
4 Al	$1.672 \pm 0.026$	$2.055 \pm 0.001$	$-19 \pm 1.6$
4 S. Steel	$1.820 \pm 0.023$	$2.142 \pm 0.005$	$-15 \pm 1.3$
4 Ta	$4.549 \pm 0.023$	$5.557 \pm 0.011$	$-18 \pm 0.54$
4 B <sub>4</sub> C	$7.595 \pm 0.02$	$8.414 \pm 0.045$	$-9.7 \pm 0.6$

In the G.F.K. analysis the uncertainties on the measured reactivities are  $\pm 5\%$ , and the uncertainty on the calculated values is estimated to be  $\pm 15\%$ , the main part of which is due to the uncertainty on the  $\beta_{\text{eff}}$  which is used to convert  $\Delta K$  to cents.

This latter error should therefore be of a systematic nature, there is, it should be of the same magnitude and direction for all reactivities measured.

Then if one compares calculated and measured relative values (i.e. with respect to a given absorber or diluent or with respect to a given size) the uncertainty over  $\frac{E-C}{C}$  comes only from the error on the measured values. If one compares calculated and measured absolute reactivities in cents, the uncertainty over  $\frac{E-C}{C}$  is mainly due to the uncertainty applied to  $\beta_{\text{eff}}$ .

The following list gives a survey over the discrepancies  $\frac{E-C}{C}$  evaluated at KARLSRUHE and at CADARACHE.

Rod	$\left(\frac{E-C}{C}\right)$ CADARACHE %	$\left(\frac{E-C}{C}\right)$ KARLSRUHE %	
		Relative values	Absolute values
1 Na	$-33 \pm 5.7$	$-8.6 \pm 5$	$-8.6 \pm 15$
1 B <sub>4</sub> C	$-15 \pm 0.7$	$-7.8 \pm 5$	$-7.8 \pm 15$
4 Na	$-24 \pm 1.2$	$-6 \pm 5$	$-6 \pm 15$
4 Al	$-19 \pm 1.6$	$-3.4 \pm 5$	$-3.4 \pm 15$
4 SS	$-15 \pm 1.3$	$-3.4 \pm 5$	$-3.4 \pm 15$
4 Ta	$-18 \pm 0.5$	$-12.3 \pm 5$	$-12.3 \pm 15$
4 B <sub>4</sub> C	$-9.7 \pm 0.6$	$-3 \pm 5$	$-3 \pm 15$

The points which may be emphasized are the following :

- The discrepancy between the Cadarache calculation and the experiment is much higher than the discrepancy between the G.F.K. evaluation and the same experiment.
- It is quite worthwhile to compare relative values of measured and calculated effects of the rods seen as a critical radius variation at Cadarache and as a reactivity change at Karlsruhe, since the uncertainty over  $\frac{E-C}{C}$  is then lower than the one concerning the absolute values. This is particularly clear for the Cadarache discrepancies  $\frac{E-C}{C}$  whose uncertainties are quite small.

One can then notice that in each case the calculations overestimate the rod effects on the reactivity.

- For the G.F.K. results, the discrepancies lie within the error quoted, especially if one considers the uncertainties due to the  $\beta_{\text{eff}}$  consideration. Recent investigations (see ref. [14]) show that the accepted value of  $\beta_{\text{eff}}$  may be increased by about 10 % simultaneously with a reduction to about 8 % of its uncertainty. In this case too, the agreement between measurements and G.F.K. calculations would still be quite satisfactory but the general tendency would be then to underestimate the rod effects on reactivity.
- Considering the individual configurations one may state that the effect of Ta is strongly overestimated by calculations of both laboratories.
- For B<sub>4</sub>C and Na the Cadarache calculations show an improvement of the agreement as one goes from 1 to 4 elements (the latter configuration is also more realistic with respect to power reactors).

## VIII.2. - Reaction rates in presence of rods

In the presence of four central elements filled with stainless steel and with  $B_4C$ , radial fission rate measurements U 235 - U 238 - Pu 239 were performed with the SNEAK fission chambers (2.4 cm length, 6 mm diameter) in the  $Z_1$  MASURCA zone with a precision of 3 % for each point.

The U 235 and U 238 relative fission rates within the 4  $B_4C$  and S.Steel rods themselves and the relative capture rates of U 238 through rods and fuel zone were measured with foils with a precision of 5 %. The measurements were made in the core mid-plane.

The main goal of these measurements was to check how the calculation evaluates the radial power distribution in the presence of a rod.

### VIII.2.1. G.F.K. analysis

The measured rates, normalized to a value outside the rod about 8.5 cm off center are indicated by crosses in Fig. 28, 29, 30.

The horizontal length of the bars corresponds to the length of the chamber response or to the size of the foil while the length of the vertical bar shows the experimental error.

The solid curves represent the S8 corrected rates per atom which were calculated in (X,Y) geometry using composition-dependent bucklings in 26 groups. The normalization point for the calculated rates is shifted by about 0.5 cm to the right with respect to the normalization point of the experimental results.

The good agreement between calculation and experiment inside the control rods was brought about by the S8 correction. This correction is negligible outside the rod.

In the calculational model  $10^{16}$  at./cm<sup>3</sup> of U235 and U238 were added to the compositions of the control rods to calculate the rates. This corresponds essentially to infinite dilution or negligible self-shielding which is a reasonable assumption, except for the U 238 capture rate in steel where the self-protection of the foil cannot be neglected. On can account approximately for the real self-protection of the foil by introducing for U 238 in steel an atom-density  $N_g'$  which is defined in the following way :

$$\frac{1}{2 d \cdot N_g} = \frac{\Sigma_t}{N_g'}$$

where  $d$  is the thickness of the foil

$N_g$  is the atom density of U 238 in the foil

$\Sigma_t$  is the total cross-section of steel.

With this atom-density one achieves a rather good agreement between the calculated and measured U 238 capture-rate traverse inside the steel rod. Due to the different self-shielding factors of the rod and of the  $Z_1$  MASURCA zone there appears a discontinuity in the calculated U 238 capture rate traverse at the surface of the rod.

The radial traverses for U 235 (fission) and U 238 (fission and capture) in the presence of the  $4 \text{ B}_4\text{C}$  rod show a minimum in the center of the rod which lies about 30-40 % below the maximum of each respective traverse in the  $Z_1$  MASURCA zone. With a central steel rod the U 238 capture and U 235 fission traverses increase towards the rod center while the U 238 fission traverse is depressed by 40 % with respect to its maximum.

#### VIII.2.2. CADARACHE analysis

The Cadarache analysis was performed from two different points of view for the  $4 \text{ B}_4\text{C}$  and 4 S.Steel rods :

- a/ comparison of the calculated and measured spectral index distributions for  $\sigma_{f_8}/\sigma_{f_5}$  and  $\sigma_{f_9}/\sigma_{f_5}$  : this gives an insight into the spectrum perturbation due to the studied central rods;
- b/ comparison of the calculated and measured relative reaction rate distributions with respect to the clean critical core, to get an information on the power distribution perturbation due to the presence of rods.

#### a/ Spectral indices : $\sigma_{f_8}/\sigma_{f_5}$ and $\sigma_{f_9}/\sigma_{f_5}$

One finds the calculated and measured fission spectral indices in Fig. 31 and 32.

The experimental indices are given with a precision of 1,5 %.

The calculated indices were obtained in multi-group diffusion approximation (25 groups) in (r,z) geometry using heterogeneous cross-sections in the  $Z_1$  MASURCA zone and homogeneous cross-sections for the rods. In the rods the self-shielding of the foils was taken into account.

$\text{B}_4\text{C}$  rod - On can observe that the spectral indices - calculated as well as measured - have a constant value from approximately the middle of the  $Z_1$  M zone (see Fig. 31).

In the rod the calculation overestimates slightly the spectral index  $\sigma_{f_8}/\sigma_{f_5}$  (by about 3 %).

Outside the rod the calculation underestimates the spectral index  $\sigma_{f_8}/\sigma_{f_5}$  by approximately 8 % and the spectral index  $\sigma_{f_9}/\sigma_{f_5}$  by 1 %.

Stainless steel rod (Fig. 32) - The spectrum perturbation due to the rod extends throught the whole  $Z_1$  M region.

In this case the  $\sigma_{f_8}/\sigma_{f_5}$  index is also overestimated in the rod, by about 8-9 %, and underestimated in the  $Z_1$  M region by 10 %.

The spectral index  $\sigma_{f_9}/\sigma_{f_5}$  is underestimated in the  $Z_1$  M region by the calculation by about 1 %.

b/ Reaction rate traverses

To get an estimate of the flux perturbation due to the rods, one compares the relative experimental and calculated radial traverses :  $T_s = \langle \sigma_{fs}, \phi(r) \rangle$ ,  $T_g = \langle \sigma_{fg}, \phi(r) \rangle$ , and  $T_g = \langle \sigma_{fg}, \phi(r) \rangle$  of the clean critical core and of the core with the central rod inserted. All the traverses are normalized in a point located at 21 cm from the core center (where the spectrum perturbation due to the rod has practically vanished).

The rod effect is characterized for each fission rate traverse by the ratio :

$$\frac{T_s(\text{rod}) - T_s(\text{ref})}{T_s(\text{ref})}, \quad \frac{T_g(\text{rod}) - T_g(\text{ref})}{T_g(\text{ref})}, \quad \frac{T_g(\text{rod}) - T_g(\text{ref})}{T_g(\text{ref})}$$

The measured and calculated spatial variation of these quantities are plotted on the Fig. 33, 34, 35, where one can observe the following points :

—  $B_4C$  rod - The flux is strongly depressed at the center of the rod : one can notice a decrease of approximately 40 % for the U 235 fission, and 50 % for the U 238 fission. Although the rod effect on the  $Z_1$  MASURCA spectrum has vanished at the normalization point (Fig. 31), this is not true for the flux perturbation which extends much further into the core.

This is not surprising if one remembers that the reactivity variation due to the rod is close to 4 000 pcm (i.e. 9 \$) according to the G.F.K. evaluation.

In order to get a good comparison with the unperturbed case it would have been necessary to measure the fission rate distribution over the whole radius of the assembly.

The agreement between calculation and experiment is rather good for the U 235 and Pu 239 traverses and this confirms the previous results obtained on the  $R_1$  MASURCA core. On the other hand, the calculation underestimates strongly the high energy flux perturbation (see  $\frac{T_s(\text{rod}) - T_s(\text{ref})}{T_s(\text{ref})}$  Fig. 33) : there is a factor 1.6 at the center of the rod between the experimental and calculated flux depression.

— Stainless steel rod - The flux perturbation due to the rod has practically vanished at the middle of the  $Z_1$  MASURCA zone for the U 235 and Pu 239 traverses, but the high energy flux perturbation extends further (see :  $\frac{T_s(\text{rod}) - T_s(\text{ref})}{T_s(\text{ref})}$  on Fig. 33) though it is much less important than in the case of the  $B_4C$  rod. This is closely related to the fact that the rod effect on the reactivity (approximately 950 pcm or 2 \$) is much lower than the one due to the  $B_4C$  rod.

In this case the perturbation  $\frac{T_s(\text{rod}) - T_s(\text{ref})}{T_s(\text{ref})}$  is not so well predicted by the calculation : this may be partly attributed to the slowing down of neutrons in the steel.

As to the ratio  $\frac{T_s(\text{rod}) - T_s(\text{ref})}{T_s(\text{ref})}$ , one observes that it is overestimated by the calculations, but the discrepancy between calculation and experiment is nevertheless much lower than with the absorber rod (approximately 12 % at the center of the rod).

### CONCLUSION

The close cooperation in fast reactor physics between the laboratories in KARLSRUHE (I.A.R./SNEAK) and CADARACHE (D.P.R.M.A./S.E.C.P.R.), which was started in 1969 with the SNEAK 2A and 2C experiments, was extended to include the study of the  $Z_1$  MASURCA zone built in the SNEAK 6D assembly. This cooperation made the building of a core including approximately 350 kg of plutonium possible (125 kg of MASURCA Pu, 220 kg of SNEAK Pu).

This allowed very useful comparisons concerning the experimental technics as well as the interpretation of the results.

### EXPERIMENTAL TECHNIQS

The common experimental work which was performed by both teams allowed to compare and eventually to check some experimental technics in particular :

- proton recoil spectra measurements;
- fission chamber calibration.

In other cases the cooperation led to the performance of experiments with technical contributions of both laboratories : the  $B_m^2$  measurements were performed by physicists of both teams according to the procedure developed at Cadarache.

For the spectral index measurements the foil detectors were counted in both places (Karlsruhe and Cadarache), a calibration of the U 238 capture - and Pu 239 fission rate was performed in the thermal column of HARMONIE.

### ANALYSIS OF THE RESULTS

The experimental program of SNEAK 6D had two main goals :

a/ to study a number of fundamental cell-parameters in order to check the cross-section sets used in both places. These parameters were :

- the spectra measured with the proton recoil technic;
- $B_m^2$  as derived from rate traverses;
- the spectral indices  $\sigma_{f8}/\sigma_{f5} - \sigma_{f8}/\sigma_{f5} - \sigma_{f9}/\sigma_{f5}$

The agreement of the measured proton recoil spectra with calculation shows an improvement with respect to previous cores using the same diluent (Na). There remains a underestimate of the spectrum between 70 and 180 keV and an overestimate between 15 and 70 keV.

The  $E_m^{\infty}$  values obtained with the MOXTOT and the CADARACHE sets are in good agreement with the experimental result (Karlsruhe :  $\frac{E-C}{C} = 0.9 \%$ , Cadarache  $\frac{E-C}{C} = 3.1 \%$ ).

The analysis of the indices gives more detailed information on the characteristics of the sets : the U 238 fission index is underestimated by both sets (by 13 % with MOXTOT, by 6.5 % with the CADARACHE set).

If the Pu 239 fission index is rather well predicted by the CADARACHE set ( $\frac{E-C}{C} = 0.8\%$ ), it is underestimated by MOXTOT ( $\frac{E-C}{C} = 9 \%$ ). As to the U 238 capture index, well evaluated at Cadarache ( $\frac{E-C}{C} = -0.1 \%$ ), it is slightly overestimated by MOXTOT ( $\frac{E-C}{C} = -1.2 \%$ ).

These results indicate that the breeding ratio would not be well predicted with the present values of  $\sigma_c$  (U 238) and  $\sigma_f$  (Pu 239) of the MOXTOT set. Recent efforts to obtain more satisfactory results comprise an improved experimental program in a Pu-core (SNEAK 9 B) and the introduction of the new G.F.K. cross section set KFK-INR.

b/ to study some project-parameters, in order to complement previous studies on other cores at SNEAK (SNEAK 2A, 2C, 6A, 6B) or at MASURCA (R1 - R2 - Z2).

These project parameters which should give useful information for the SNR and the PHENIX projects are :

- criticality
- axial power distribution
- sodium-void
- $\gamma$ -heating
- worths of control rods and their influence on the power distribution.

In spite of some discrepancies in the correction terms calculated at Karlsruhe and Cadarache, the critical mass is well predicted by the MOXTOT and the CADARACHE sets. The discrepancy between the experimental and calculated  $k_{eff}$  values is about 160 pcm (i.e. 25 cents). From this one may deduce that the sets are rather well suited for criticality calculations for this type of core.

The axial power distribution is well predicted by the calculations of the two teams. This holds also at the core-blanket interface : on the core side of the interface, MOXTOT and the CADARACHE set yield a slight overestimation (1.3 % and 1.9 %) of the power; on the blanket side one observes a more important underestimation (4 %) with the CADARACHE set than with MOXTOT (0.6 %).

The sodium void effect is well predicted by the G.F.K. procedure : the mean discrepancy  $\frac{E-C}{C}$  between calculation and measurement is 10 %, but there is no systematic over- or underestimate of the calculation. The procedure of calculating the sodium void effect has to be improved by the use of the REMO correction (see ref [ 2 ]) which was not included here.

The French predictions with the reference method defined in section VI.3 (including systematically a correction equivalent to the REMO one) are rather far from the measured results : the mean value of the discrepancy  $\frac{E-C}{C}$  is about 40 %. The G.F.K. procedure is now under study at Cadarache.

The  $\gamma$ -heating was analyzed only in Karlsruhe till now. But these measurements will also be analyzed in Cadarache. In fact systematic studies will be performed in the next MASURCA cores.

The analysis of the control rod reactivities was performed on both sides under a slightly different point of view.

The G.F.K. analysis only considers reactivity changes using a calculated  $\beta_{\text{eff}}$  value to convert the  $\Delta k/k$  values into cents.

The Cadarache analysis studies mainly the critical radius variations.

The G.F.K. calculated results are in a rather good agreement (between 3 % and 12 %) with the experimental worths, but there is an important uncertainty (15 %) due to the use of  $\beta_{\text{eff}}$ .

The Cadarache calculated results are rather far from the experimental values (between 10 % and 33 %), with a low uncertainty which makes the discrepancies significant.

Nevertheless some common conclusions arise from the results :

- The tantalum capture cross-sections seem to be too large in both sets.
- The worth of diluent rods is not well predicted by either set. The CADARACHE set yields discrepancies between 24 % and 33 %, for the MOXTOT set they are 6 % to 9 %. Considering the fact that the diluent rods (at least Na and Al) are similar to a voided core region, where streaming effect occurs, one has to investigate if the calculational procedures used are really well adapted to the situation.

Further conclusions which concern the influence of the fuel geometry (U - Pu - Fe rodlets in SNEAK 6D and  $\text{PuO}_2$  -  $\text{UO}_2$  platelets in SNEAK 6A and 6B) on similar measurements are given in ref. [1].

The present report represents an attempt to write for the first time a common report by two teams from laboratories of different countries which have jointly investigated a fast critical assembly. It turned out that certain evaluation procedures were identical and so provided a useful mutual check. On the other side, some evaluation methods were different and no attempt was made to come to an agreement to use a particular method. In such cases the results of both methods are quoted and the methods are explained as well as possible. The authors hope that in this way also the second goal of this common report could be reached : a better understanding of each other's method which could be the base for further improved cooperation of the French and German teams.

REFERENCES

- [1] SNEAK 6A, 6B, 6D      K.F.K. report to be published.
- [2] H. KÜSTERS et al.      K.F.K. report 793 (1968).
- [3] H. WERLE              K.F.K. report INR 4/70-25  
                            ORNL report TR 2415 - 1970.
- [4] A. LERIDON et al. - Spectrométrie par compteurs proportionnels à protons de recul  
                            Note CEA-N 1525.
- [5] G. HUMBERT - Private communication.
- [6] D. WINTZER - "Zur Berechnung von Heterogenitätseffekten in periodischen Zellstruk-  
                            turen Thermischer und Schneller Kernreaktoren"  
                            Report KFK-743 (1969).
- [7] A. KHAIRALLAH, J. RECOLIN - Calcul de l'autoprotection résonnante dans les cal-  
                            culs complexes, par la méthode des sous-groupes.  
                            IAEA - Journées d'études sur les calculs numériques de ré-  
                            acteurs, Vienne 17-21 janvier 1972 - SM 154/37.
- [8] J.L. CAMPAN - Private communication.
- [9] J.P. BRUNET - Private communication.
- [10] J.P. CHAUDAT, G. HUMBERT - Private communication.
- [11] J.Y. BARRE, J. DJABALI, L. GOUTANY - Private communication.
- [12] F. HELM, G. JOURDAN, S. PILATE, H. REICHEL - Physics investigations of sodium  
                            cooled fast reactors : SNEAK-assembly 2 - KFK Report 1399.
- [13] S. PILATE, F. PLUM - Control rod experiments in SNEAK 6A and SNEAK 6D -  
                            KFK Report to be published.
- [14] FISHER, MAC GRATH - Private communication.

LIST OF TABLES

- Table 1 - Atom densities for the clean critical core SNEAK 6D (core zones).
- Table 2 - Atom densities for the clean critical core SNEAK 6D (blankets).
- Table 3 - Experimental and calculated spectra (Karlsruhe).
- Table 4 - SNEAK 6D spectrum measurements (Cadarache).
- Table 5 - Atom densities for the SNEAK 6D control rods.
- Table 6 - Control rod experiments : reactivity changes measured.
- Table 7 - Control rod experiments : comparison between measured and calculated reactivity changes.

LIST OF FIGURES

- Fig. 1 - SNEAK 6D - Axial cut through a quarter of the clean critical core.
- Fig. 2 - SNEAK 6D - Cross section.
- Fig. 3 -  $Z_1$  MASURCA,  $Z_1$  SNEAK,  $R_1$  SNEAK cells.
- Fig. 4 - G.F.K. and Cadarache proton recoil counter disposals.
- Fig. 5 - Neutron spectrum SNEAK 6D : small core (SR in).
- Fig. 6 - Neutron spectrum SNEAK 6D : small core (SR out).
- Fig. 7 - Neutron spectrum SNEAK 6D.
- Fig. 8 - Comparison of measured and calculated spectra.
- Fig. 9 - Spectrum measurements SNEAK 6D : comparison between Cadarache and Karlsruhe.
- Fig. 10 - Experimental axial fission rate traverse for U 235.
- Fig. 11 - Experimental axial fission rate traverse for U 238.
- Fig. 12 - Experimental axial fission rate traverse for Pu 239.
- Fig. 13 - Experimental axial fission rate traverse for Np 237.
- Fig. 14 - Experimental radial fission rate traverse for U 235.
- Fig. 15 - Experimental radial fission rate traverse for U 238.
- Fig. 16 - Experimental radial fission rate traverse for Pu 239.
- Fig. 17 - Experimental radial fission rate traverse for Np 237.
- Fig. 18 - Cell-models for calculating the heterogeneity.
- Fig. 19 - Axial fission rate traverse for U 235.
- Fig. 20 - Axial fission rate traverse for U 238.
- Fig. 21 - Axial fission rate traverse for Pu 239.
- Fig. 22 - Radial fission rate traverse for U 238.
- Fig. 23 - Axial power distribution.
- Fig. 24 - Positions of the detectors for the spectral index measurements.
- Fig. 25 - Experimental reactivity change as a result of voiding four central elements of SNEAK 6D up to a height.
- Fig. 26 - Axial  $\gamma$ -heating traverse in steel at 350 W of reactor power.
- Fig. 27 - Axial  $\gamma$ -heating traverse in steel for fission.
- Fig. 28 - Control rod experiment : fission rate traverse for U 235 normalized to one atom.

Fig. 29 - Control rod experiment : Radial fission rate traverse for U 238 normalized to one atom.

Fig. 30 - Control rod experiment : Radial capture rate traverse for U 238 normalized to one atom.

Fig. 31 - B<sub>4</sub>C rod : Radial distribution of  $\sigma_{f8}/\sigma_{f5}$  and  $\sigma_{c8}/\sigma_{c5}$ .

Fig. 32 - Stainless steel rod : Radial distribution of  $\sigma_{f8}/\sigma_{f5}$  and  $\sigma_{c8}/\sigma_{c5}$ .

Fig. 33 - Influence of the rods on the radial fission rate traverse for U 238.

Fig. 34 - Influence of the rods on the radial fission rate traverse for U 235.

Fig. 35 - Influence of the rods on the radial fission rate traverse for Pu 239.

TABLE 1

ATOM-DENSITIES ( $\times 10^{-24}$ ) FOR THE CLEAN CRITICAL CORE SNEAK 6D

Nuclide	Z1. MASURCA Zone (Z1-M)	Z1. SNEAK Zone (Z1-A)		R1. SNEAK Zone (R <sub>1</sub> )	
	cell-composition	for $k_{eff}$ calculations	cell-composition	for $k_{eff}$ calculations	cell- composition
U 235	$1,6035 \cdot 10^{-5}$	$1,9602 \cdot 10^{-4}$	$4,6372 \cdot 10^{-5}$	$1,8789 \cdot 10^{-3}$	$1,8774 \cdot 10^{-3}$
U 238	$5,9296 \cdot 10^{-3}$	$6,8440 \cdot 10^{-3}$	$6,7860 \cdot 10^{-3}$	$6,5990 \cdot 10^{-3}$	$6,5159 \cdot 10^{-3}$
Pu 239	$1,2104 \cdot 10^{-3}$	$1,1118 \cdot 10^{-3}$	$1,2107 \cdot 10^{-3}$	-	-
Pu 240	$1,1163 \cdot 10^{-4}$	$9,9875 \cdot 10^{-5}$	$1,0876 \cdot 10^{-4}$	-	-
Pu 241	$1,0588 \cdot 10^{-5}$	$9,0765 \cdot 10^{-6}$	$9,8839 \cdot 10^{-6}$	-	-
Pu 242	$1,3180 \cdot 10^{-6}$	$4,5617 \cdot 10^{-7}$	$4,9675 \cdot 10^{-7}$	-	-
Fe	$1,2550 \cdot 10^{-2}$	$1,1830 \cdot 10^{-2}$	$1,1908 \cdot 10^{-2}$	$1,2171 \cdot 10^{-2}$	$1,2386 \cdot 10^{-2}$
Cr	$3,4421 \cdot 10^{-3}$	$3,2289 \cdot 10^{-3}$	$3,2283 \cdot 10^{-3}$	$3,6293 \cdot 10^{-3}$	$3,6953 \cdot 10^{-3}$
Ni	$1,7644 \cdot 10^{-3}$	$2,2252 \cdot 10^{-3}$	$2,2762 \cdot 10^{-3}$	$1,8957 \cdot 10^{-3}$	$1,9210 \cdot 10^{-3}$
Al	-	$5,0112 \cdot 10^{-4}$	$5,3316 \cdot 10^{-5}$	$8,5241 \cdot 10^{-3}$	$8,5301 \cdot 10^{-3}$
O	$1,1599 \cdot 10^{-2}$	$1,1796 \cdot 10^{-2}$	$1,1995 \cdot 10^{-2}$	$5,2213 \cdot 10^{-3}$	$4,8412 \cdot 10^{-3}$
C	-	$2,0976 \cdot 10^{-4}$	$4,9208 \cdot 10^{-5}$	$6,1682 \cdot 10^{-3}$	$6,5227 \cdot 10^{-3}$
Na	$8,8568 \cdot 10^{-3}$	$8,1066 \cdot 10^{-3}$	$8,4797 \cdot 10^{-3}$	$2,8635 \cdot 10^{-3}$	$2,7703 \cdot 10^{-3}$
Si	$4,5325 \cdot 10^{-5}$	$1,5289 \cdot 10^{-4}$	$1,5271 \cdot 10^{-4}$	$2,0091 \cdot 10^{-4}$	$2,0510 \cdot 10^{-4}$
Ti	-	$1,2332 \cdot 10^{-5}$	$9,2277 \cdot 10^{-6}$	$4,0261 \cdot 10^{-5}$	$4,0300 \cdot 10^{-5}$

Note - In this table, Mn has been assimilated to Cr  
 Co has been assimilated to Ni  
 Mg has been assimilated to Al.

TABLE 2

ATOM DENSITIES ( $\times 10^{-24}$ ) FOR THE CLEAN CRITICAL CORE SNEAK 6D

Nuclide	Axial breeder blanket with MASURCA rodlets	Axial breeder blanket with SNEAK platelets	Axial alternate blanket	Radial blanket
U 235	$3,6499.10^{-5}$	$4,9864.10^{-5}$	$5,4978.10^{-5}$	$1,6245.10^{-4}$
U 238	$8,4912.10^{-3}$	$6,8744.10^{-3}$	$8,4617.10^{-3}$	$3,9940.10^{-2}$
Fe	$9,2575.10^{-3}$	$8,9830.10^{-3}$	$1,0191.10^{-2}$	$1,6132.10^{-2}$
Cr	$2,6194.10^{-3}$	$2,6636.10^{-3}$	$3,0584.10^{-3}$	$4,8788.10^{-4}$
Ni	$1,2729.10^{-3}$	$1,4252.10^{-3}$	$1,4466.10^{-3}$	$6,4568.10^{-4}$
Al	—	$3,3669.10^{-3}$	$1,2107.10^{-2}$	$3,0755.10^{-3}$
O	$1,7055.10^{-2}$	$1,3698.10^{-2}$	$1,3079.10^{-2}$	—
C	$1,356.10^{-5}$	$4,6274.10^{-5}$	$4,3201.10^{-5}$	$5,5316.10^{-6}$
Na	$8,8568.10^{-3}$	$6,1963.10^{-3}$	—	—
Si	$4,5330.10^{-5}$	$1,4829.10^{-4}$	$2,3259.10^{-4}$	$2,5295.10^{-5}$
Ti	—	$2,7149.10^{-6}$	$2,3240.10^{-5}$	$3,4640.10^{-7}$

Note : In this table, Mn has been assimilated to Cr  
 Co has been assimilated to Ni  
 Mg has been assimilated to Al.

TABLE 3

EXPERIMENTAL AND CALCULATED SPECTRA (KARLSRUHE)

( $\phi_i$  group fluxes, calculated spectra normalized to experiment between 1,4 - 0,1 MeV)

Core Configuration	$E_i$ MeV	EXPERIMENT	CALCULATION 1 Dim., P <sub>1</sub> , 208 gr		CALCULATION 1 Dim., Diff, 26 gr MOXTOT (+ REMO)	
			$\phi_i$	$\frac{\text{CALC.}}{\text{EXP.}}$	$\phi_i$	$\frac{\text{CALC.}}{\text{EXP.}}$
1 Large core Shut down	1,4 - 0,8	1,03	0,854	0,829	0,89	0,864
	0,8 - 0,4	1,86	1,753	0,942	1,59	0,855
	0,4 - 0,2	1,93	2,065	1,070	2,18	1,129
	0,2 - 0,1	1,89	2,045	1,082	2,04	1,079
	0,1 - 0,0465	1,52	1,642	1,080	1,73	1,138
	0,0465 - 0,0215	0,80	1,170	1,462	1,24	1,55
	0,0215 - 0,010	-	0,703	-	0,76	-
3 Small core Shim rods in	1,4 - 0,8	1,34	1,173	0,875		
	0,8 - 0,4	2,53	2,38	0,94		
	0,4 - 0,2	2,69	2,82	1,05		
	0,2 - 0,1	2,65	2,82	1,06		
	0,1 - 0,0465	2,27	2,28	1,00		
	0,0465 - 0,0215	1,67	1,65	0,99		
	0,0215 - 0,010	0,98	1,00	1,02		
4 Small core 9 shim rods out (B <sub>4</sub> C in the core)	1,4 - 0,8	0,886	0,775	0,875		
	0,8 - 0,4	1,66	1,568	0,945		
	0,4 - 0,2	1,71	1,822	1,065		
	0,2 - 0,1	1,70	1,791	1,053		
	0,1 - 0,0465	1,43	1,433	1,002		
	0,0465 - 0,0215	1,02	1,016	0,996		
	0,0215 - 0,010	0,63	0,607	0,964		
4/3 Small core (S.R. out) Small core (S.R. in)	1,4 - 0,8	0,66	0,66	1,00		
	0,8 - 0,4	0,66	0,66	1,00		
	0,4 - 0,2	0,635	0,65	1,024		
	0,2 - 0,1	0,64	0,635	0,992		
	0,1 - 0,0465	0,63	0,63	1,00		
	0,0465 - 0,0215	0,61	0,62	1,016		
	0,0215 - 0,010	0,64	0,61	0,953		
1/3 Large core (shut down) Small core (S.R. in)	1,4 - 0,8	0,77	0,73	0,948		
	0,8 - 0,4	0,735	0,74	1,007		
	0,4 - 0,2	0,72	0,73	1,014		
	0,2 - 0,1	0,71	0,73	1,028		
	0,1 - 0,0465		0,72			
	0,0465 - 0,0215		0,71			
	0,0215 - 0,010		0,70			

TABLE 4  
SNEAK 6D SPECTRUM MEASUREMENTS

Energy Range MeV	CADARACHE Measurements Configuration 2 ( $k_{eff}$ # 0,98)	KARLSRUHE Measurements Configuration 3 ( $k_{eff}$ # 0,95)	Karlsruhe- Cadache Karlsruhe	KARLSRUHE Measurements corrected for the $k_{eff}$ variation	Karls.(corrected) - Cadache Karlsruhe (corrected)
1,35 -0,82	8,33	8,54	+2,2 %	8,16	-2,1 %
0,82 -0,498	13,01	13,15	+1,1 %	12,95	-0,5 %
0,498 -0,302	11,92	12,93	+7,7 %	12,72	+6,3 %
0,302 -0,183	14,54	14,57	+0,2 %	14,38	-1,1 %
0,183 -0,111	15,59	14,48	-7,7 %	14,54	-7,2 %
0,111 -0,0674	12,72	11,98	-6,2 %	12,15	-4,8 %
0,0674-0,0409	9,55	9,82	+2,8 %	10,02	+4,7 %
0,0409-0,0248	7,74	8,63	+10 %	8,91	+13,1 %
0,0248-0,015	6,60	5,90	-11,8 %	6,16	-6,8 %

All fluxes correspond to 100 neutrons between 15 keV and 1,35 MeV.

TABLE 5

ATOM DENSITIES ( $\times 10^{-24}$ ) FOR THE SNEAK 6D CONTROL RODS

	B <sub>4</sub> C - rod	Ta - rod	Al - rod	SS - rod	MASURCA Na - rod
Al	0.0504-2	2.5868-2	4.3865-2	—	—
C	1.2096-2	0.0029-2	0.0029-2	2.023152-4	1.356164-5
Cr	0.2552-2	0.3505-2	0.3505-2	1.635943-2	2.366883-3
Fe	0.8293-2	1.1789-2	1.1789-2	5.535268-2	8.316323-3
Na	—	—	—	—	1.771355-2
Ni	0.1176-2	0.1633-2	0.1633-2	7.57888 -3	1.148239-3
Si	0.0172-2	0.0365-2	0.0505-2	6.323868-4	4.532545-5
Ti	—	0.0117-2	0.0167-2	2.839825-4	—
B 10	0.9449-2	—	—	—	—
B 11	3.8762-2	—	—	—	—
Ta	—	1.6537-2	—	—	—

Note : In this table Mn has been assimilated to Cr  
 Co has been assimilated to Ni  
 Mg has been assimilated to Al.

TABLE 6

CONTROL ROD EXPERIMENTS : REACTIVITY CHANGES MEASURED

Core configuration	Rod inserted at the core center	Reactivity change with respect to the precedent configuration in cents
1. Clean critical core + 5 Edge elements	—	0.0
2. " + 5 E.E.	1 Na	-52.3
3. " + 19 E.E.	1 Na	+139.8
4. " + 19 E.E.	4 Na	-145.4
5. " + 21 E.E.	4 Na	+16.1
6. " + 19 E.E.	4 Na	-16.0
7. " + 19 E.E.	4 Al	-13.2
8. " + 25 E.E.	4 Al	+56.6
9. " + 25 E.E.	3 Al + 1 SS	-5.7
10. " + 25 E.E.	4 SS	-17.6
11. " + 23 E.E.	4 SS	-16.3
12. " + 28 E.E.	4 SS	+40.9
13. " + 28 E.E.	4 SS <sup>(+)</sup>	-23.8
14. " + 26 E.E.	4 SS <sup>(+)</sup>	-15.3
15. " + 31 E.E.	4 SS <sup>(+)</sup>	+42.8
16. " + 31 E.E.	3 SS <sup>(+)</sup> + 1 B <sub>4</sub> C <sup>(+)</sup>	-220.3 (subcritical measurement)
17. " + 31 E.E.	1 B <sub>4</sub> C <sup>(+)</sup>	+162.2
18. " + 32 E.E.	1 B <sub>4</sub> C <sup>(+)</sup>	+8.8
19. " + 32 E.E.	4 Ta <sup>(+)</sup>	-230.2
20. " + 52 E.E.	4 Ta <sup>(+)</sup>	+181.7
21. " + 57 E.E.	4 Ta <sup>(+)</sup>	+44.9
22. " + 59 E.E.	4 Ta <sup>(+)</sup>	+17.0
23. " + 59 E.E.	4 Ta'' <sup>(+)</sup>	-6.4
24. " + 60 E.E.	4 Ta'' <sup>(+)</sup>	+6.0
25. " + 61 E.E.	4 Ta'' <sup>(+)</sup>	+6.8
26. " + 59 E.E.	4 Ta'' <sup>(+)</sup>	-12.7
27. " + 60 E.E.	4 Ta'' <sup>(+)</sup>	+8.1

.../...

TABLE 6 (continued)

Core configuration	Rod inserted at the core center	Reactivity change with respect to the precedent configuration in cents
28. Clean critical core + 61 E.E.	4 Ta <sup>''</sup> (+)	+7.6
29. " + 62 E.E.	4 Ta <sup>''</sup> (+)	+7.6
30. " + 62 E.E.	4 B <sub>4</sub> C <sup>(+)</sup>	-345.7 (subcritical measurement)
31. " +101 E.E.	4 B <sub>4</sub> C <sup>(+)</sup>	+342.9
32. " +102 E.E.	4 B <sub>4</sub> C <sup>(+)</sup>	+5.2

Note : a) + 5 E.E. means, for example, that 5 Edge Elements were added to the clean critical core configuration.

b) 4 S.S. mean, for example, that the four central elements of the Z1 MASURCA zone were filled with stainless steel blocks over the total core height.

c) 4 Ta<sup>(+)</sup> means, for example, that the four central elements of the Z1 MASURCA zone were filled with the tantalum rodlets inserted in aluminium matrices over the total core height. The part of these tubes corresponding to the upper blanket was filled with B<sub>4</sub>C.

d) 4 Ta and 4 Ta<sup>''</sup> elements have the same homogeneous atom densities, but correspond to two different cells as shown in the following figure :

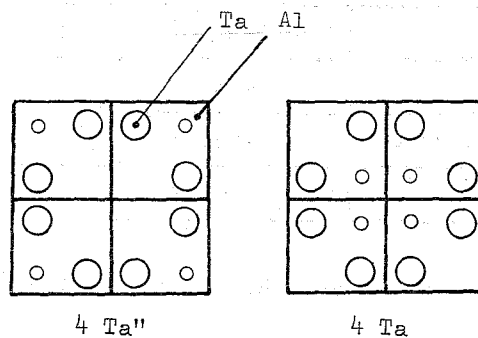


TABLE 7

CONTROL ROD EXPERIMENTS :  
COMPARISON BETWEEN MEASURED AND CALCULATED REACTIVITY CHANGES

Type of measurement	Experiment Reactivity change in cents	Calculation Reactivity change in cents	C/E
1 Na → Reference core	-52.3	-57.2	1.09
4 Na → 1 Na	-145.4	-153.2	1.05
4 Na → Reference core	-197.7	-210.4	1.06
4 Al → 4 Na	-13.2	-7.9	0.59
4 Al → Reference core	-210.9	-218.3	1.03
4 SS → 4 Al	-23.3	-24.2	1.03
4 SS → Reference core	-234.2	-242.5	1.03
4 SS <sup>(+)</sup> → Reference core	-258.0	-267.6	1.03
4 SS <sup>(+)</sup> → 4 SS	-23.8	-25.1	1.05
1 B <sub>4</sub> C <sup>(+)</sup> → 4 SS <sup>(+)</sup>	-58.1	-75.2	1.29
1 B <sub>4</sub> C <sup>(+)</sup> → Reference core	-316.1	-342.8	1.08
1 B <sub>4</sub> C <sup>(+)</sup> → 1 Na	-263.8	-285.6	1.08
4 Ta <sup>(+)</sup> → 1 B <sub>4</sub> C <sup>(+)</sup>	-230.2	-280.2	1.21
4 Ta <sup>(+)</sup> → Reference core	-546.3	-623.0	1.14
4 Ta'' <sup>(+)</sup> → 4 Ta <sup>(+)</sup>	-6.4	-	-
4 Ta'' <sup>(+)</sup> → Reference core	-552.7	-623.0	1.12
4 Ta'' <sup>(+)</sup> → 4 Al	-341.8	-404.7	1.18
4 Ta <sup>(+)</sup> → 4 Al	-335.4	-404.7	1.20
4 B <sub>4</sub> C <sup>(+)</sup> → 4 Ta'' <sup>(+)</sup>	-345.7	-303.5	0.87
4 B <sub>4</sub> C <sup>(+)</sup> → 4 Ta <sup>(+)</sup>	-352.1	-303.5	0.86
4 B <sub>4</sub> C <sup>(+)</sup> → Reference core	-898.4	-926.5	1.03
4 B <sub>4</sub> C <sup>(+)</sup> → 4 Na	-700.7	-716.1	1.02

Note : The Reference core is here the clean critical core with five additional edge elements.

(+) The part of the central rod located in the upper blanket is filled with B<sub>4</sub>C.

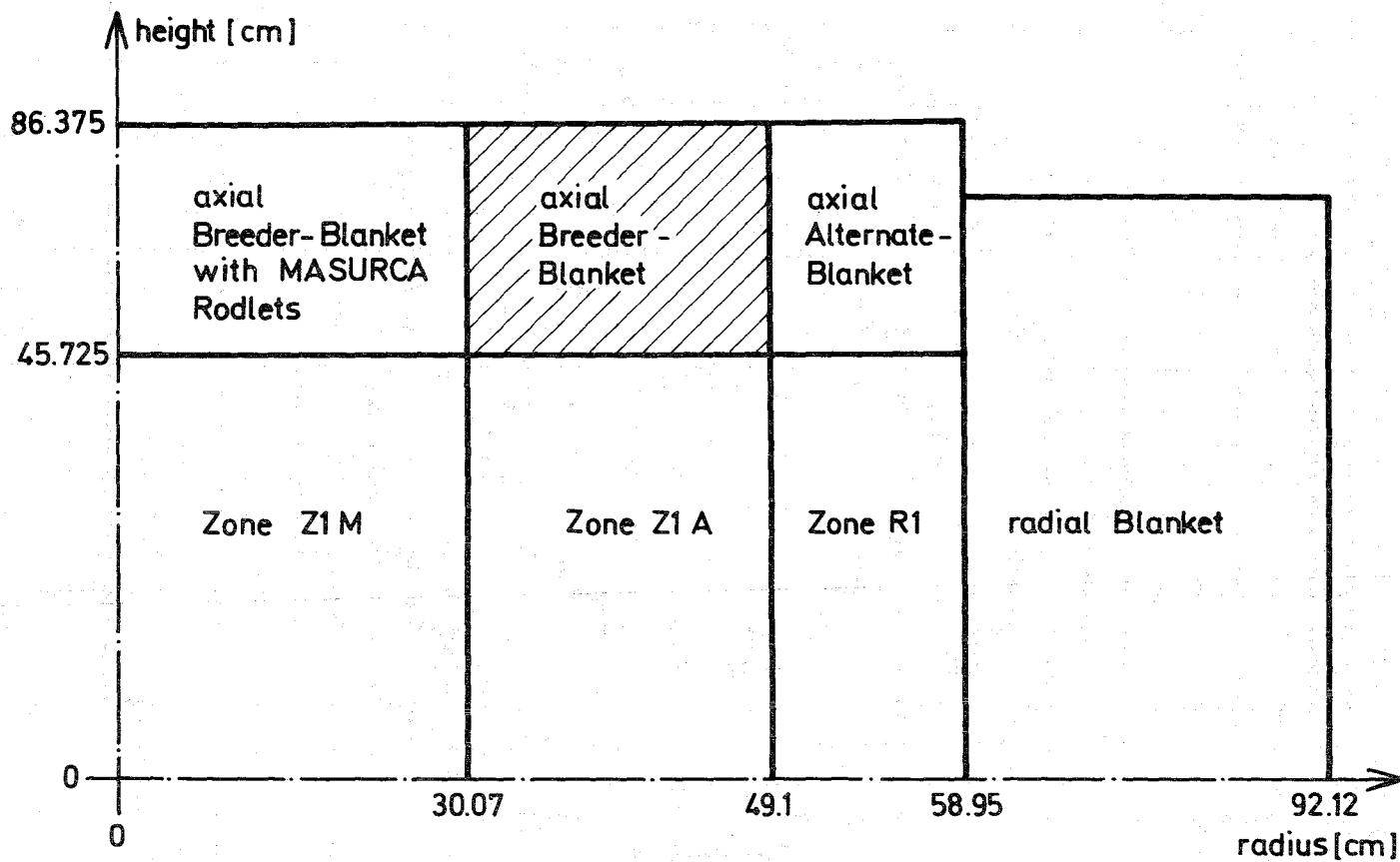


Fig. 1 SNEAK-6D  
 Axial Cut through a Quarter of the "Clean Critical"  
 Core

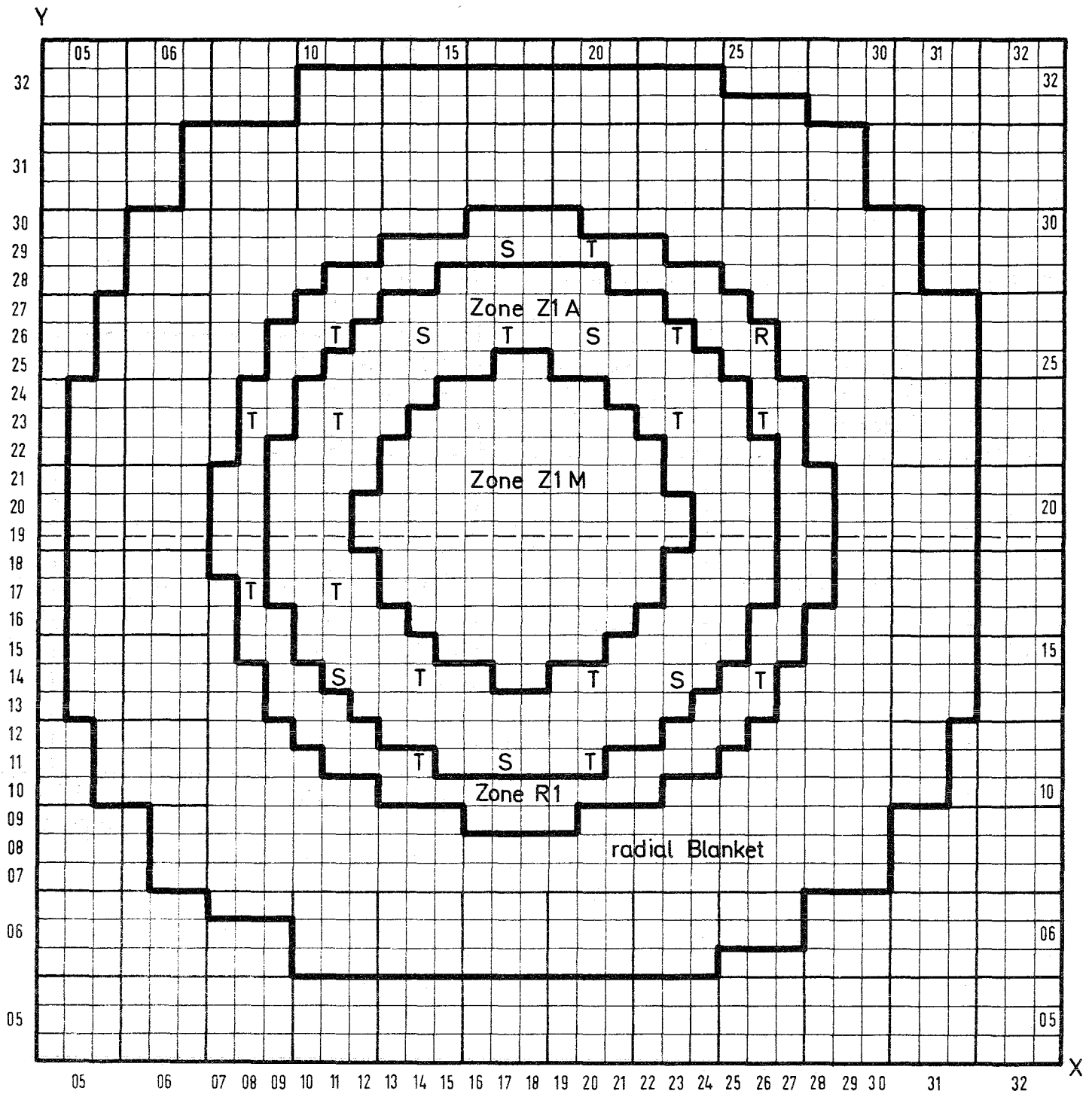
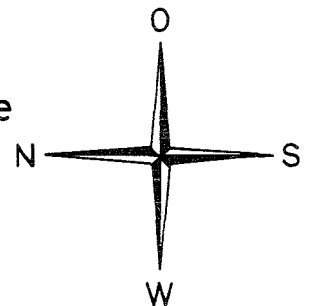


Fig. 2  
SNEAK - 6D Cross Section of the Clean Critical Core

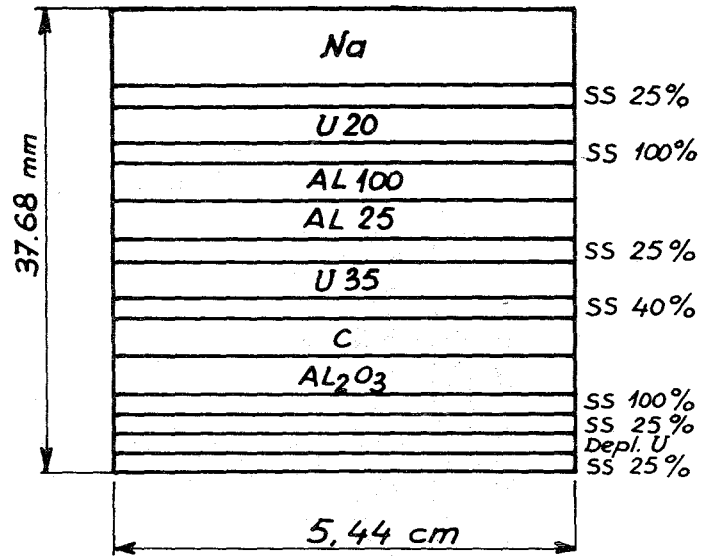
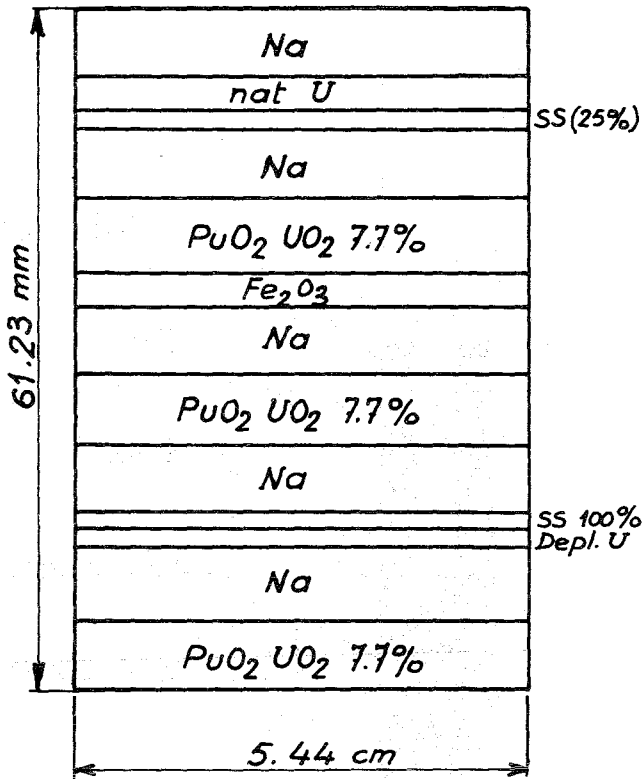
- Zone Z1 M (96 fuel elements )
- Zone Z1 A (147 fuel elements, 8T-rods, 5 S-rods )
- Zone R1 (104 fuel elements, 7T-rods, 1S-rod , 1R-rod )



- S = safety rod
- T = shim rod
- R = regulating rod
- radial chamber traverse

### Z1-SNEAK CELL

### R1-SNEAK CELL



### Z1-MASURCA CELL

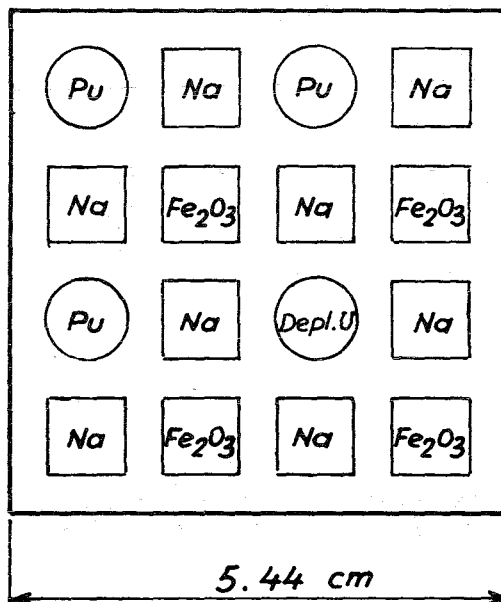
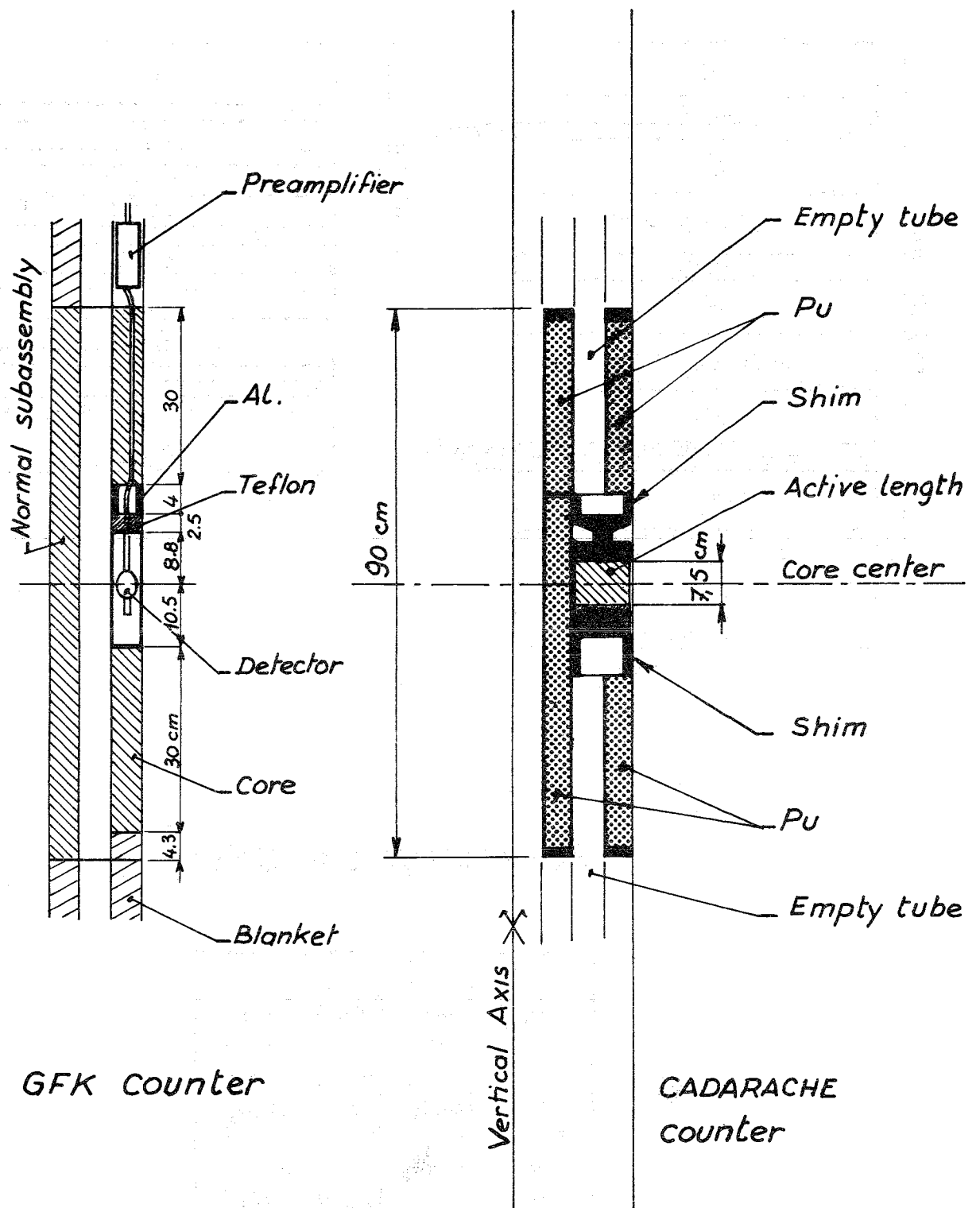


Fig. 3



**COUNTER POSITION**

*Fig. 4*

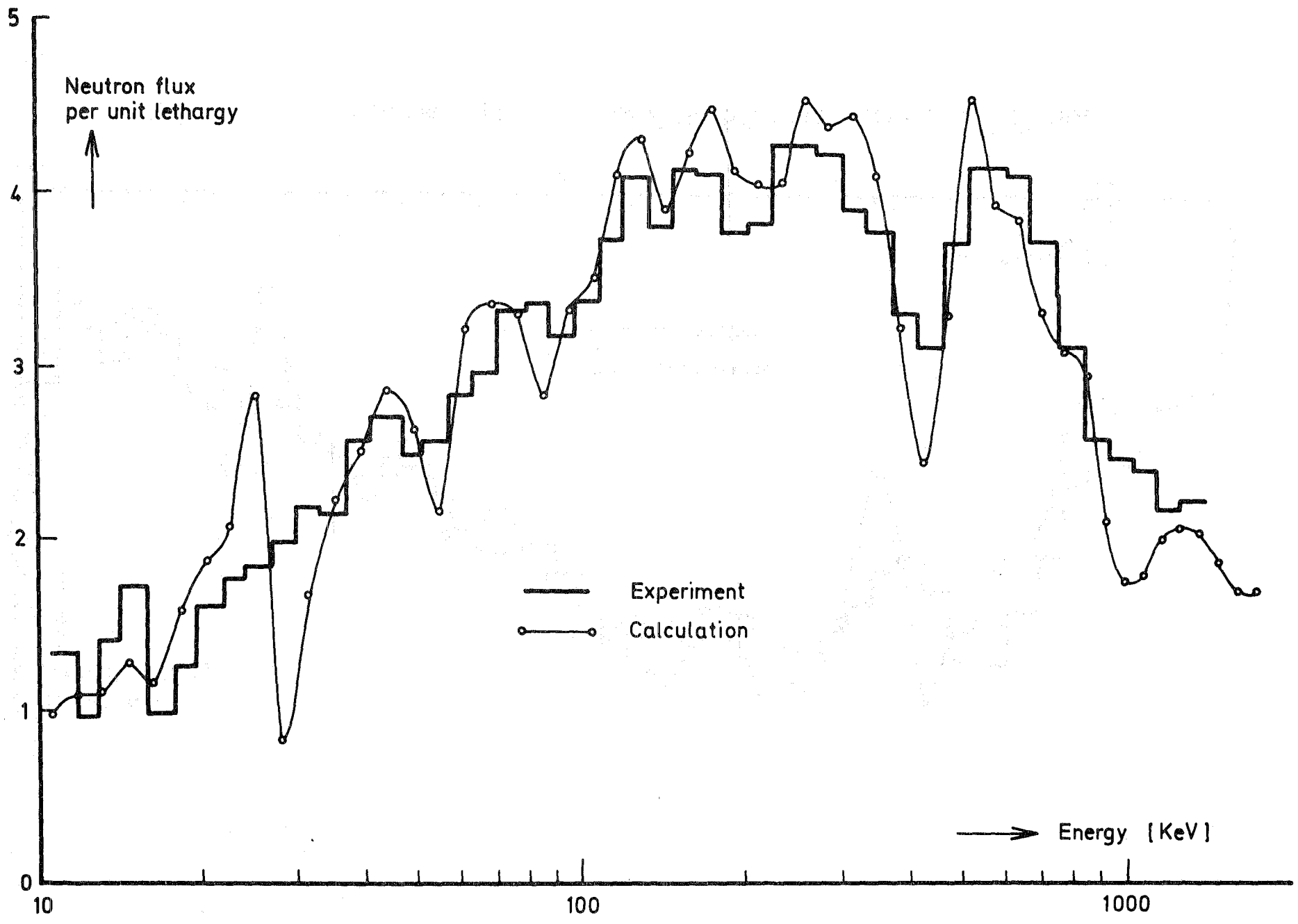


Fig. 5

Neutron Spectrum SNEAK - 6D small Core - 9 SR in

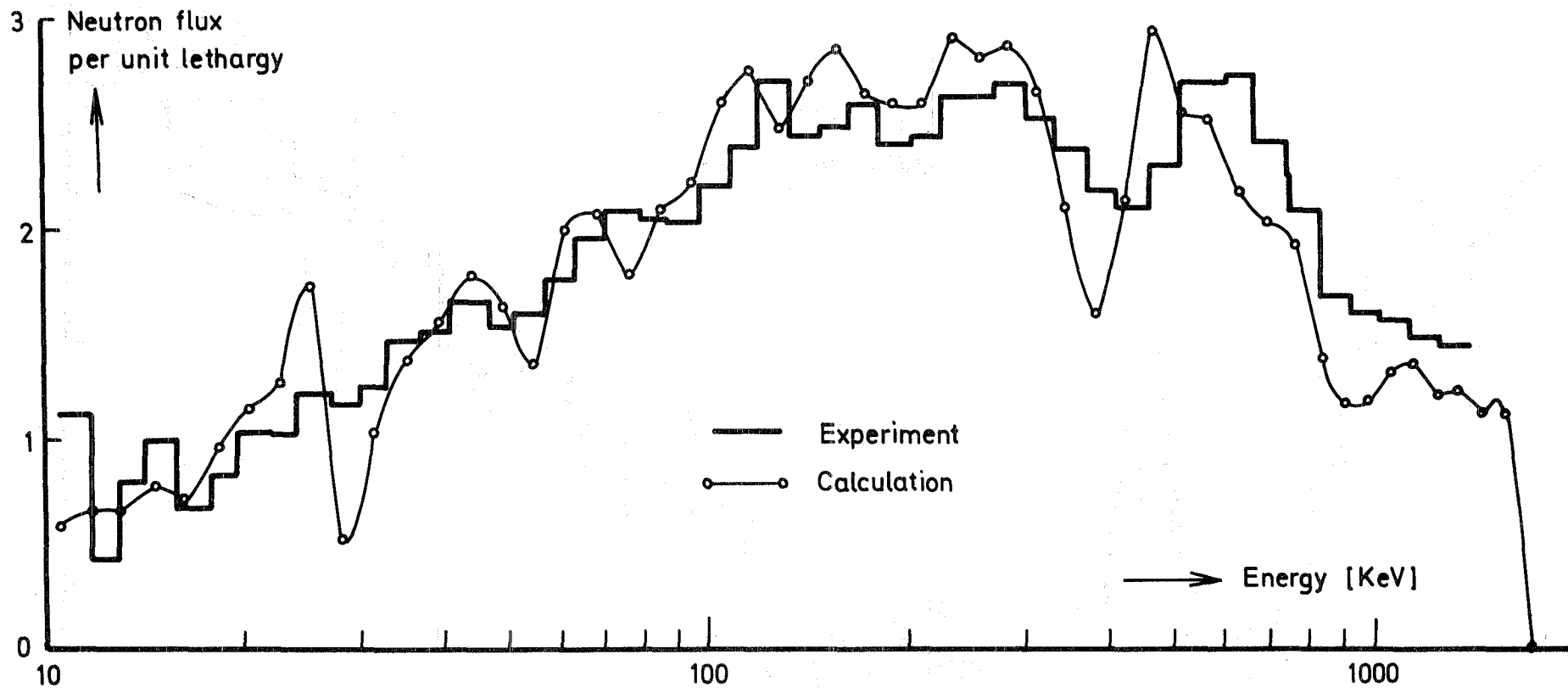
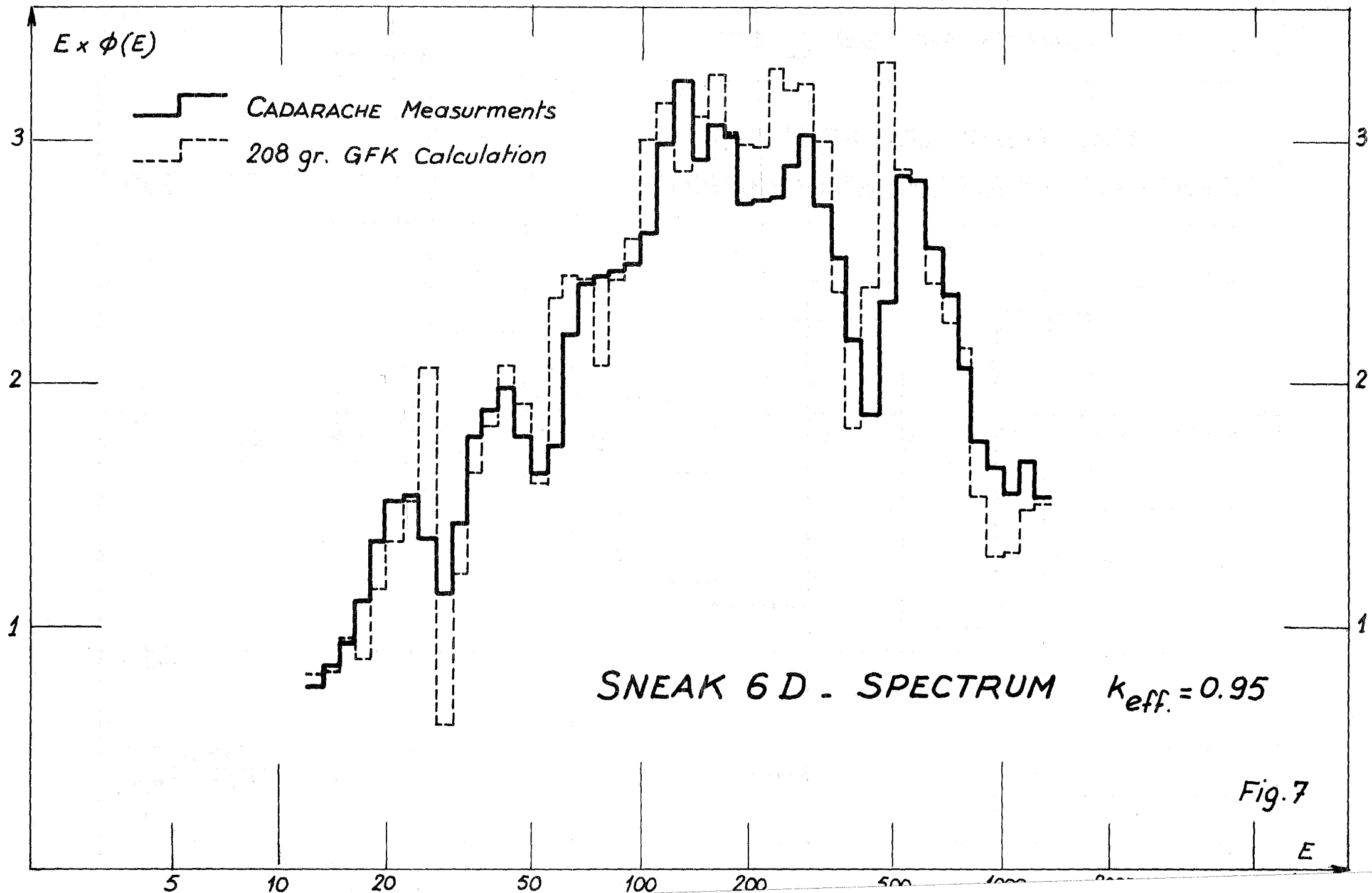


Fig. 6

Neutron Spectrum SNEAK-6D small Core . 9 SR out



$\frac{\text{Meas.} - \text{Calc.}}{\text{Calc.}}$

+10%

9.12

24.8

15.0

40.9

67.4

111

183

302

498

820

1350

E (keV)

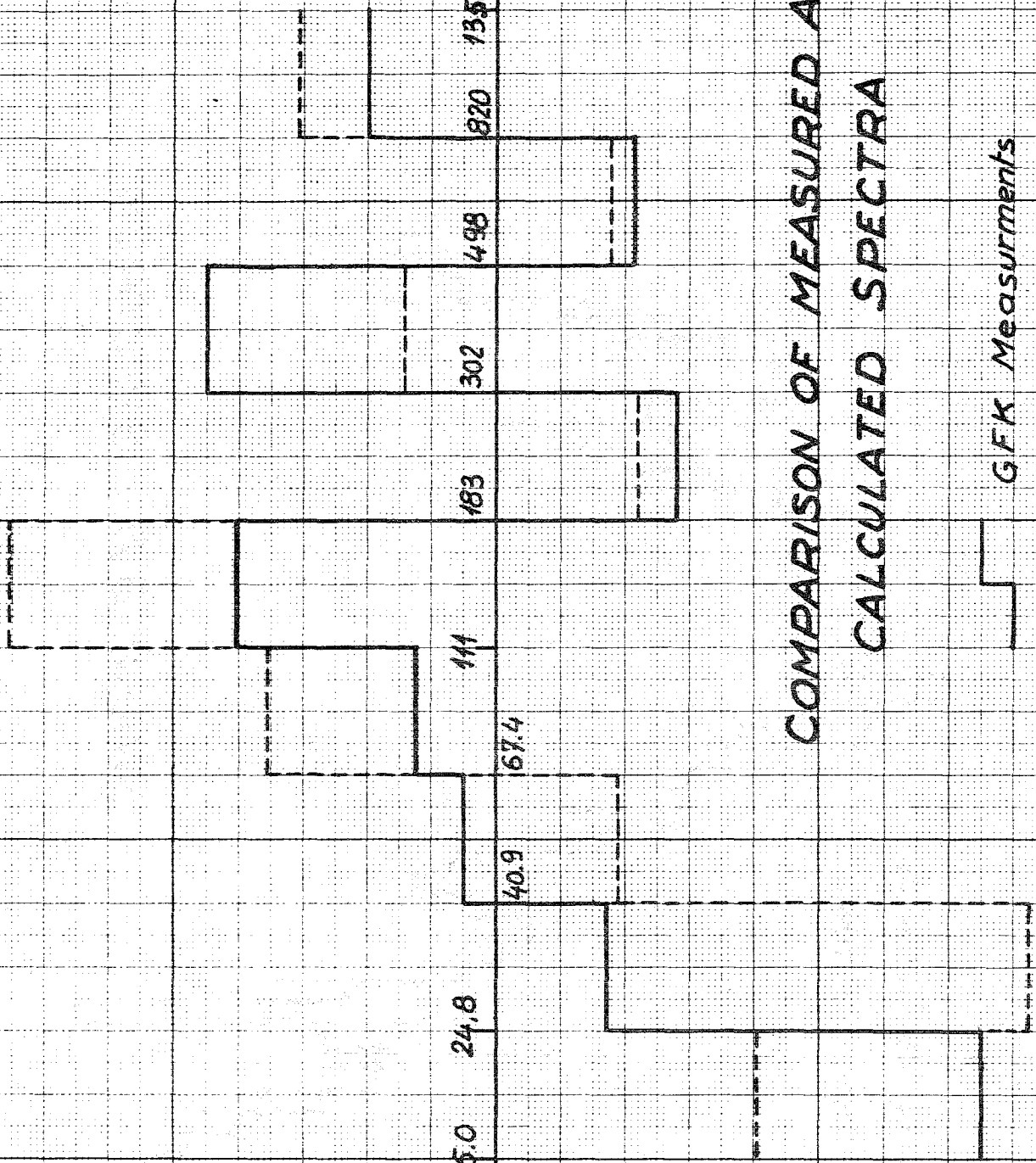
-10%

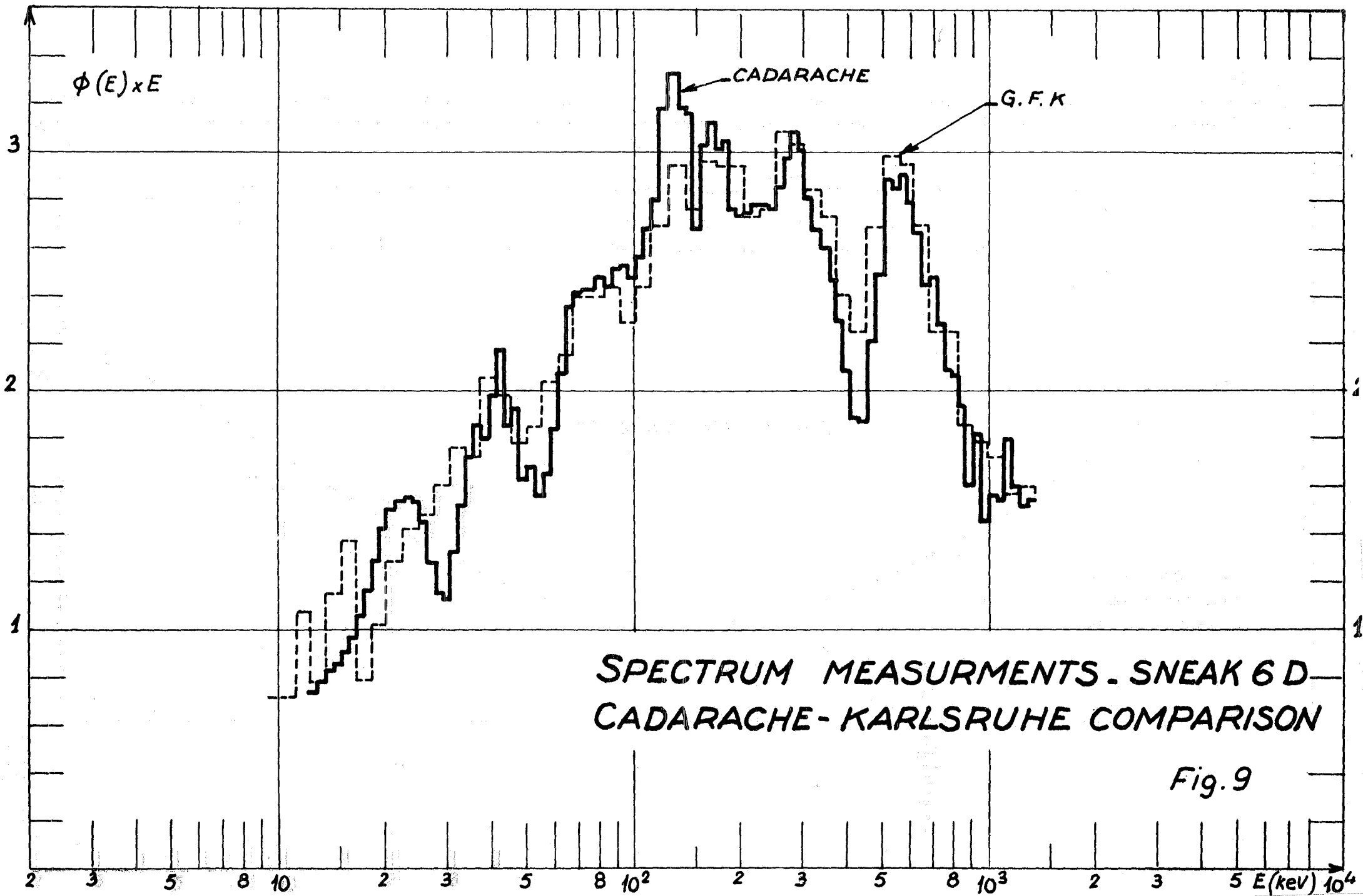
COMPARISON OF MEASURED AND  
CALCULATED SPECTRA

GFK Measurements

CADARACHE Measurements

Fig. 8





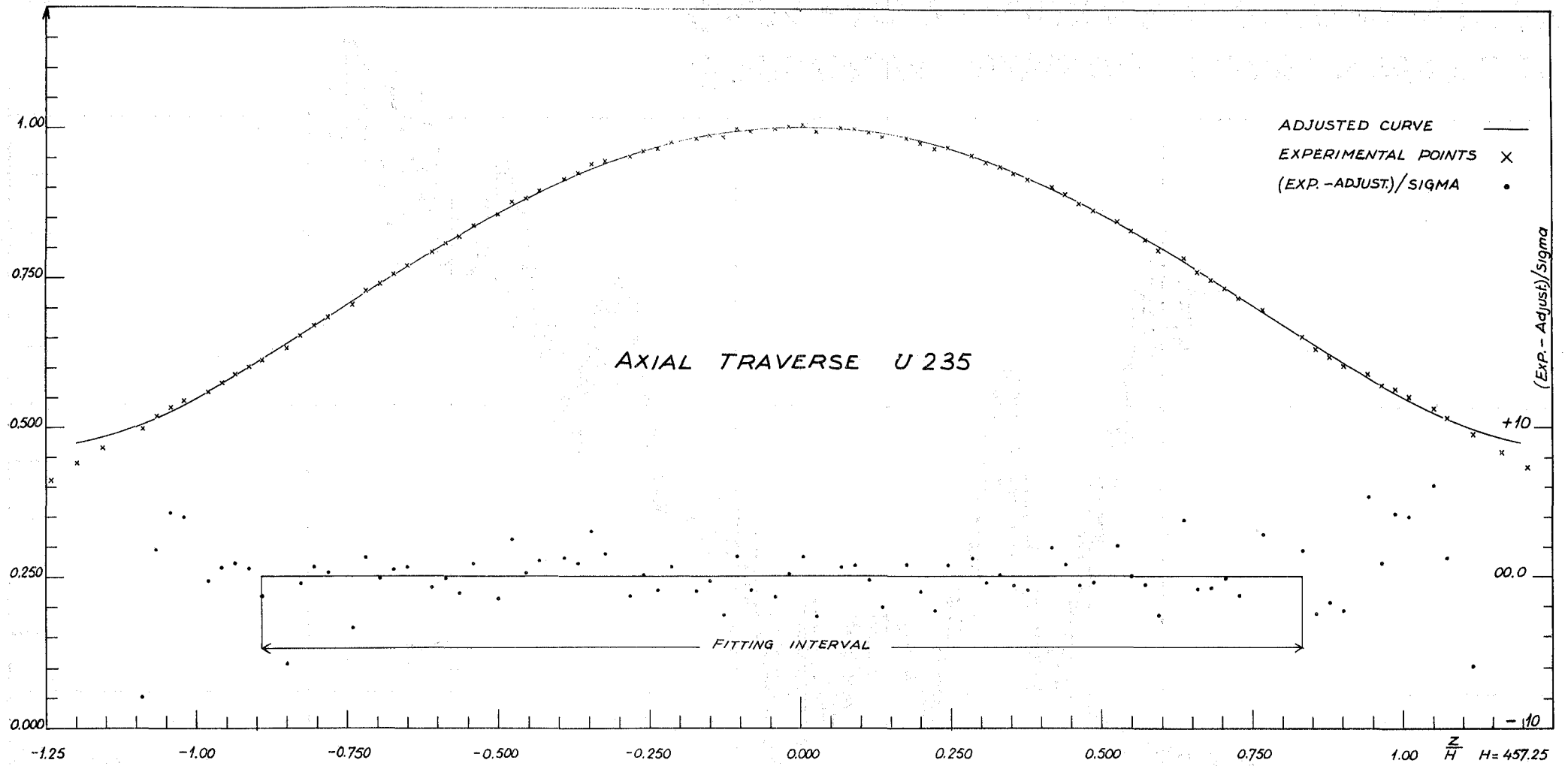


Fig. 10

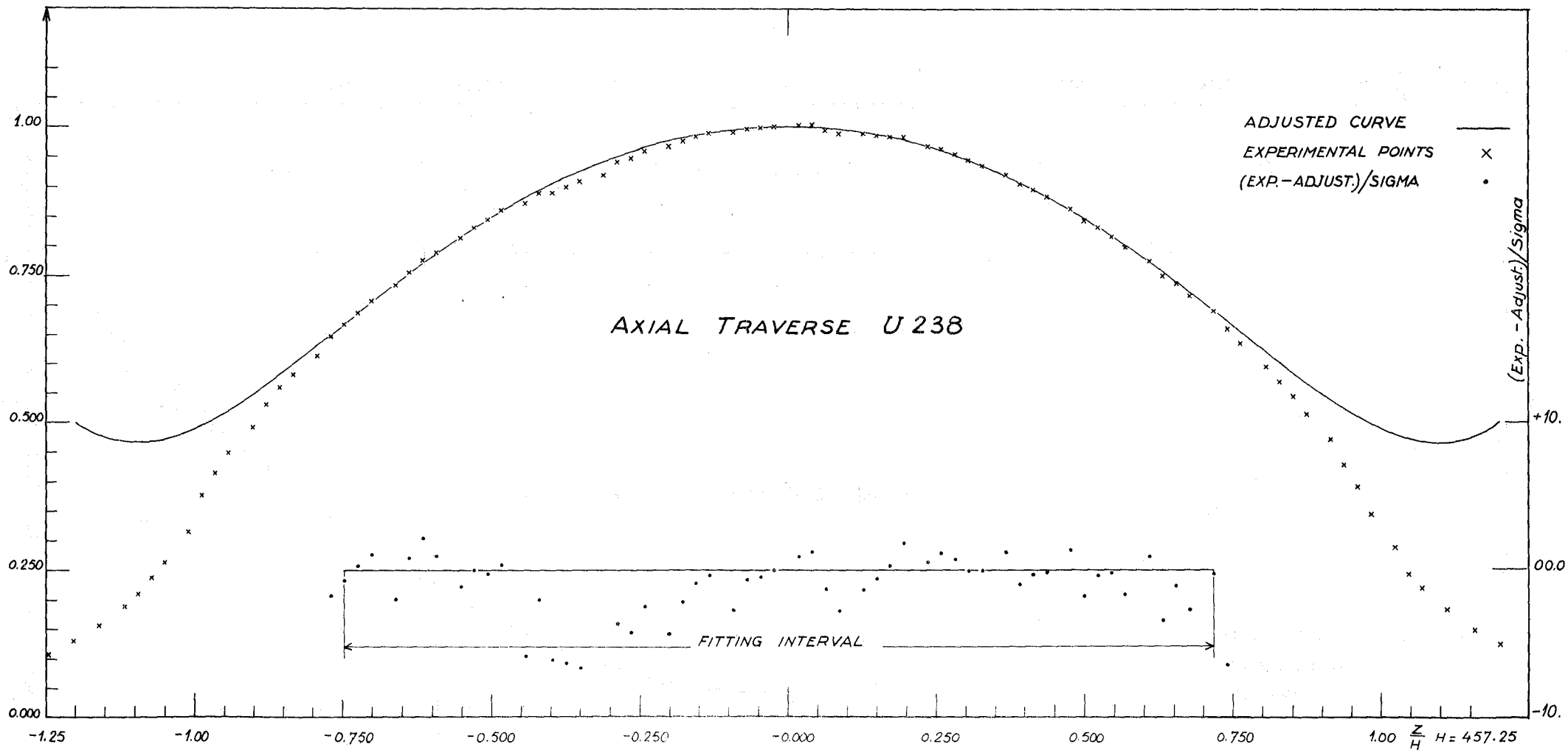


Fig. 11

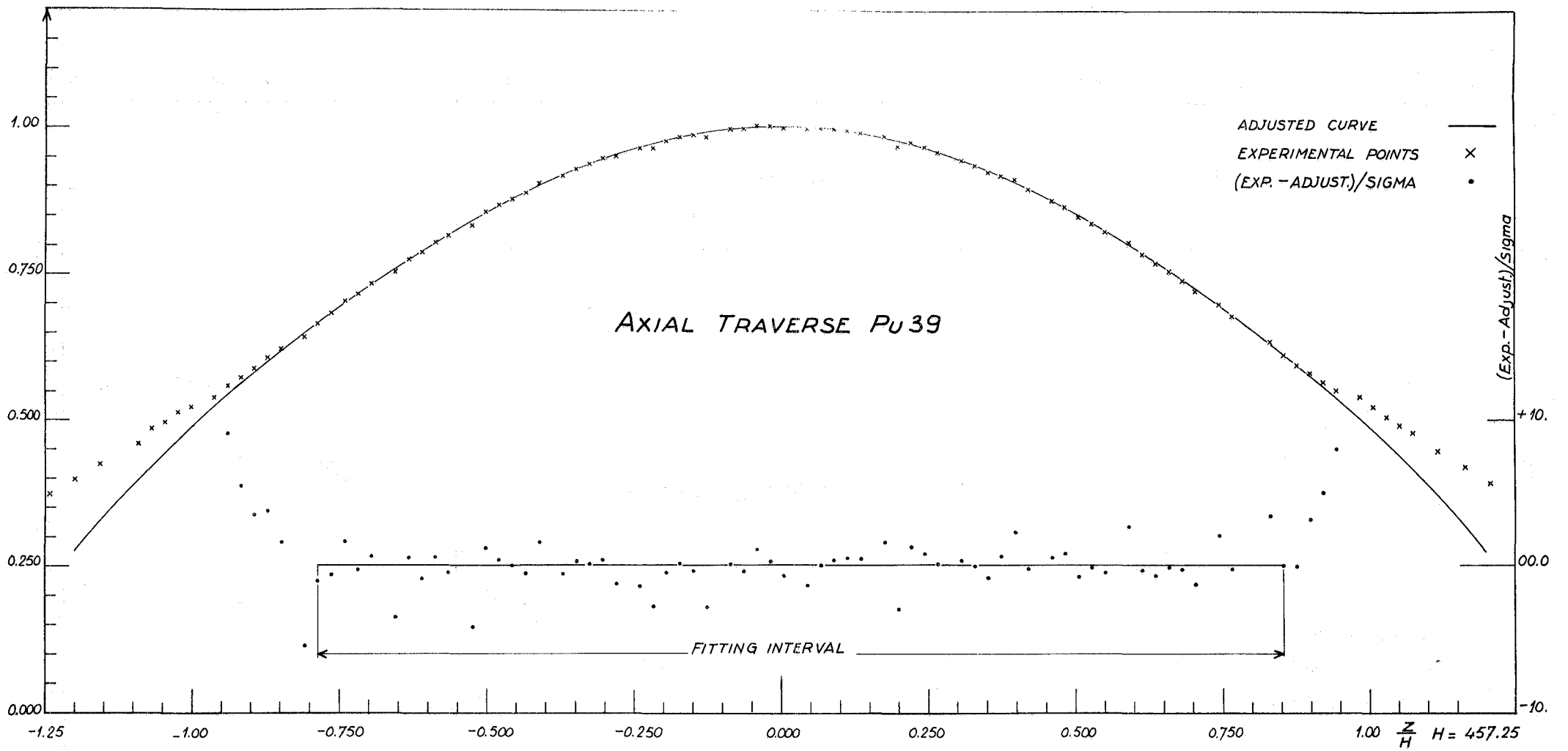


Fig. 12

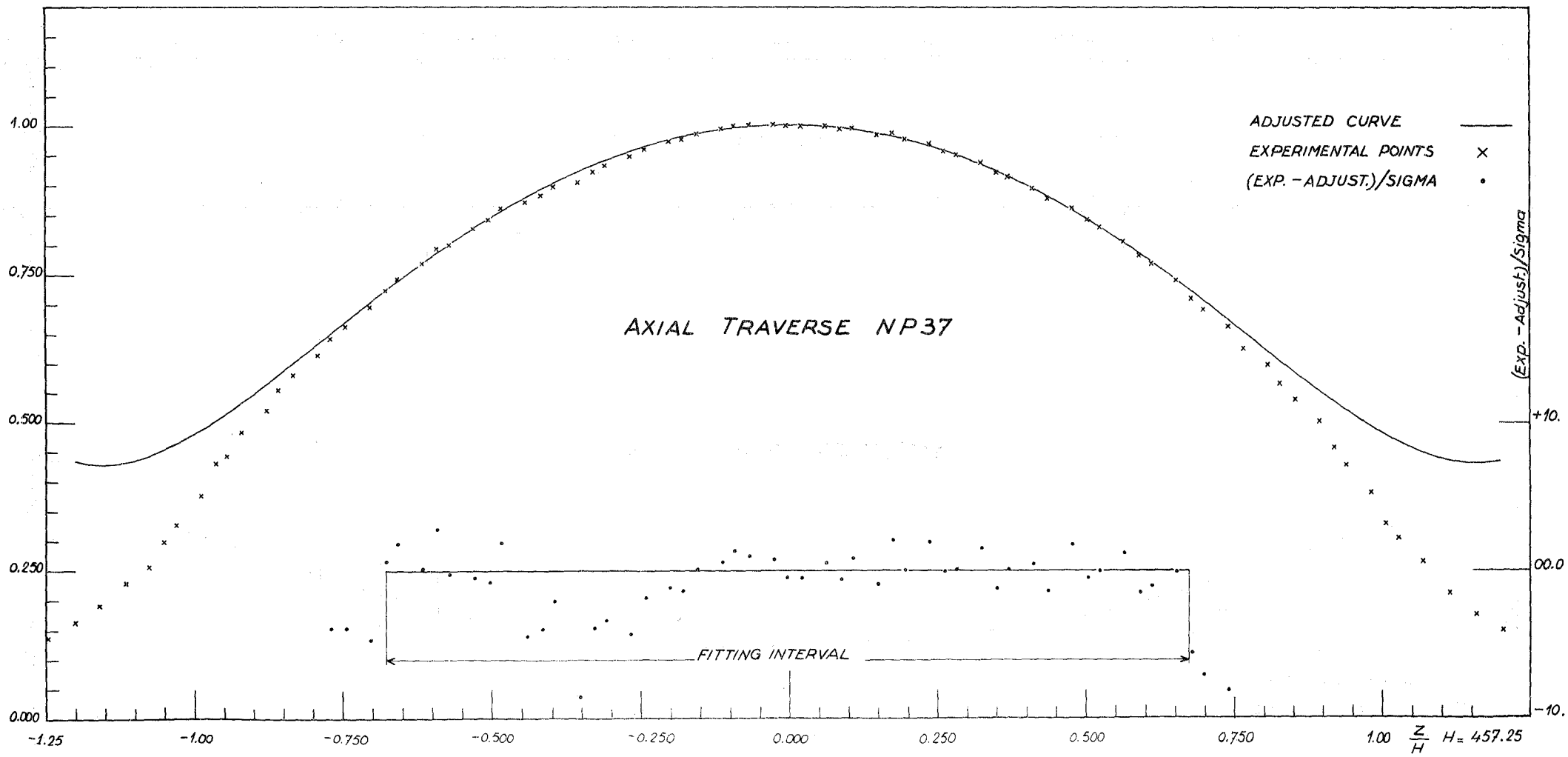


Fig. 13

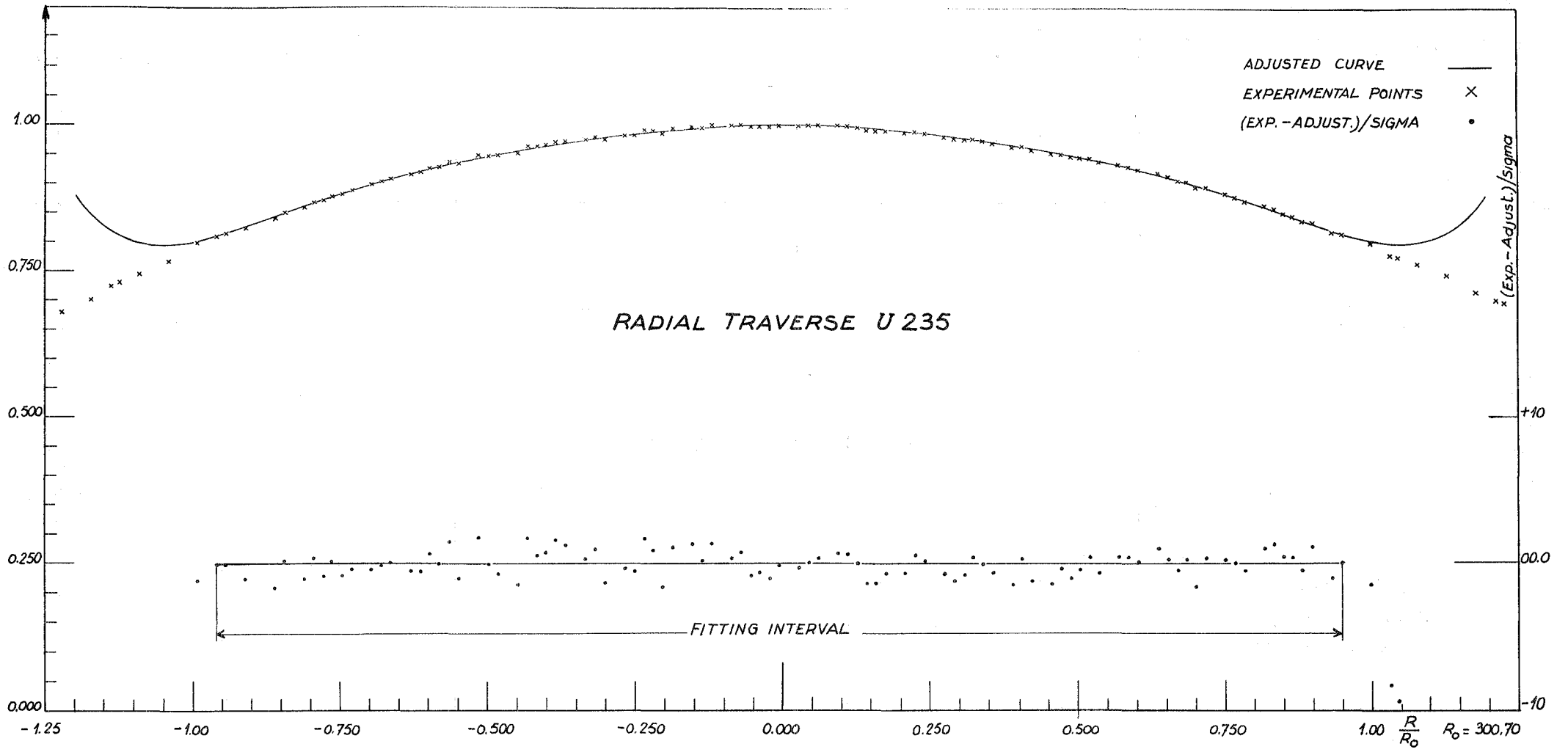


Fig. 14

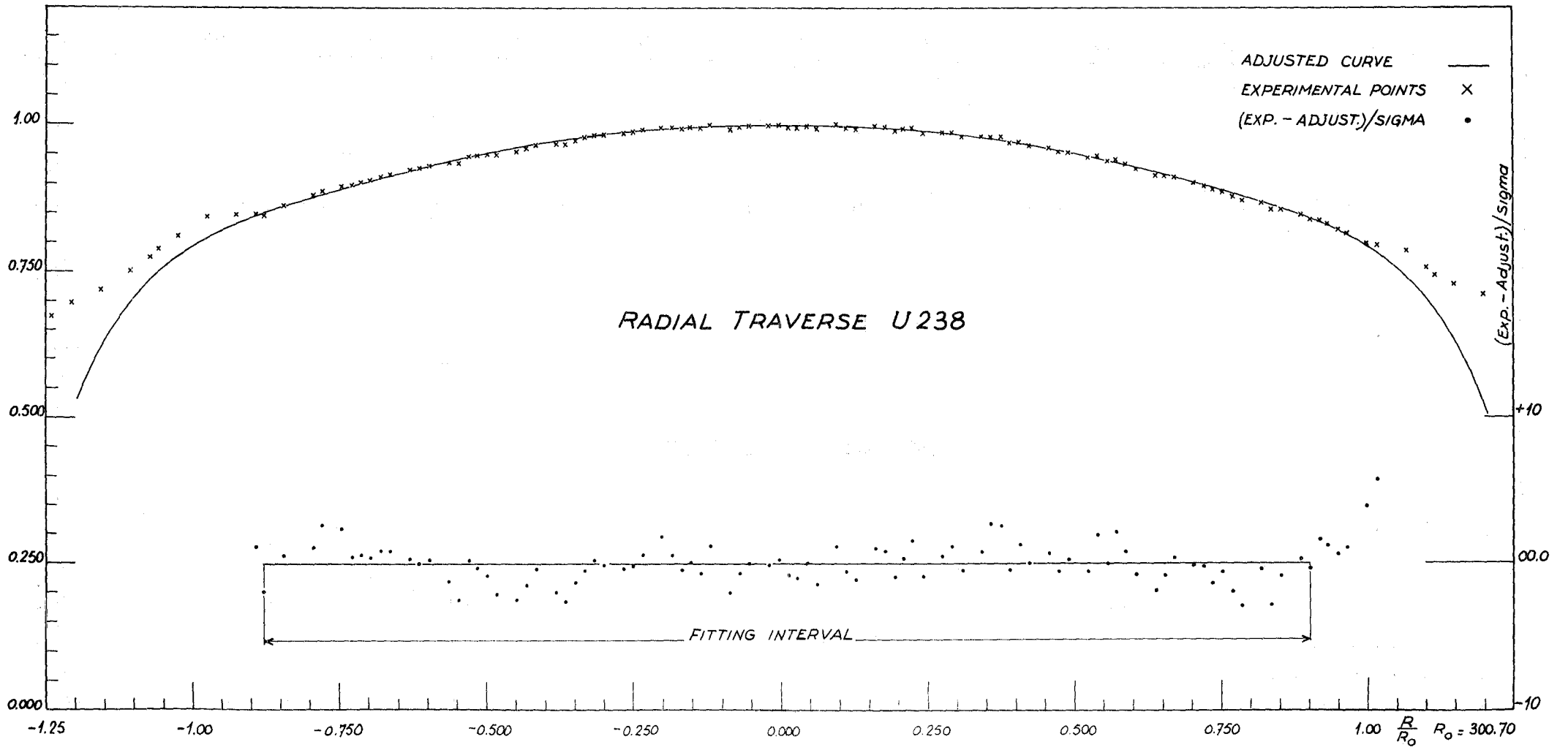


Fig. 15

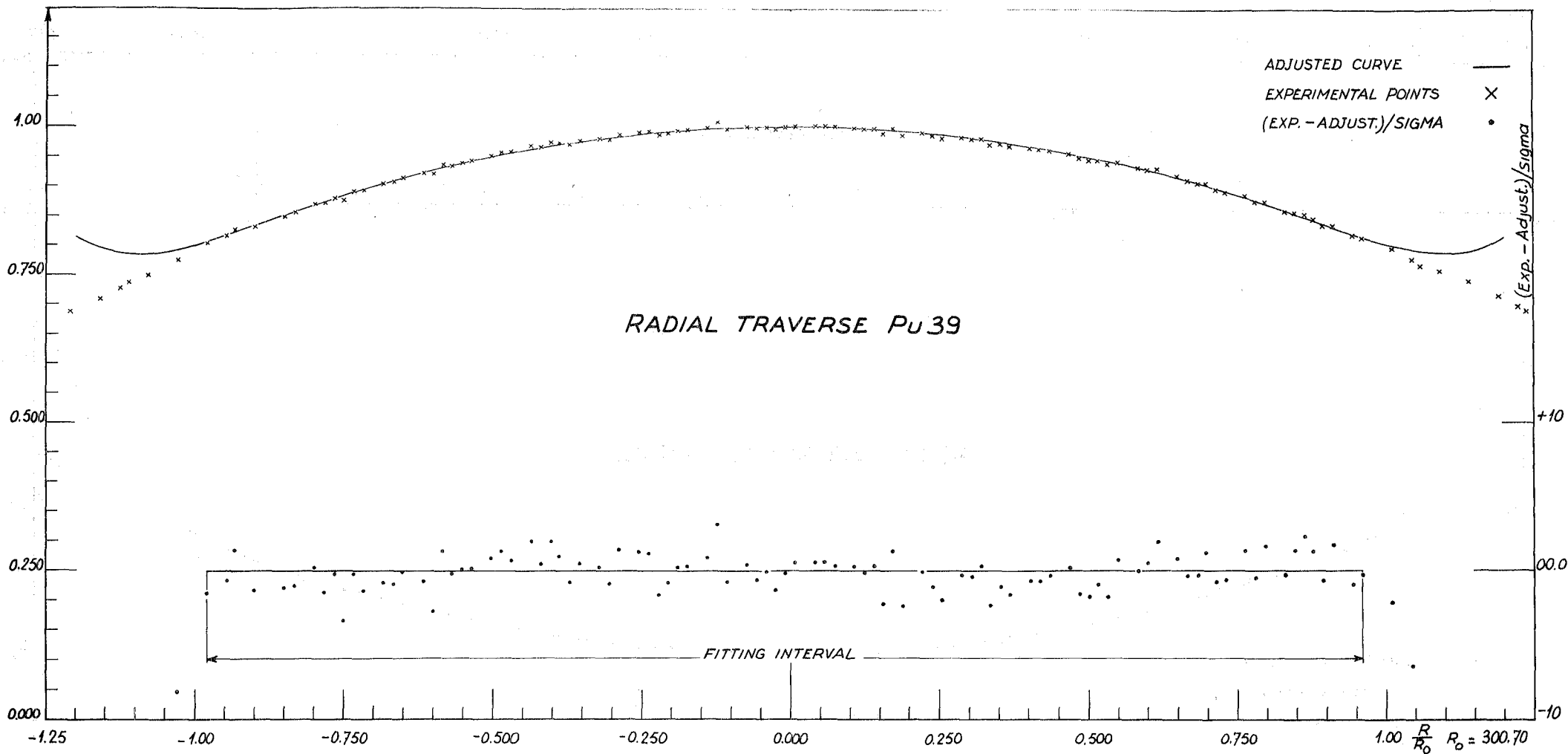


Fig. 16

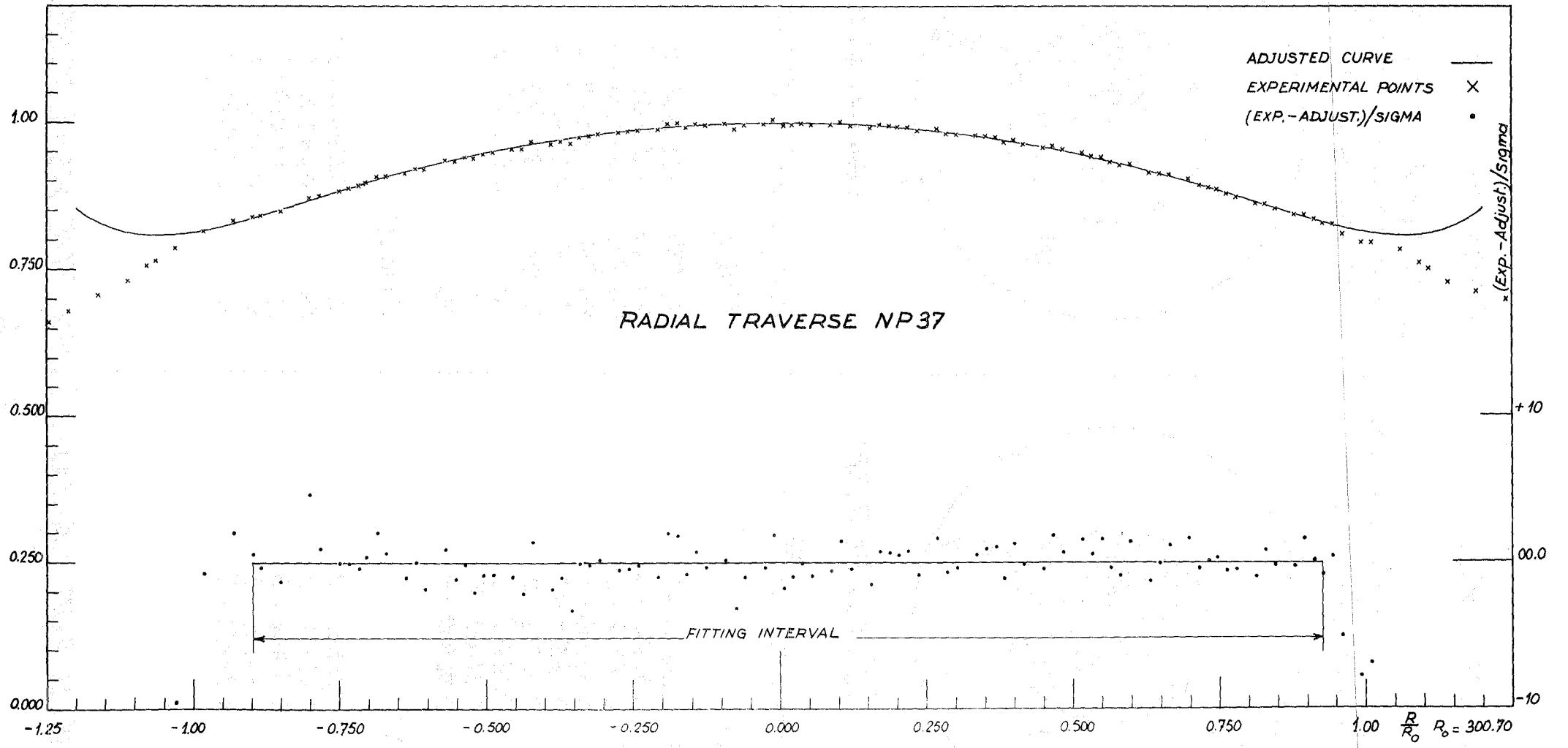
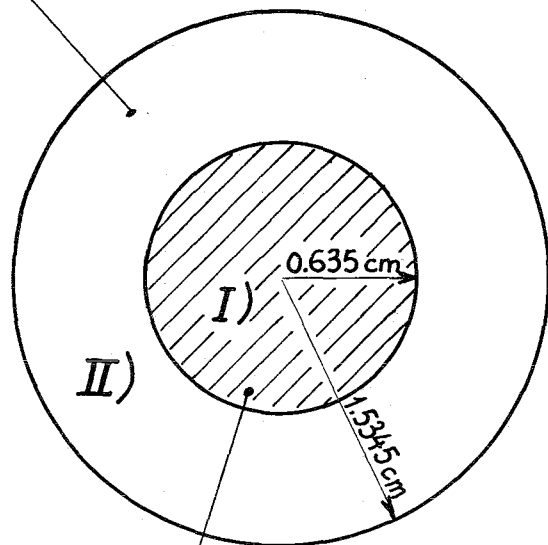


Fig. 17

## KARLRUHE MODEL

1 Fe<sub>2</sub>O<sub>3</sub> + 2 Na + 1/4 structural material of the element tube



3/4 Pu + 1/4 U depl.

Atom densities  $\times 10^{-24}$  for:

Zone I):

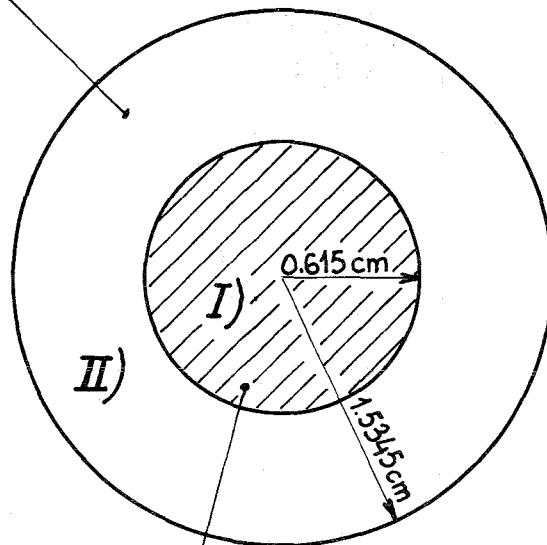
Pu 239	7.06844	-3
Pu 240	6.51900	-4
Pu 241	6.18272	-5
Pu 242	7.69638	-6
U 235	9.36373	-5
U 238	3.46269	-2
Fe	4.16942	-3
Cr	7.61260	-4
Ni	8.82860	-4

Zone II):

Na	1.06868	-2
Fe	1.42812	-2
Cr	3.99608	-3
Ni	1.94659	-3
O	1.39954	-2

## CADARACHE MODEL

1 Fe<sub>2</sub>O<sub>3</sub> + 2 Na + 1/4 structural material of the element tube + the cladding of the fuel rodlets



3/4 Pu + 1/4 U depl.

Atom densities  $\times 10^{-24}$  for:

Zone I):

Pu 239	0.753646	-2
Pu 240	0.695055	-3
Pu 241	0.659253	-4
Pu 242	0.820642	-5
U 235	0.998406	-4
U 238	0.369202	-1
Fe	0.142274	-2
Cr		
Ni		

Zone II):

Na	0.105514	-1
Fe	0.146790	-1
Cr	0.410069	-2
Ni	0.210199	-1
O	0.138183	-1

## MODELS FOR CALCULATING THE HETEROGENEITY

Fig. 18

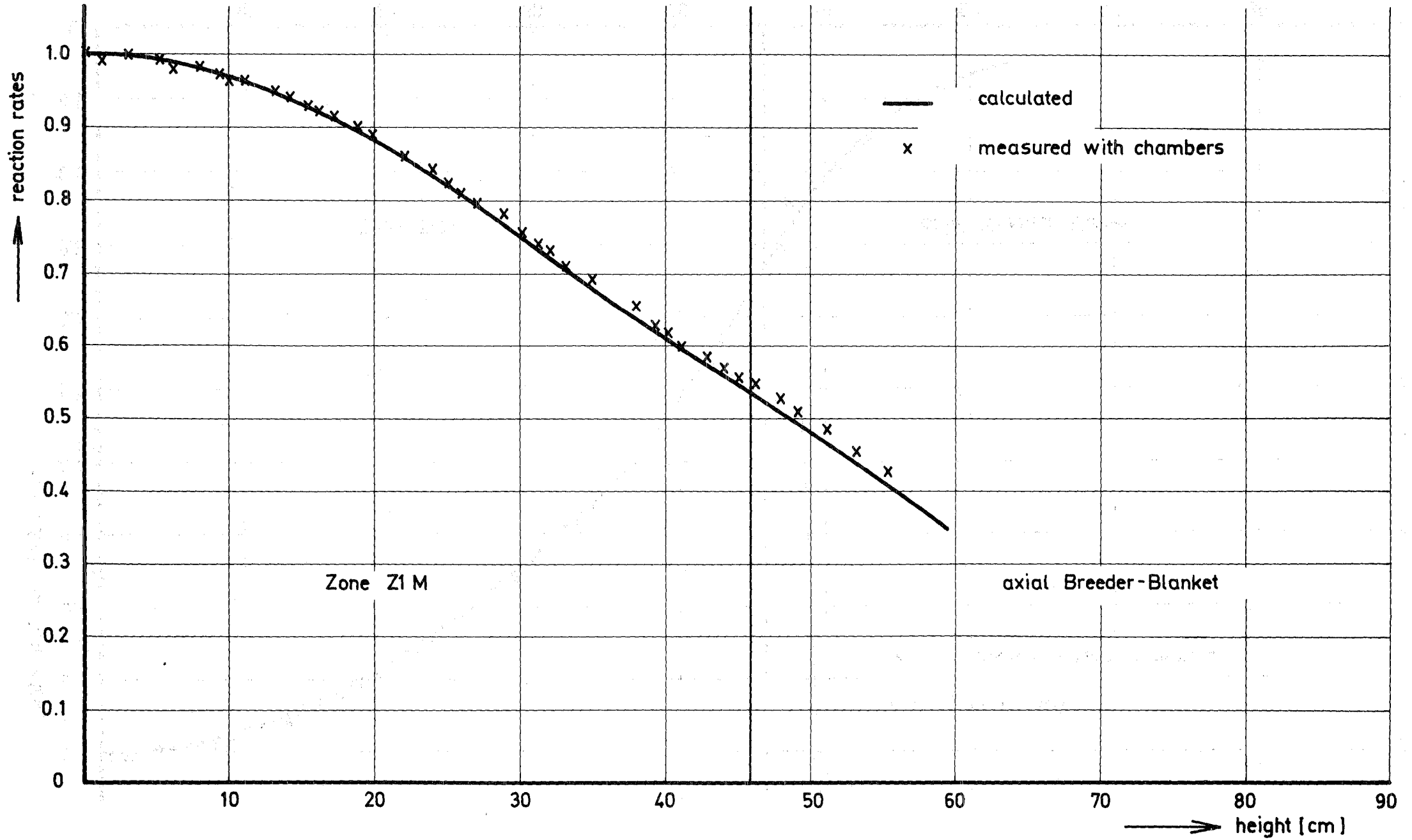


Fig. 19

Axial Fission Rate Traverse for U235

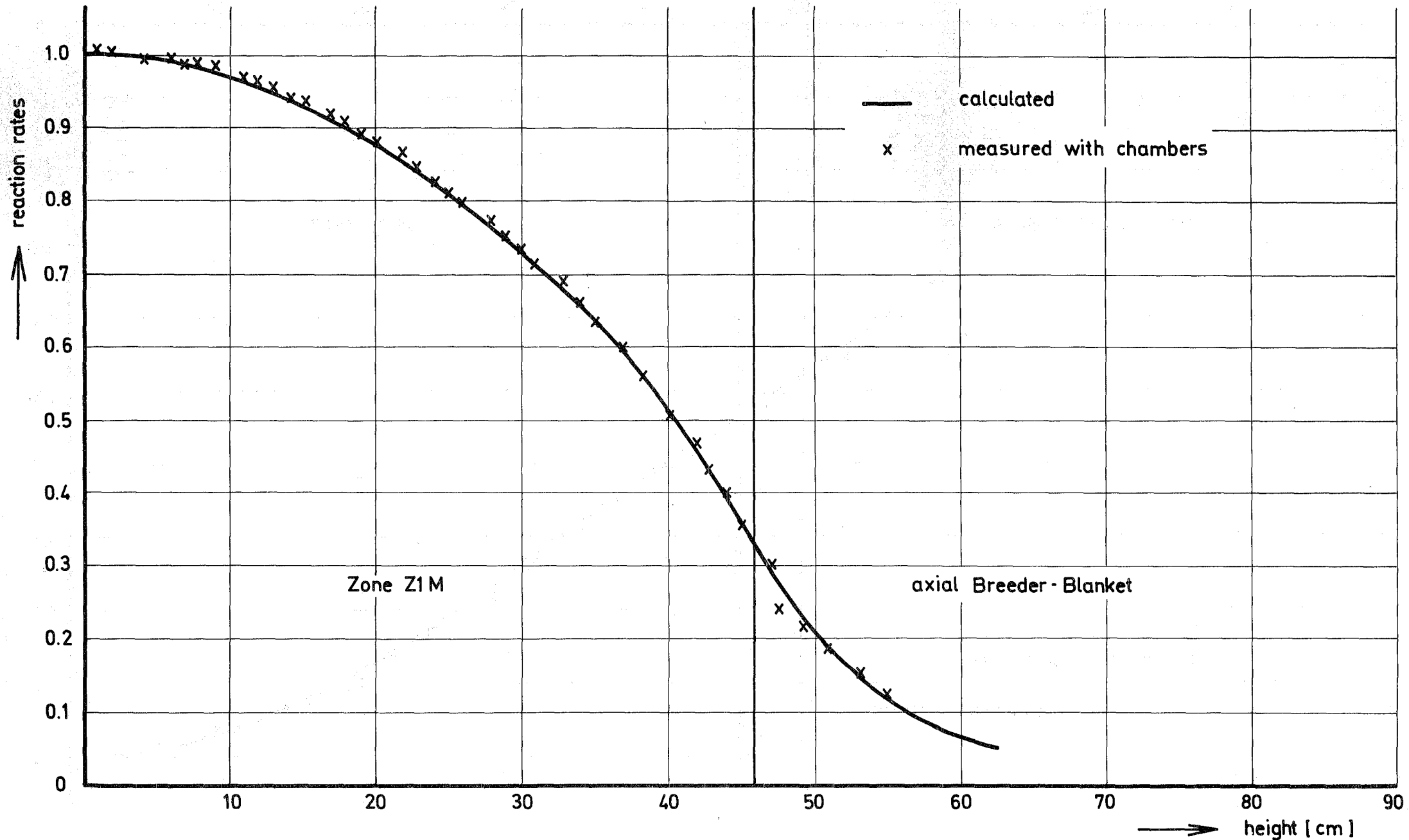


Fig. 20

Axial Fission Rate Traverse for U238

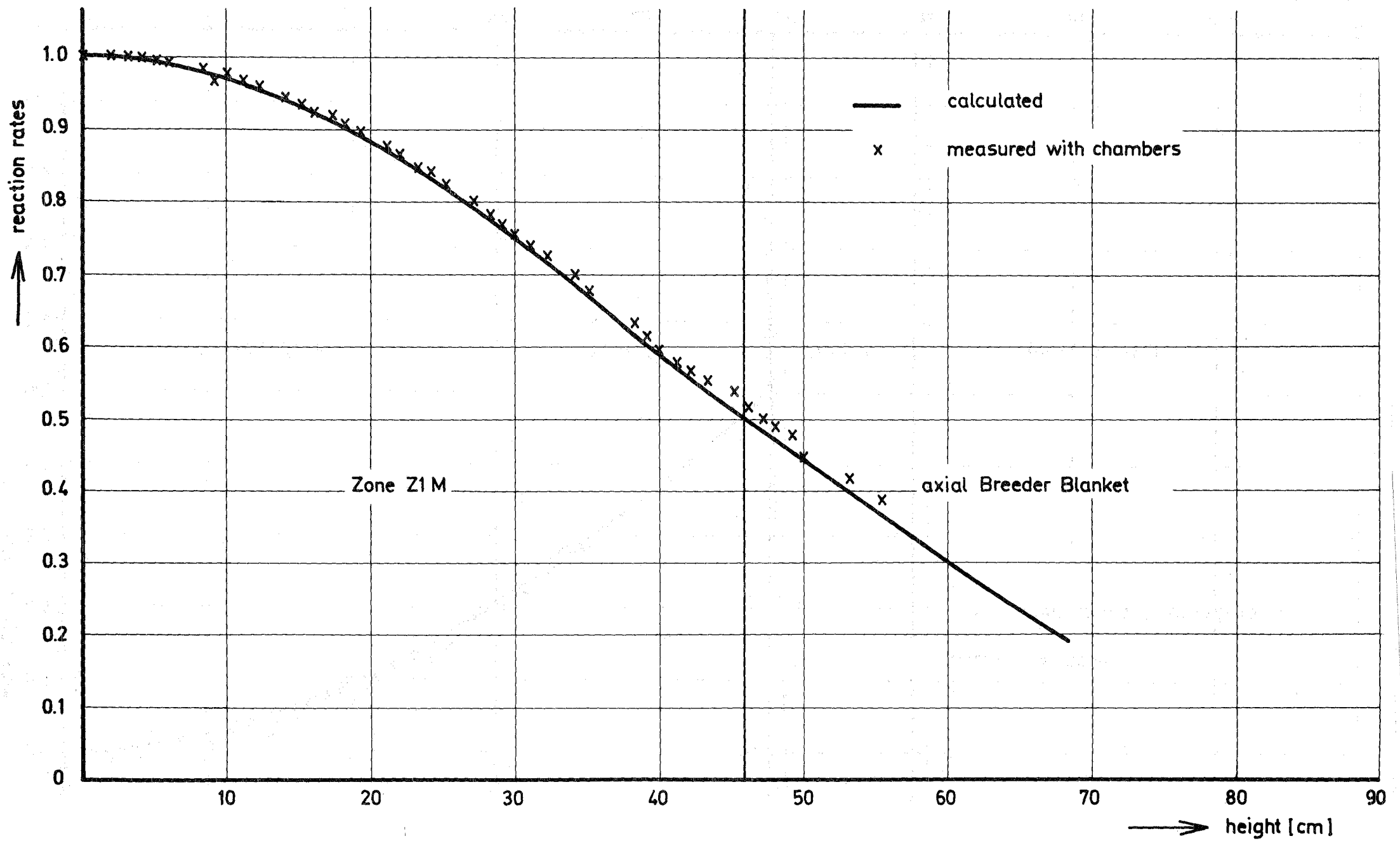


Fig. 21

Axial Fission Rate Traverse for Pu 239

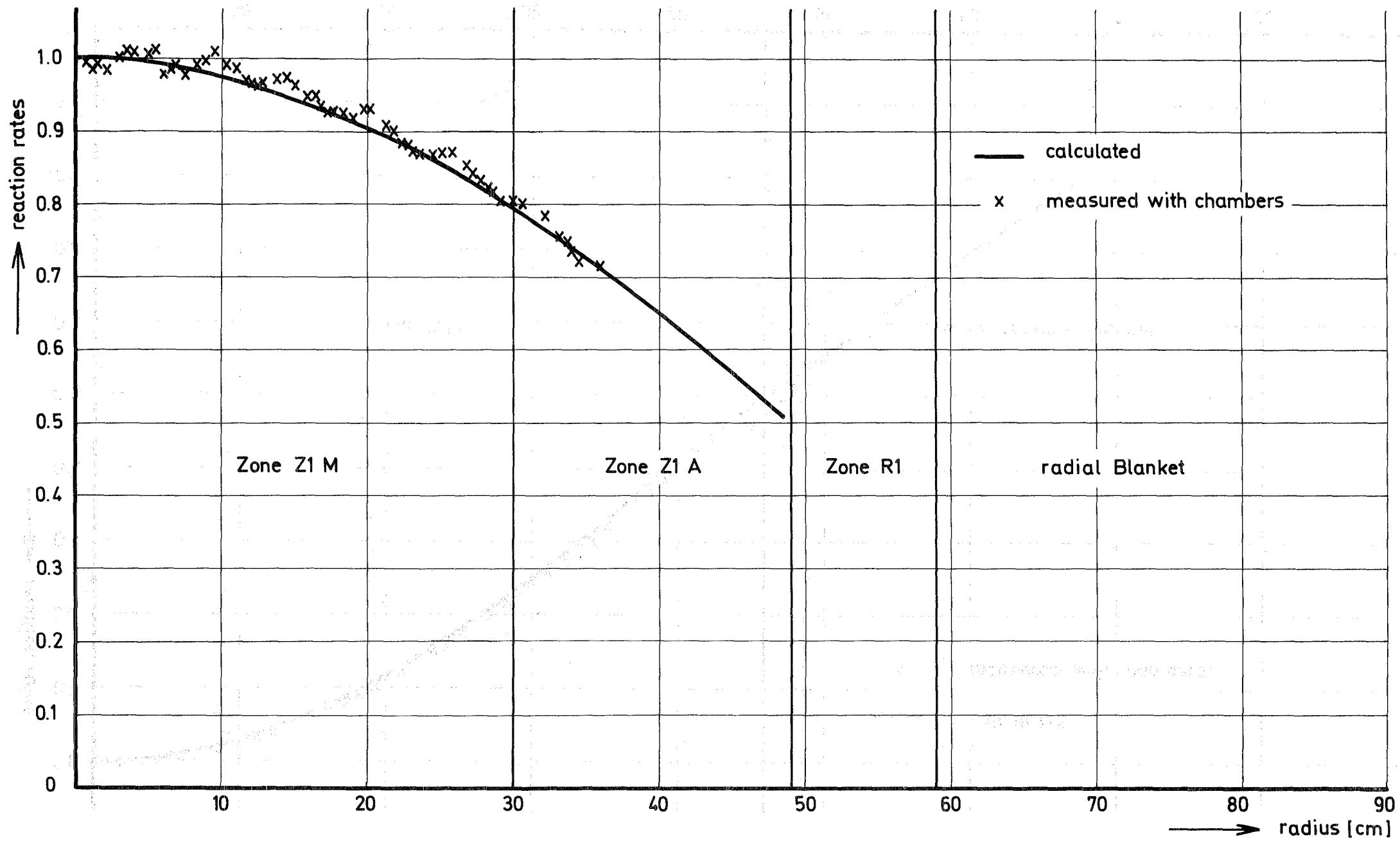


Fig. 22 Radial Fission Rate Traverse for U238

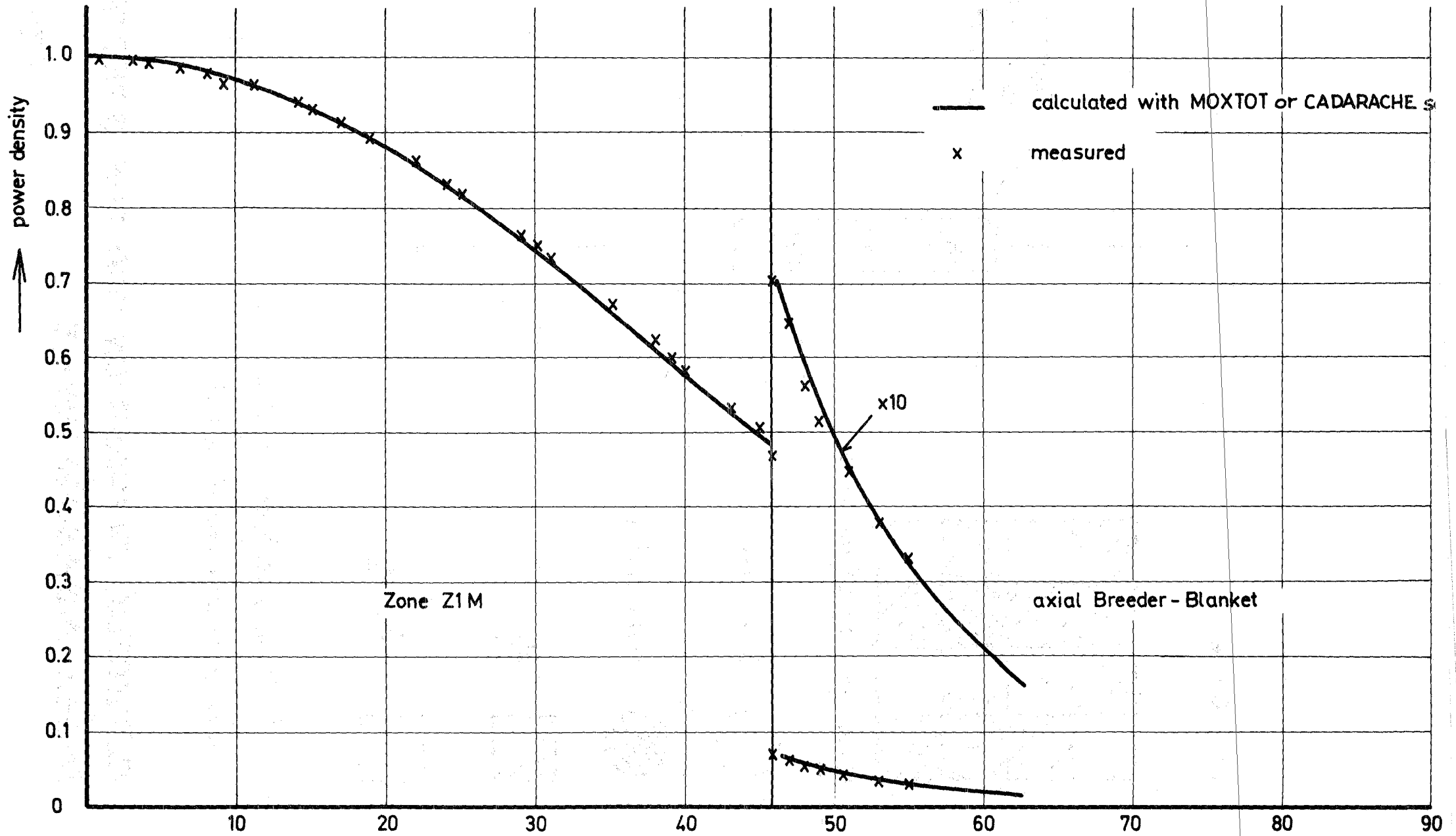
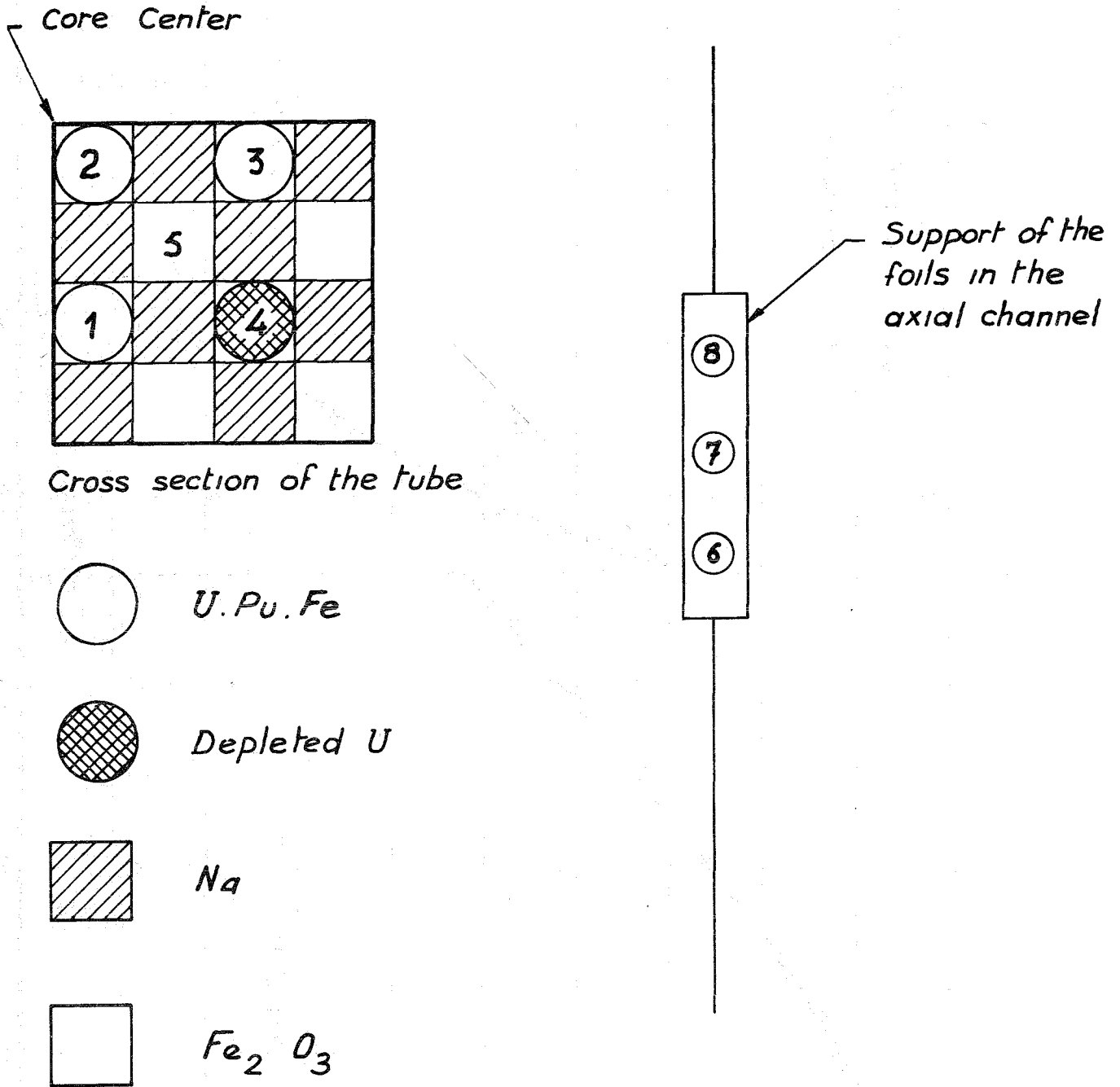


Fig. 23

Axial Power Distribution



Foils in position 1, 2, 3, 4, 5,  
and in axial channel 6, 7, 8.

**DETECTOR DISPOSITION FOR THE SPECTRAL INDEX MEASUREMENTS**

Fig. 24

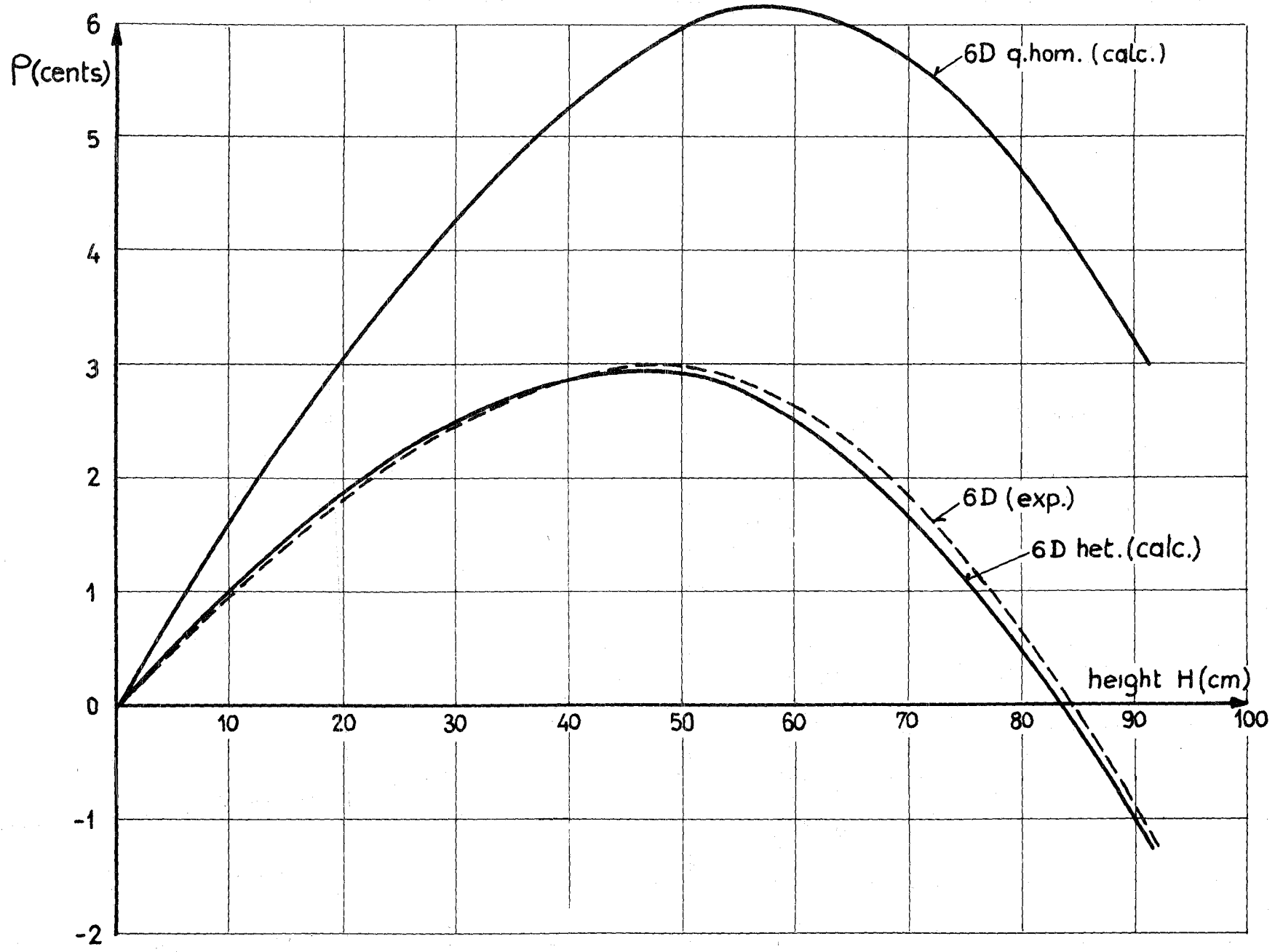
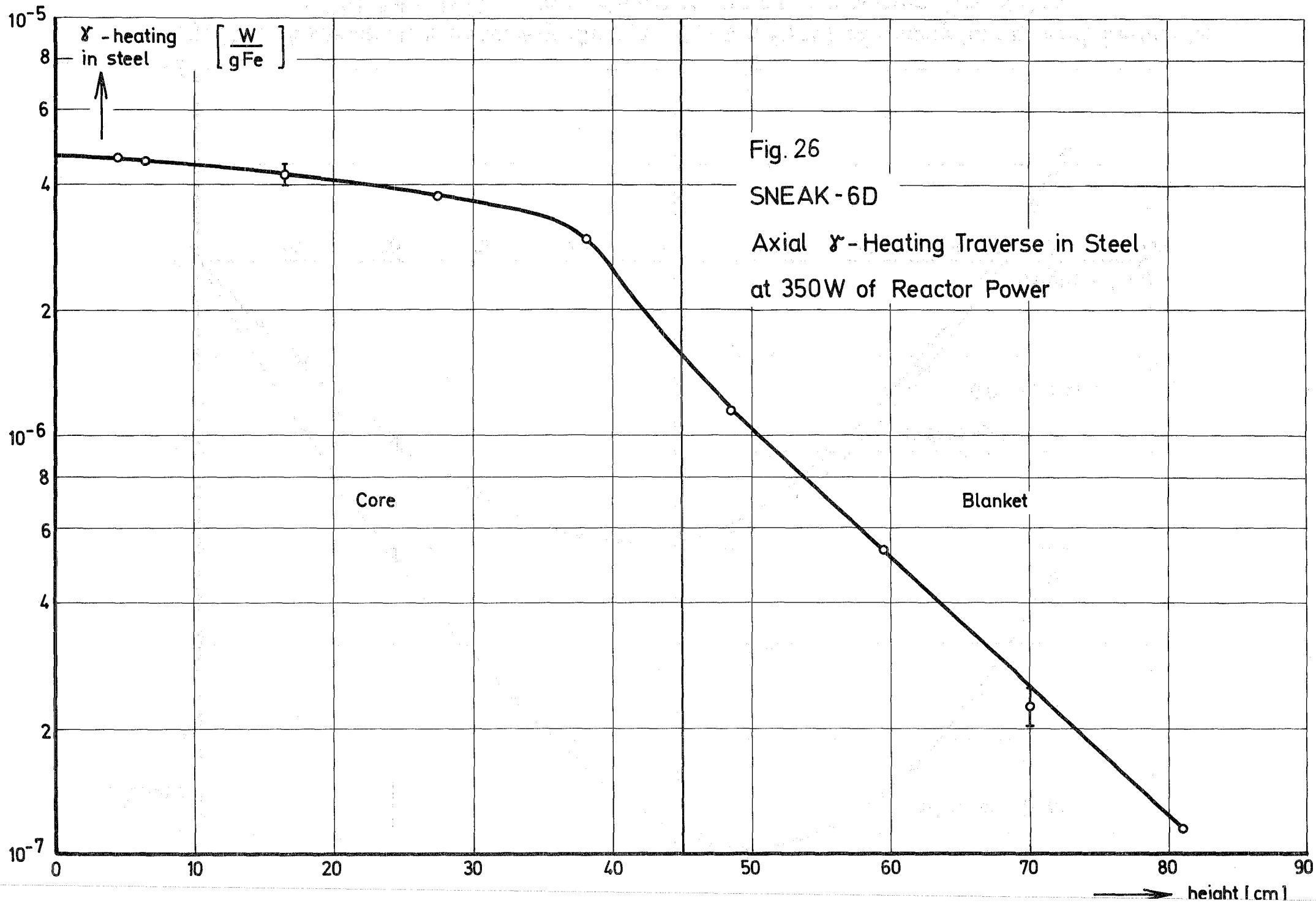


Fig. 25 . Experimental Reactivity Change,  $P$ , as a Result of voiding four central Elements of SNEAK - 6 D up to a Height  $H$  and corresponding Calculations.





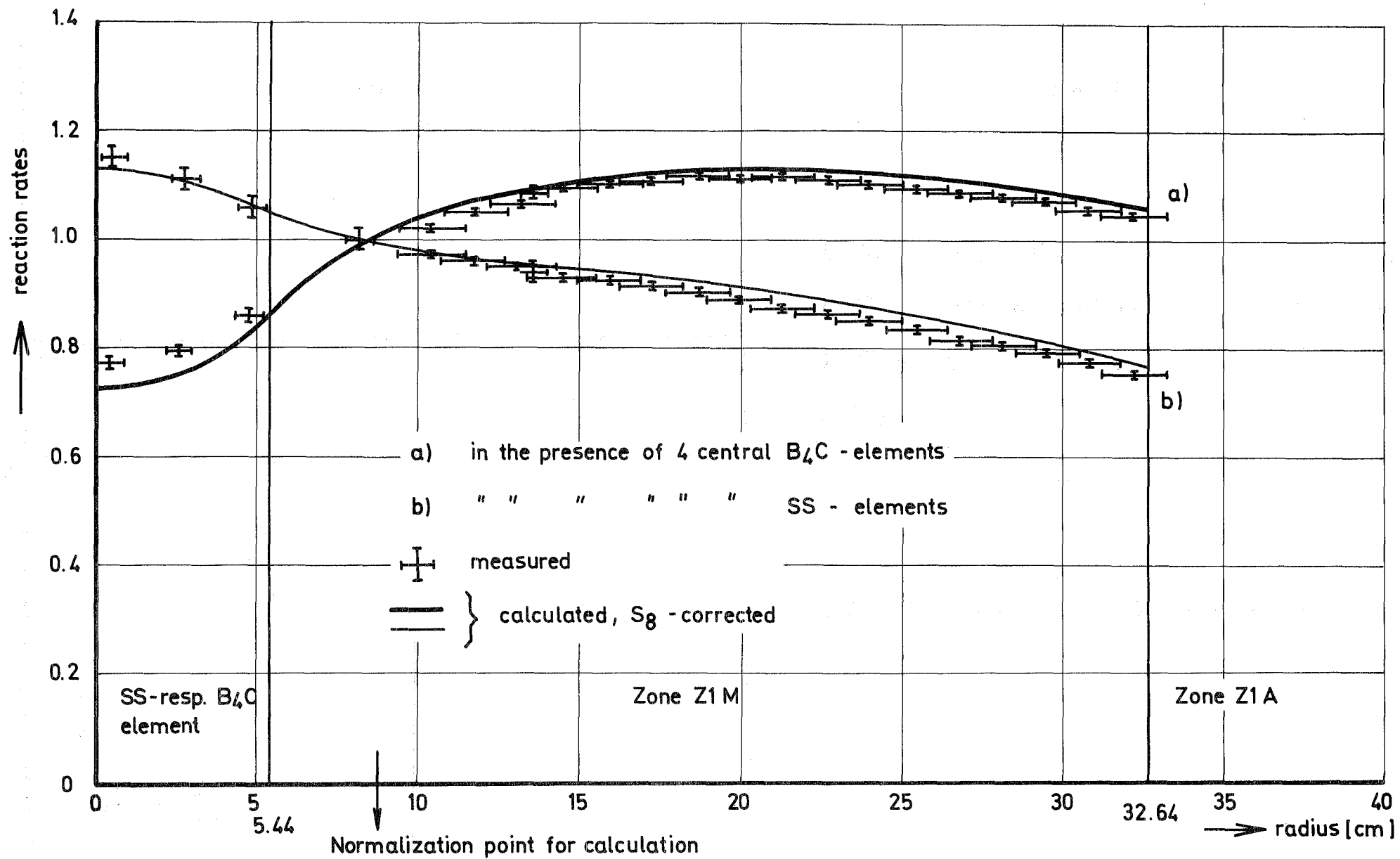


Fig. 28 SNEAK-6D Fission Rate Traverse for U235 normalized to one Atom

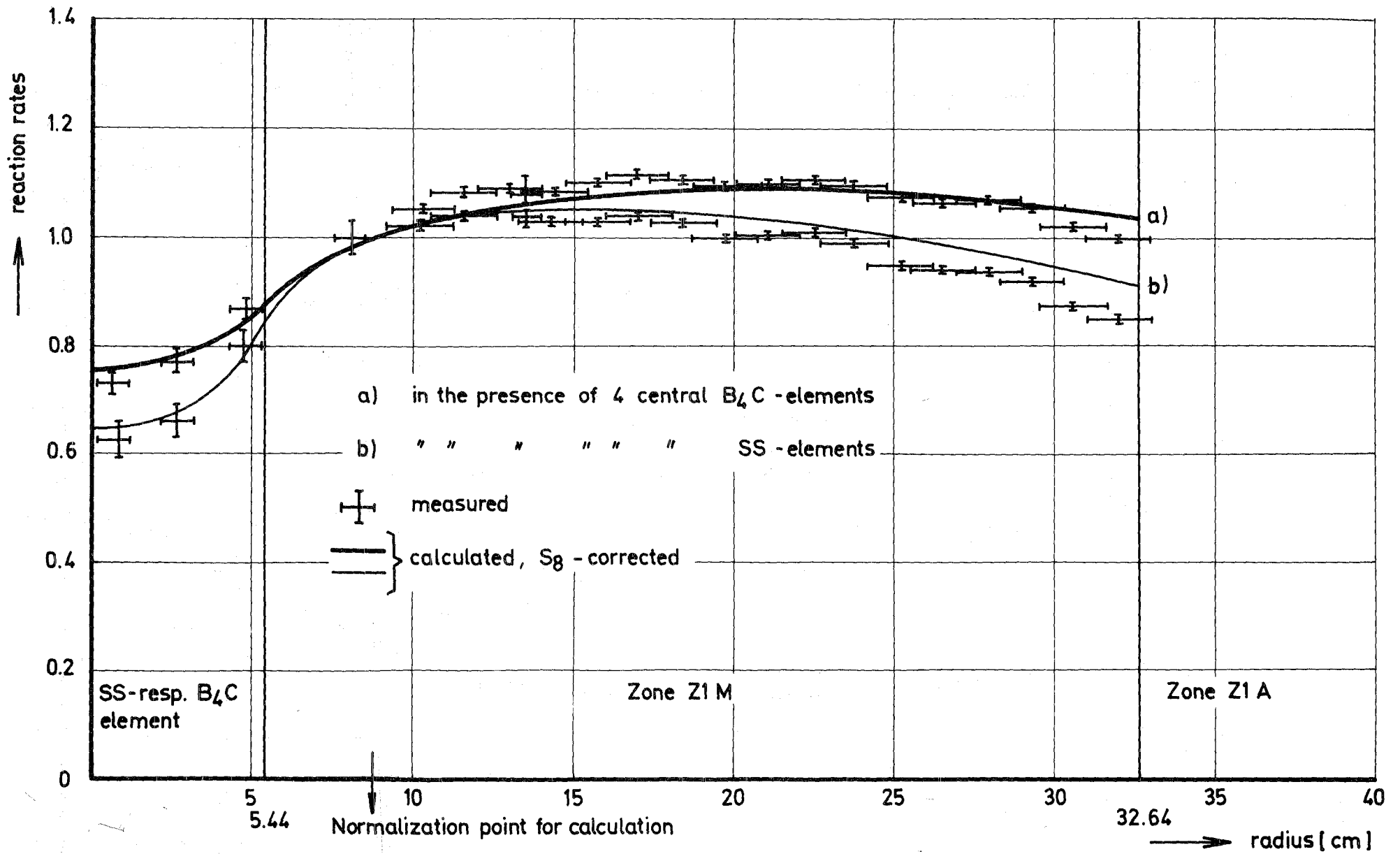


Fig. 29

SNEAK-6D Radial Fission Rate Traverse for U238  
normalized to one Atom

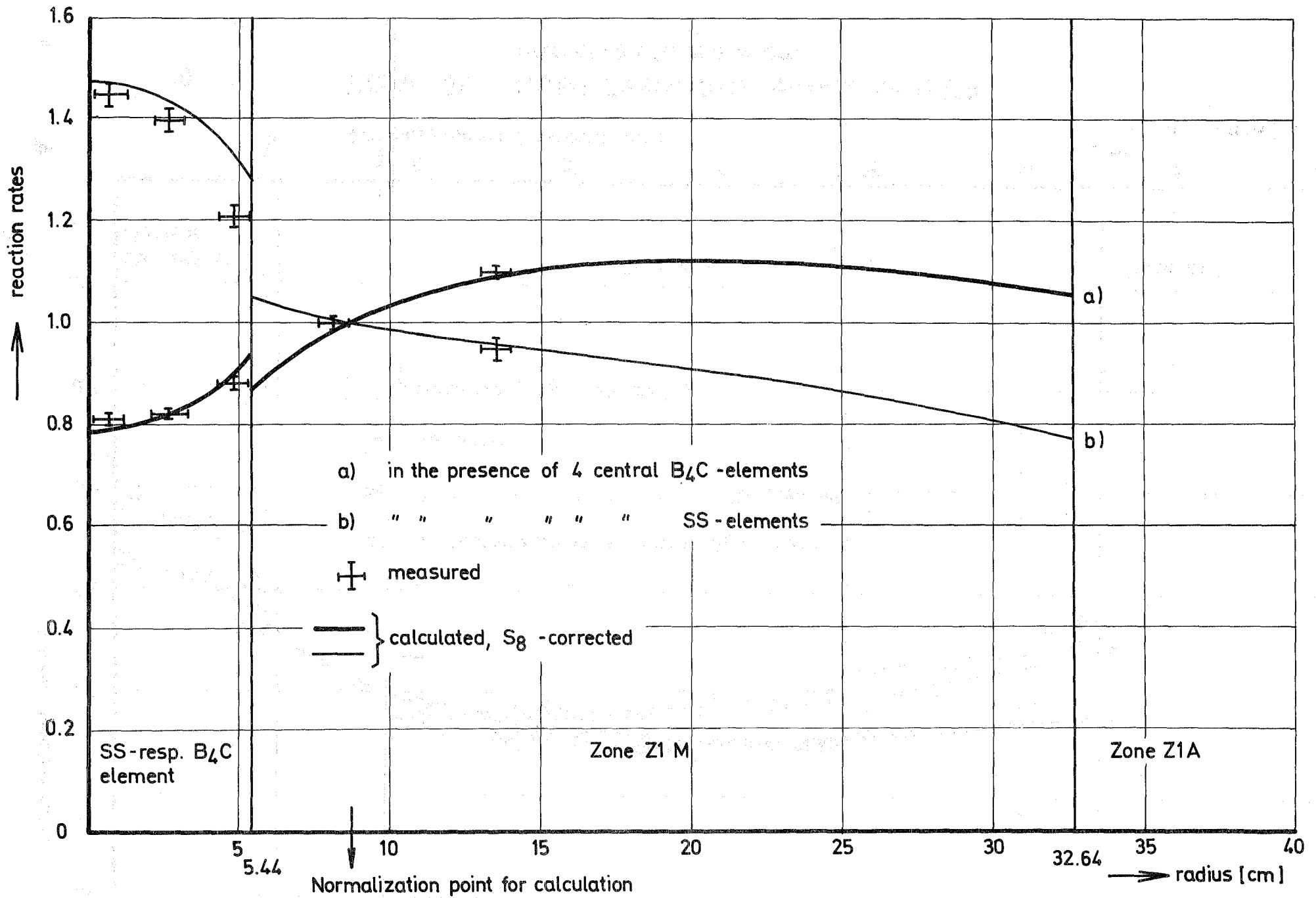
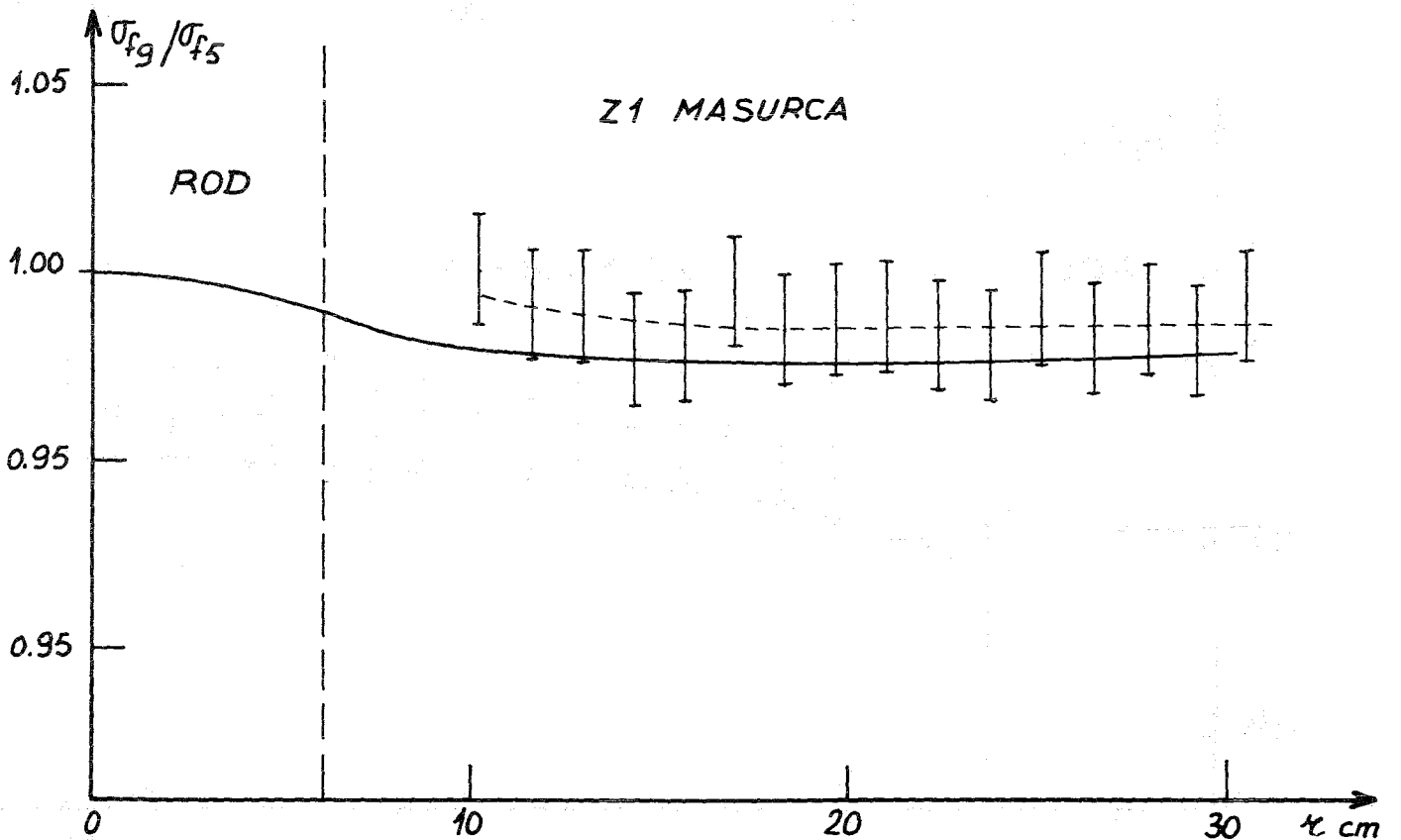
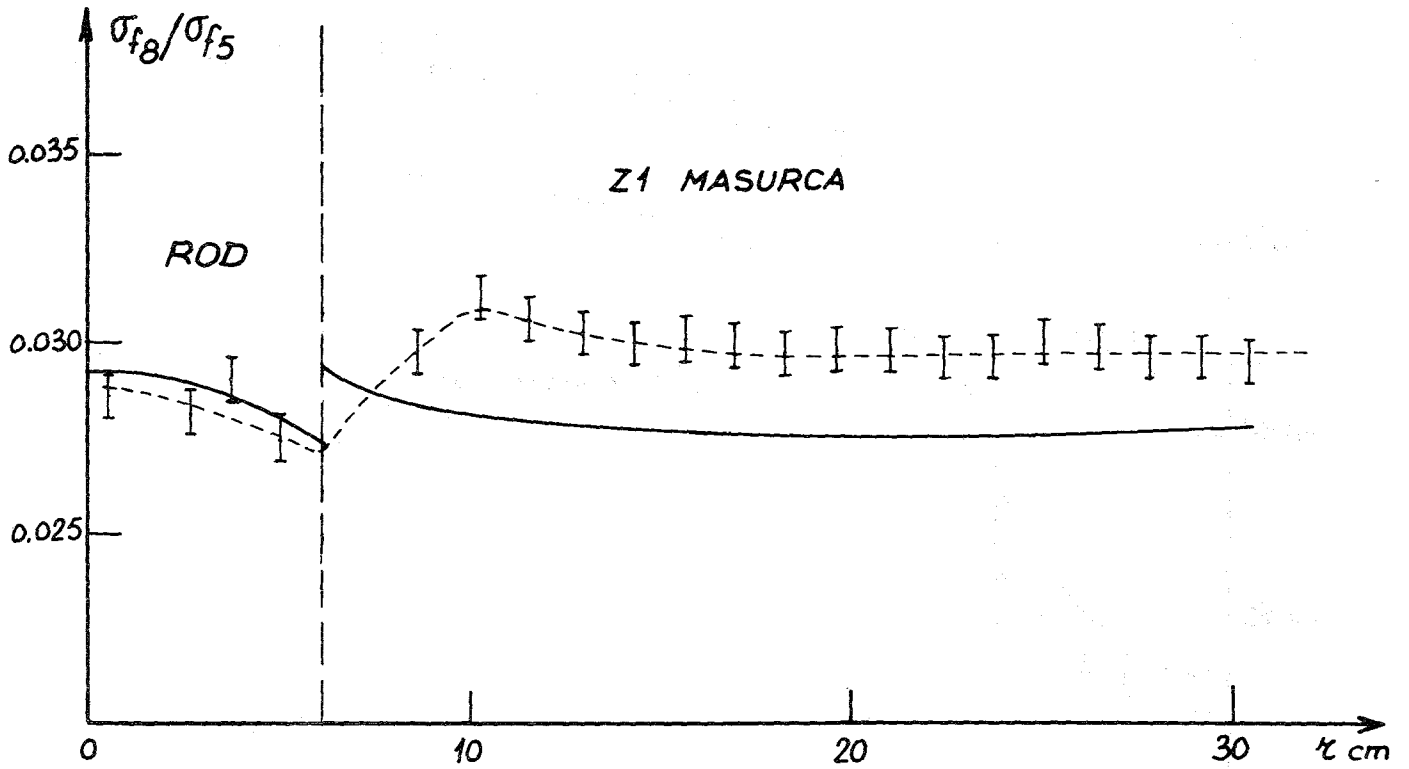


Fig. 30

SNEAK - 6D Radial Capture Rate Traverse for U238  
normalized to one Atom

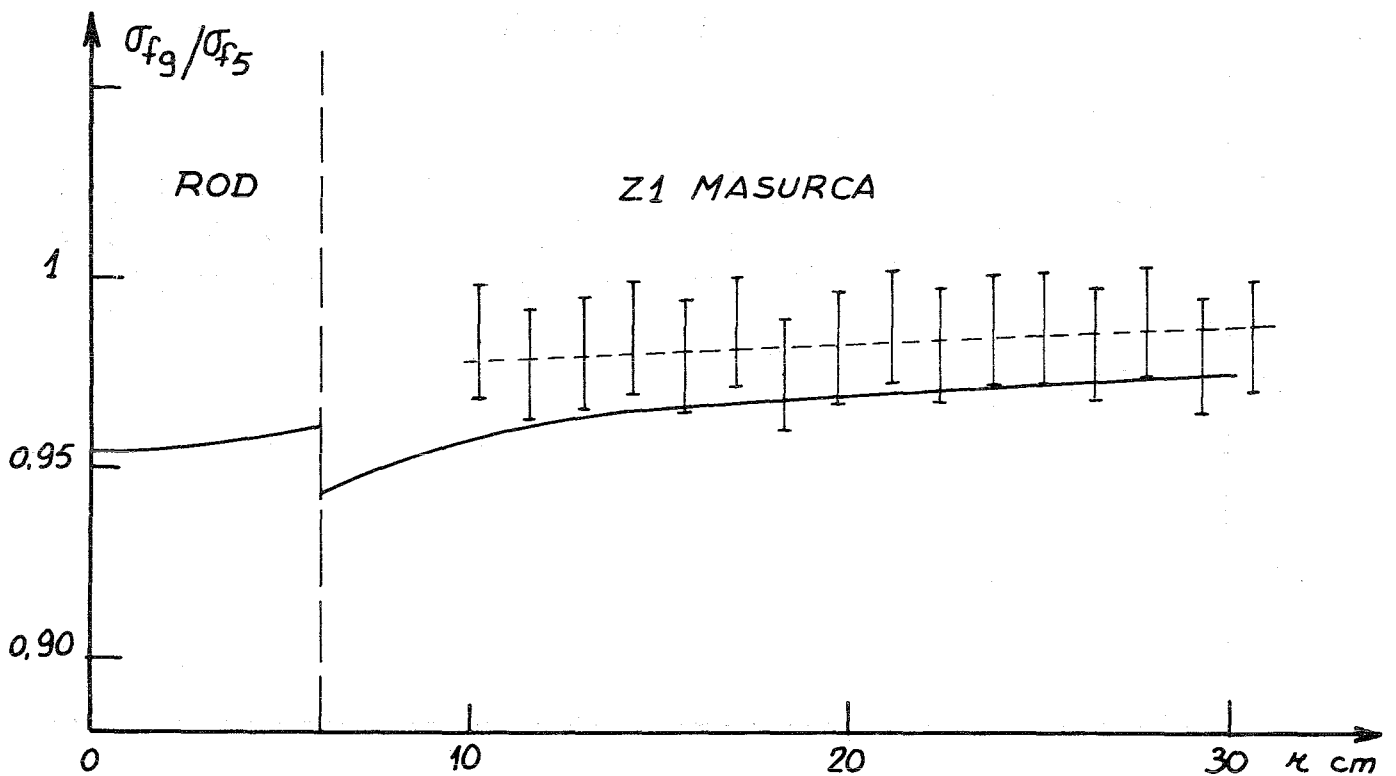
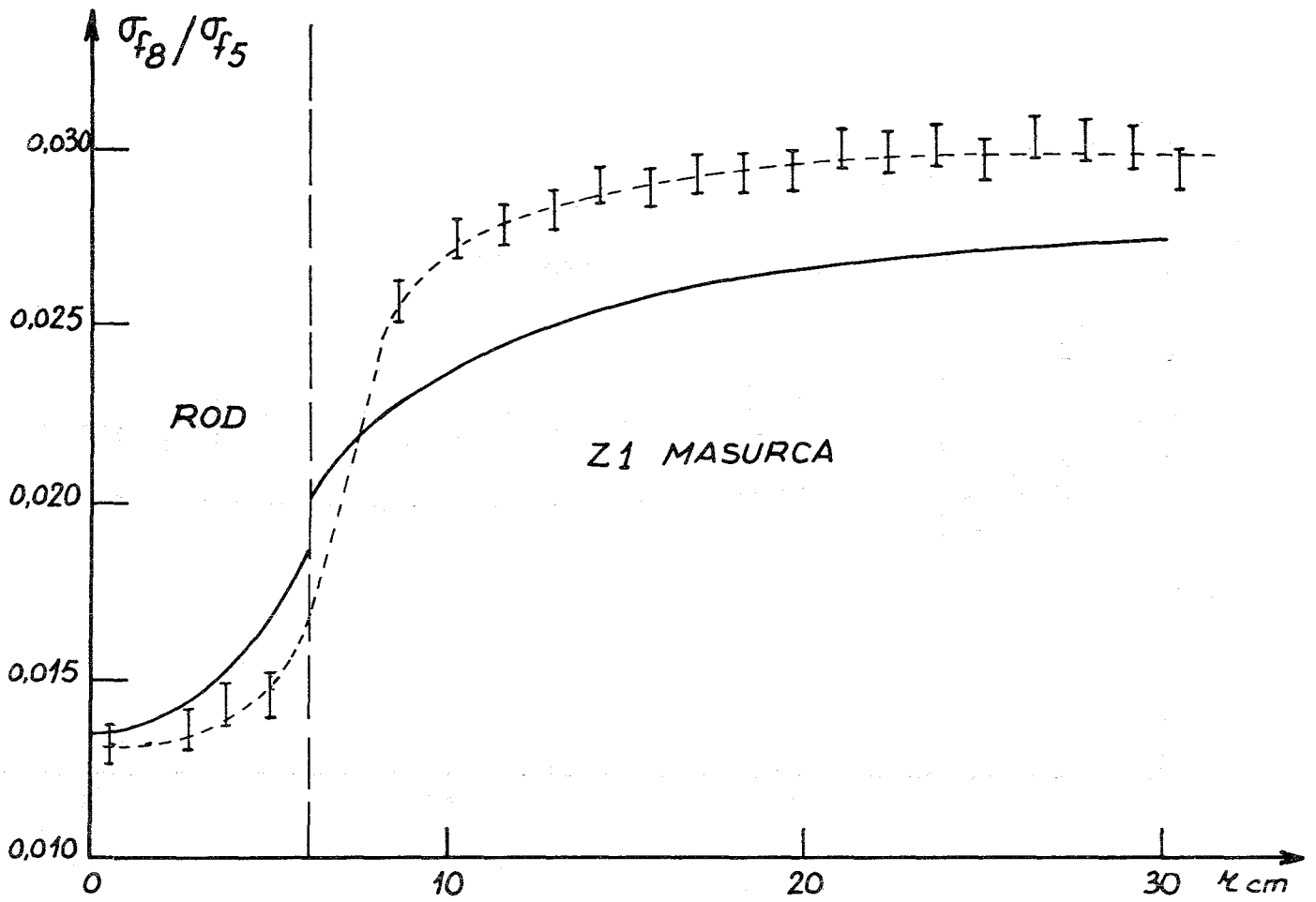


**$B_4C$  ROD : SPECTRAL INDEX DISTRIBUTION**

— Calculated distribution

- - - Experimental results

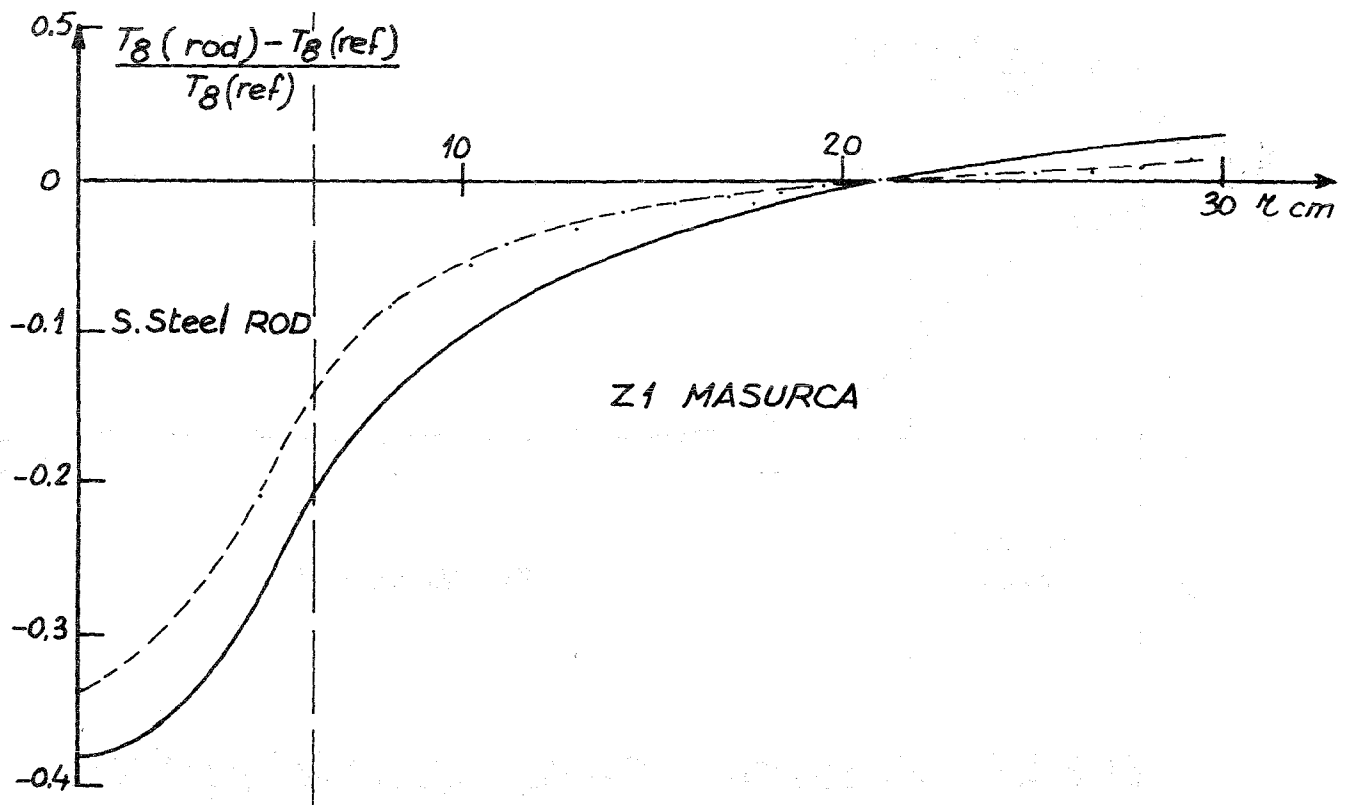
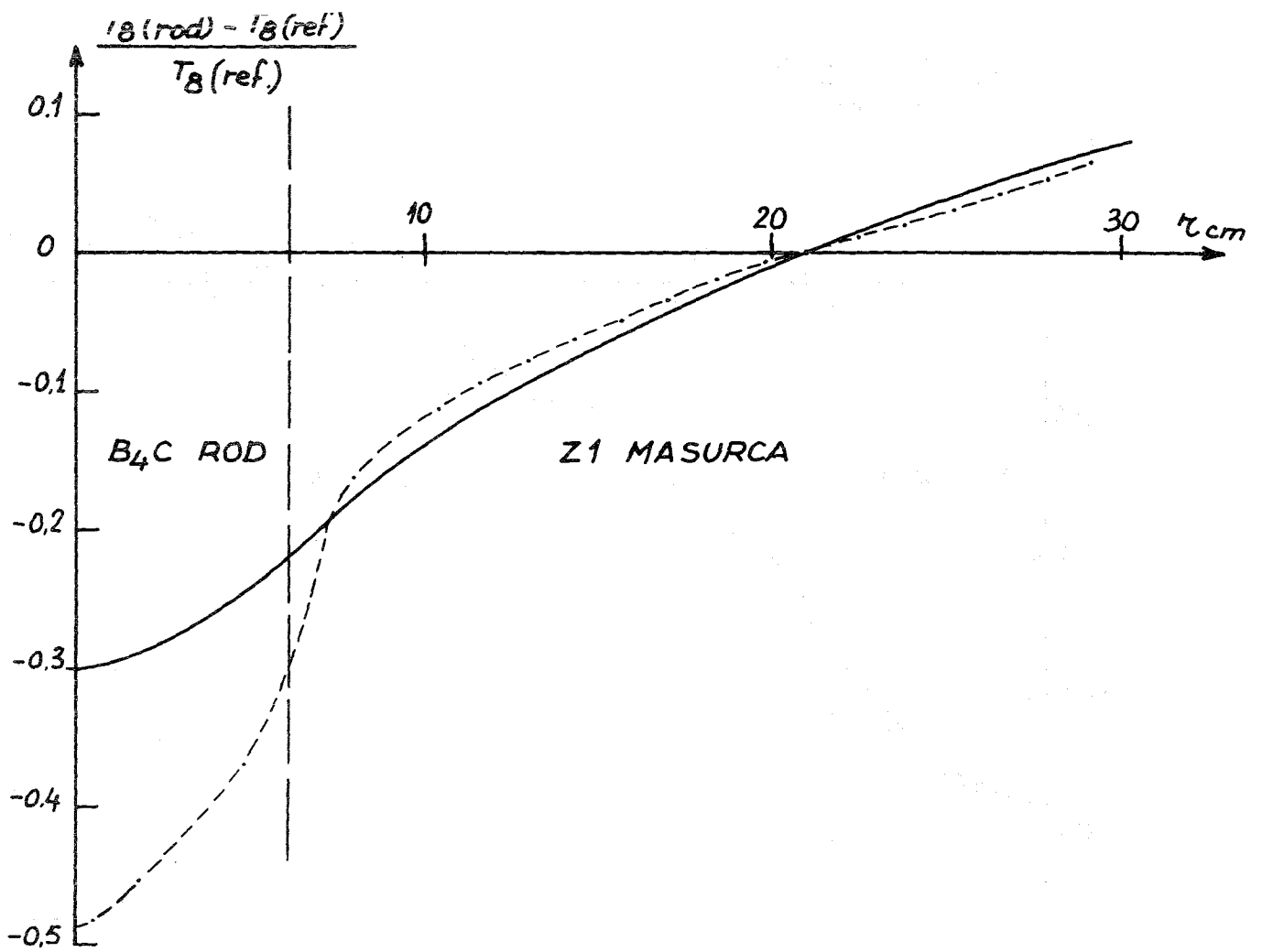
Fig.31



**STAINLESS STEEL ROD: SPECTRAL INDEX DISTRIBUTION**

- Calculated distribution
- - I - - Experimental results

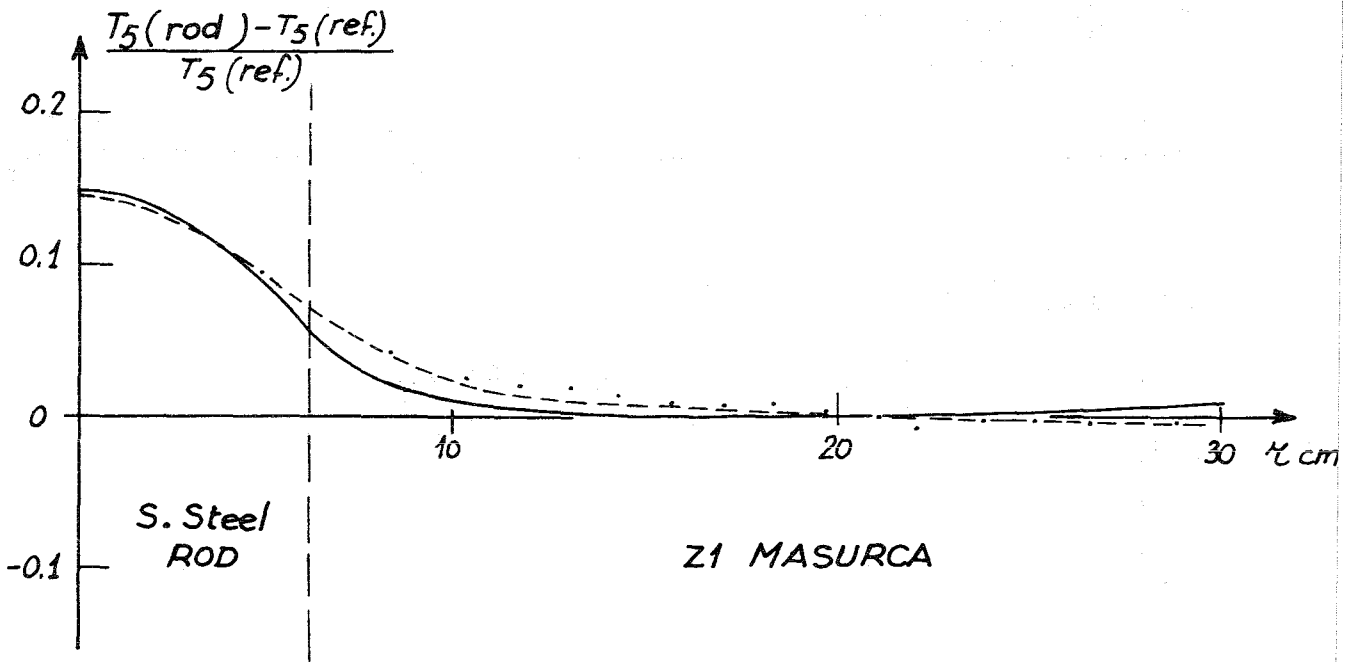
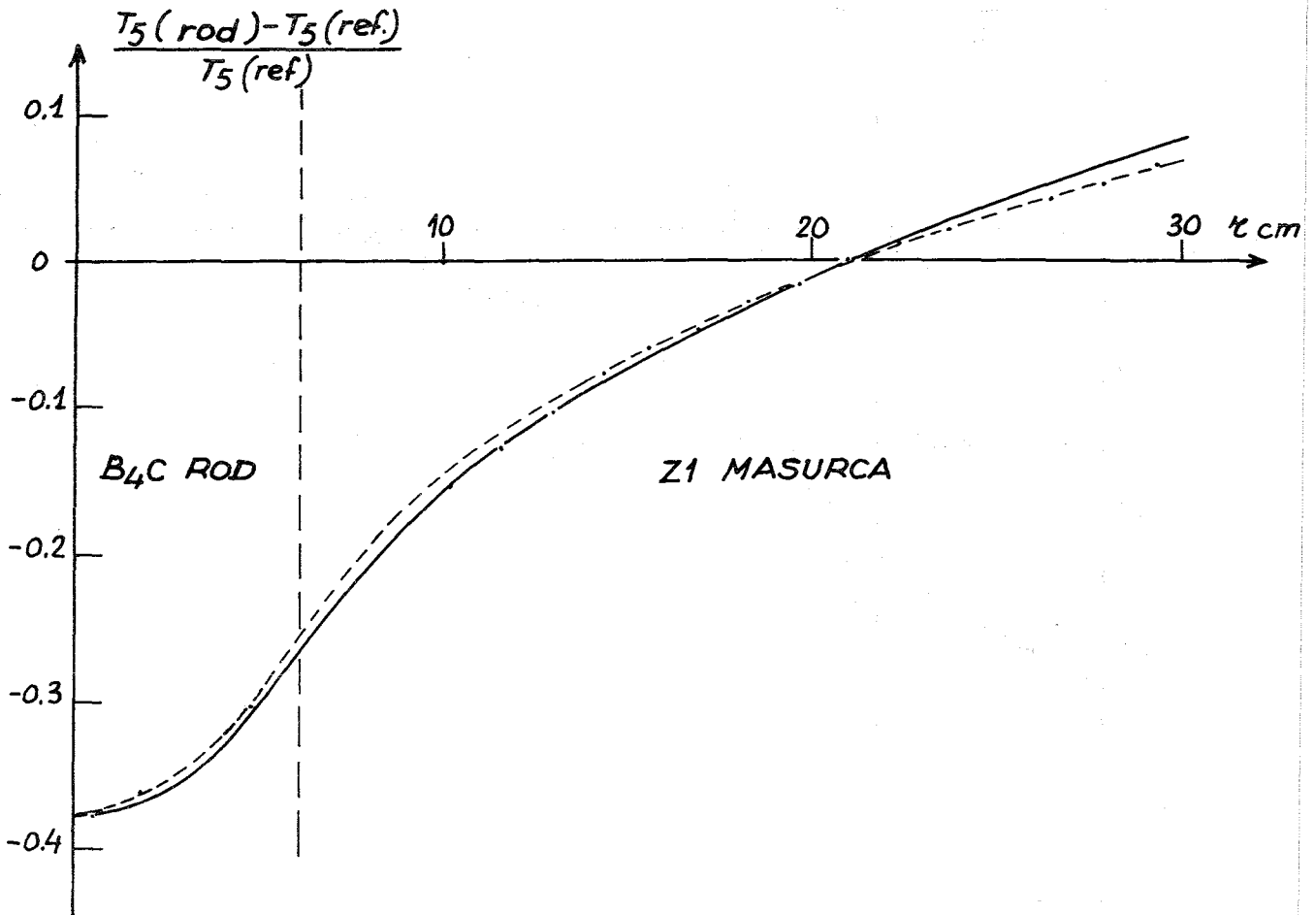
Fig.32



**U 238 FISSION RATE DISTRIBUTION ; PERTURBATION  
 DUE TO A CENTRAL ROD**

— Calculation  
 - - - Experimental results

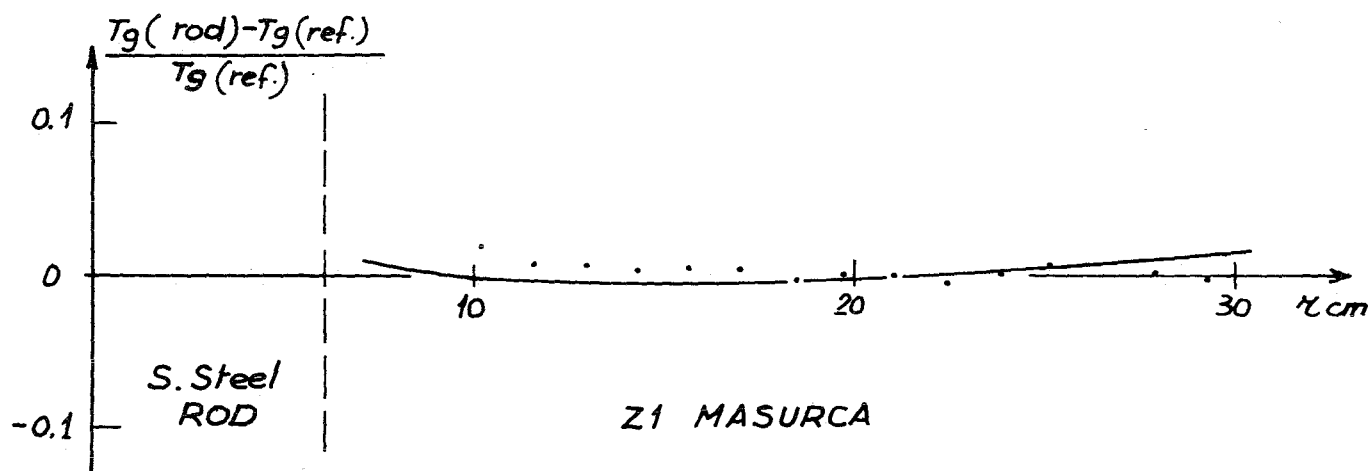
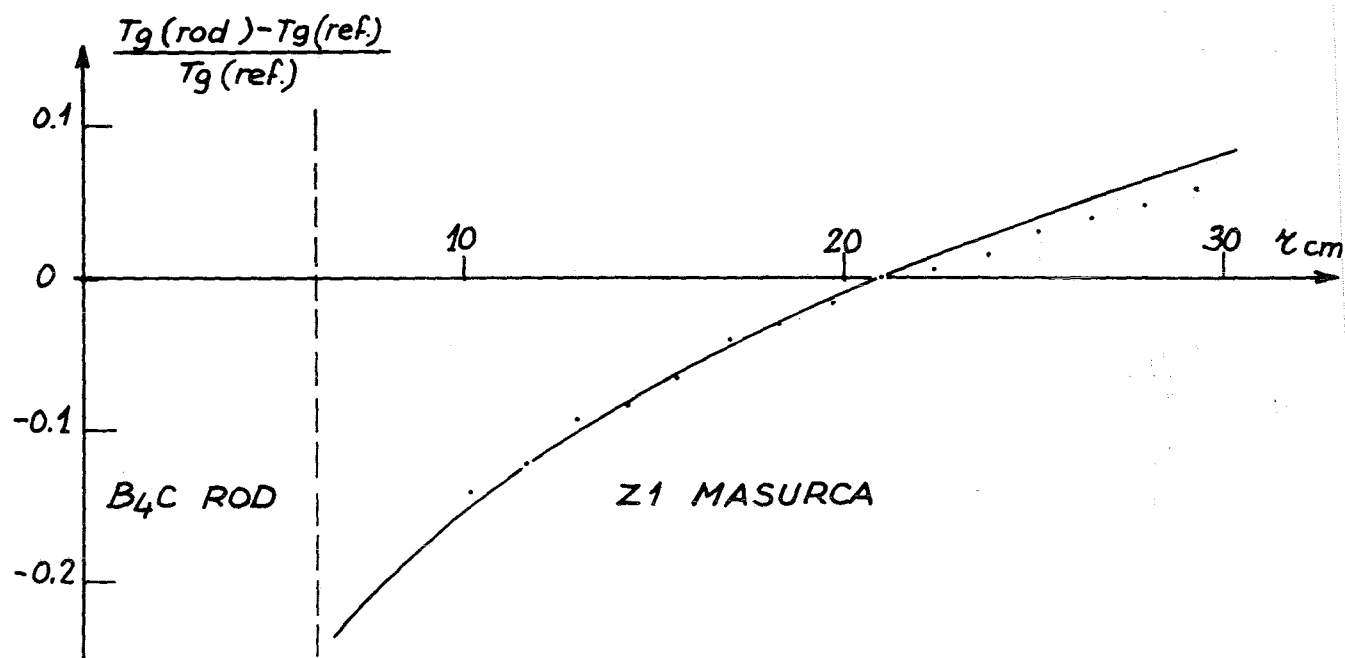
Fig. 33



**U 235 FISSION RATE DISTRIBUTION :  
 PERTURBATION DUE TO A CENTRAL ROD .**

— Calculation  
 - - - Experimental results

Fig. 34



**U 239 FISSION RATE DISTRIBUTION ;  
 PERTURBATION DUE TO A CENTRAL ROD**

——— Calculation  
 - - - - Experimental results

Fig. 35



Imprimé  
par le Bureau de Documentation  
C.E.N./CADARACHE

